UNIVERSITY OF CALIFORNIA

SANTA CRUZ

ILLUMINATING THE ROLES OF OUTER MEMBRANE PROTEINS AND OUTER MEMBRANE VESICLES IN VIBRIO CHOLERAE BIOFILM

A thesis submitted in partial satisfaction of the requirements for the degree of

MASTER OF SCIENCE

in

MICROBIOLOGY AND ENVIRONMENTAL TOXICOLOGY

by

William Garvey

September 2019

The Thesis of William Garvey is Approved:

Professor Fitnat H. Yildiz, Ph.D., Chair

Professor Karen M. Ottemann, Ph.D.

Professor Glenn Millhauser, Ph.D.

Quentin Williams
Acting Vice Provost and Dean of Graduate Studies

TABLE OF CONTENTS

LIST OF FIGURES

Illuminating the Roles of Outer Membrane Proteins and Outer Membrane Vesicles in *Vibrio cholerae* Biofilm

by

William Garvey

ABSTRACT

Biofilms are matrix-encased microbial communities, composed of lipids, proteins, exopolysaccharides, eDNA, and outer membrane vesicles. Residence in biofilm facilitates increased microbial fitness in both the environment and host. Biofilm formation is critical for the infection cycle of *Vibrio cholerae*, the causative agent of cholera. To gain insight into the *V. cholerae* biofilm matrix we performed proteomic analysis of the biofilm matrix and identified a set of outer membrane proteins (OMPs) in the *V. cholerae* biofilm matrix. Strains lacking these OMPs were generated and assessed for biofilm formation potential and production of matrix components. The role of outer membrane vesicles (OMVs), the primary mechanism of OMP extracellular secretion, in formation of biofilm was also investigated. The results of this study suggest that both outer membrane proteins and outer membrane vesicles participate in *V. cholerae* biofilm architecture, helping fill a knowledge gap regarding an aspect of the infection cycle of this pathogen.

ACKNOWLEDGEMENTS

I would like to thank Dr. Fitnat Yildiz, who spotted me in an undergraduate lecture, took a chance, and helped me start this incredible scientific journey. Her support and tutelage have helped turn my childhood dream of being a scientist into a modern-day reality. I hope, one day, I will be able to inspire other scientists-to-be with the same level passion I have seen from Dr. Yildiz over these past few years.

This work would not have been possible without the support from my committee members, Dr. Fitnat Yildiz, Dr. Karen Ottemann, and Dr. Glenn Millhauser. I want to also thank Dr. Donald Smith, Dr. Manel Camps, Dr. Chad Saltikov, and Dr. Victoria Auerbach Stone, each of whom I have had the privilege to study under. Without the incredible METX faculty and administration, I would not be half the scientist or student I am now.

Similarly, I would not be where I am today without the unfathomable support, mentorship, and companionship of each of the members of the Yildiz lab, both past and present. Thank you, Dr. Carmen Schwechheimer, Dr. Kyle Floyd, Dr. Jin Hwan Park, Dr. Fernando Pagliai, Dr. Ana Gallego, Dr. Jennifer Teschler, Joseph Kiblen, Giordan Kitts, Michael Trebino, Megan Mouw, Bao Nguyen, Giselle Aguayo, Sarah Delon, Daniel Wu, Kassidy Hebert, and Maya Modak.

I would also like to thank my mom, dad, and sister for their unconditional love and support. Finally, thank you to all my friends who stood by me during this journey, even when it was not the easiest or most fun thing to do: T.K., A.M., H.M., H.B., M.S., C.K., K.G., and, especially, N.C.

CHAPTER 1: Introduction

William Garvey & Fitnat H. Yildiz

Vibrio cholerae and Cholera

Vibrio cholerae is the Gram-negative causative agent of cholera. Cholera is an infectious, gastrointestinal disease caused by the consumption of contaminated food and water[1]. After ingestion, the disease can result in severe diarrhea and dehydration, which, in the absence of treatment, may result in death. Historically, there have been seven cholera pandemics, having first been cataloged in South-East Asia and moving as far as South America[2]. The most recent epidemiological survey, published in 2015, estimates there still remain 2.9 million cases of cholera annually in endemic countries, primarily those in Sub-Saharan Africa, alongside a number of disturbing outbreaks across the globe[3]. However, the World Health Organization predicts that only 5-10% of annually occurring cases are ever reported, increasing the difficulty in truly understand the global burden of this disease. Said cases are also estimated to result in 95,000 deaths annually[2]. Levels of morbidity and mortality have remained almost constant over the past decade, highlighting how cholera still remains an important public health concern.

Biofilms Have Wide-Ranging Impact

Biofilms are microbial-produced matrices, composed of microorganisms and cell-produced secreted substances[4, 5] and have important implications for human health, environmental, and industrial fields[6]. Microbes living within the biofilm community are able to function cooperatively in their actions and compete with other

microorganisms[7]. Microbial growth and secretion of biofilm matrix components results in the formation of mature, three-dimensional biofilm structures. The multi-component matrix aids in the coaggregation of microbes on both biotic and abiotic surfaces[8, 9]. Production of and subsequent protection by biofilms has been shown to increase bacterial resistance to a number of environmental stresses such as nutrient limitation, reactive oxygen species, acid stress, heat stress, protozoa and bacteriophages[10, 11]. In addition to increased survivability, against the aforementioned factors, biofilm has also been shown to increase the difficulty in treating bacterial infection and contamination through the use of antibiotics and disinfectants, when compared to non-biofilm-associated cells[12]. Increased bacterial persistence is a threat to both heath and food industries, in the context of both patient welfare and as hot beds for horizontal gene transfer of antibiotic resistance cassettes and virulence genes, respectively[13]. Biofilm production has been shown to be involved in the persistence of certain chronic infections, such as cystic fibrosis-induced pneumonia, urinary tract infections, and contaminated implants (catheters, artificial heart valves, etc…)[14].

Composition of Gram-Negative Biofilms

Composition of biofilm is diverse, varying between different bacterial species, but contain a number of conserved components: exopolysaccharides (EPS), proteins, DNA molecules, and outer membrane vesicles (OMVs) [8, 15]. Different matrix components serve specific roles:

EPS: The major component of the biofilm matrix is exopolysaccharide, massive sugar molecules with molecular masses ranging from $0.5x10^6$ to $2.0x10^6$ daltons[16.] Exopolysaccharide molecules are consistently implicated in antimicrobial peptide resistance, host colonization, and mature biofilm formation[17, 18]. EPS is secreted from cells through a number of mechanisms: a WZY secretion mechanism exports polysaccharide precursors to the periplasm, where they are oligomerized before being exported across the outer membrane[19]; ATP binding cassette systems transport fully formed polysaccharide molecules across the inner membrane, but rely on a WZY/WZA-like channel protein to cross the outer membrane[20]; synthase-dependent exopolysaccharide secretion uses a membrane-associated glycosyl transferase which polymerizes monomers while facilitating transport across the inner membrane and ultimately relies on a β-barrel porin for final secretion[21]. Produced by single cells in response to growth phases shift and chemical signals, the EPS meshwork has been shown to increase resistance to antimicrobial compounds[22], host immune system factors[23], and various chemical disinfectants[24]. EPS connects individual microbes and microcolonies, small masses of bacteria, forming the major meshwork that constitutes the biofilm[25]. Additionally, the EPS matrix has been shown to provide mechanical stability to biofilm[26]. One notable EPS molecule, identified in *E. coli*, is cellulose. The cellulose glucose polymer is observed to form wide sheets, with the polymeric layers produced from one cell interacting with those of another cell[27]. Additionally, cellulose structures can be observed to form composite structures with the curli matrix protein forming tissue-like sheaths which cover and connect cells within the

matrix[27]. Certain species of bacteria are identified to produce multiple types of exopolysaccharides; for example, *Pseudomonas aeruginosa* produces the EPS molecules alginate, Pel, and Psl, with each EPS playing a different role in biofilm formation[28]. Alginate, composed of β-1,4-linked D-mannuronic acid and L-guluronic acid[29], has been shown to be essential to forming microcolonies during early stages of biofilm formation and maintenance of mature biofilms[28]. Pellicle formation, biofilm growth at air-liquid interface, is dependent on Pel, a positively charged polysaccharide composed of partially acetylated 1-4-glycosidic linkages of N-acetylgalactosamine and N-acetylglucosamine[30]. Psl, a pentasaccharide containing D-glucose, D-mannose, and L-rhamnose, is shown to be involved in *P. aeruginosa* surface attachment and cell-surface interaction[31]. Pel has also been identified to interact with another biofilm matrix component, eDNA, to promote matrix structural stability[32]. *V. cholerae* biofilm formation involves, among other things, the production of *Vibrio* polysaccharide (VPS), a *Vibrio*-specific exopolysaccharide molecule and major component of the *V. cholerae* biofilm[20, 73]. *V. cholerae* produces two VPS variants: the major variant is composed of [-4)-α-GulNAcAGly3OAc-(1-4)-β-D-Glc-(1-4)-α-Glc-(1-4)-α-D-Gal-(1-] repeating units; in the minor structure, the α-D-Gal is replaced with α-D-GclNAc[34]. VPS is required for the formation of mature biofilm, intestinal colonization, and subsequent pathogenesis, as several of the VPS genes have been shown to be expressed in human infection[35]. One mechanism of VPS-mediated biofilm strength is recruitment and retention of VPS molecules to the

cell surface through interaction with the fibronectin type III-containing RbmA matrix protein[36, 37].

Matrix Proteins: Matrix proteins, secreted proteins identified to contribute to biofilm formation and stabilize the biofilm matrix, either through facilitating cell-surface, cell-cell, or cell-exopolysaccharide interaction. Development of *E. coli* biofilm includes expression of type I fimbriae and curli fimbriae[38]. Type I fimbriae, filamentous adhesins, are implicated in initial attachment of *E. coli* to surfaces[39, 40]. *fimA*, the major fimbriae subunit, mutants are noted to suffer from decreases in initial attachment[41]. Interestingly, activity of type I fimbriae has been shown to decrease expression of certain outer membrane proteins (OmpA, OmpX), which in turn upregulates pili expression and associated adhesion[42]. Curli fimbriae, cell surface aggregating proteins[43], form extracellular structures that facilitate attachment to extracellular proteins, like fibronectin and plasmidogen[44]. Additionally, adhesive curli fibers also promote biofilm formation by facilitating initial cell–surface interactions and subsequent cell–cell interactions[45, 46]. Other proteins, implicated in *E. coli* biofilm formation are AidA and TibA. Both AidA and TibA are surface autotransporter proteins involved into both adhesion to eukaryotic surfaces and formation of biofilm through both auto and cellular aggregation[47]. LecA and LecB are two secreted lectin proteins, proteins specifically characterized to bind carbohydrates, identified to be essential to *P. aeruginosa* biofilm construction and preservation; competitive inhibitors for LecB have been shown to prevent biofilm formation and induce

dispersal of mature matrix structure[48]. In addition to lectin proteins, adhesins, proteins that facilitate cell-surface, cell-EPS, and EPS-surface connections, also aid in biofilm structure. LapA and LapF are two secreted proteins identified in *Pseudomonas putida* biofilms. LapA has been shown to be important for cell-surface attachment, while LapF has been shown to be important for cell-cell interaction along with biofilm maturation[49]. In addition to their aforementioned functions, LapA and LapF have been observed to bind exopolysaccharide molecules in *P. aeruginosa* biofilms[50]. Interestingly, expression of the Lap proteins are influenced by the absence or presence of certain EPS in *P. putida*[49], further highlighting the importance of interactions between the different species of biofilm components. In *V. cholerae*, RbmA, Bap1, and RbmC, three secreted proteins[51], facilitate biofilm formation through several mechanisms including mother-daughter cell attachment[52], cell-surface attachment[53], and protein-protein interaction[54]. Interesting work has been done in determining a timeline for protein-mediated *V. cholerae* biofilm formation and structure in *V. cholerae*. Following bacterial attachment to the environmental surface, RbmA was noted to accumulate sporadically on the cell surface, this is later described as aiding in the aggregation of mother and daughter cells[55]. RbmA is observed to be critical for *Vibrio cholerae* biofilm structure and affords increased resistance to sodium dodecyl sulfate[56]. Increased biofilm durability is thought to be garnered through the cleavage of RbmA, into the cationic "RbmA*" form, to recruit additional anionic VPS molecules, as the addition of exogenous RbmA* was show to significantly increase incorporation of VPS into biofilm structure[37]. Other studies

have also shown that one of the two FnIII domains of RbmA binds to VPS[36]. The same study showed that RbmA has a bistable switch, which affects protein dimerization and VPS-binding potential[36]. Regulation of RbmA structure by plays an essential role in its ability to participate in biofilm formation. Bap1 was then observed to accumulate between cells and at the surface of the biofilm. Shown to be specific to cells forming the biofilm-surface interface, Bap1 promotes biofilm adhesion to the surface, perhaps through self-aggregation of the proteins after having been secreted[57]. Upon expression, Bap1 and RbmC were finally noted to form sheath-like structures, incorporating VPS molecules, around the cells within the biofilm[55]. RbmC was discovered to contain two β-prism domains. These domains were observed to target a number of complex N-glycans containing a $GlcNAc_2$-Man_3 polysaccharide core[58], defining a role for RbmC in binding extracellular polysaccharide molecules in the environment or present by host cells. Finally, *V. cholerae* matrix proteins are post-translationally regulated via proteolytic activity, namely HapA, a secreted protease[37].

eDNA: Extracellular nucleic acid polymers, or eDNA, have been identified as a fundamental component of various bacterial biofilms. Varying greatly in length, eDNA is observed to be a structural component of the biofilm, linking its various components into the network necessary for proper function. eDNA is found to be produced through multiple mechanisms: cell lysis[59], active secretion of genomic DNA[60], and synthesis of non-genomic, linear DNA molecules[60]. eDNA has been identified to have at least two roles in biofilm, such as an adhesin, aiding bacterial

adhesion to physical surfaces[61] and as a connective polymer to facilitate bacterial aggregation[62]. One form of eDNA induced biofilm structure has been identified in uropathogenic *E. coli* (UPEC). DNABII family proteins play a role in binding and shaping nucleic polymers within the biofilm, increasing biofilm integrity[32, 40]. Additionally, the negatively charged phosphate backbone of DNA has been shown to chelate environmental cations[64]. The PhoPQ signal transduction pathway, common to intracellular pathogens such as *Pseudomonas aeruginosa,* is known to respond to limited Mg^{2+} conditions, a common condition during the infection cycle[65]. It has been shown that the PhoPQ two component system regulates multiple lipopolysaccharide modifications, resulting in an increase in outer membrane resistance to bile salts[66]. This system highlights an interesting interplay between different biofilm components. Furthermore, eDNA-induced cation-limitation, namely magnesium, has been shown to promote LPS modification increasing *P. aeruginosa* biofilm resistance to aminoglycosides, like gentamycin and tobramycin[64]. eDNA, in *V. cholerae* biofilm, is shown to be involved in both formation and detachment[67]. *V. cholerae* encodes two extracellular endonucleases: Dns and Xds[68]. Xds is observed to be expressed during late stage of infection[69], perhaps suggesting a role in degradation of biofilm-associated eDNA. *Dns* and *Xds* mutants show increases in biofilm formation[67], leading authors to establish eDNA as an integral component of *V. cholerae* biofilm.

OMVs: Outer membrane vesicles (OMVs) are phospholipid micelles, ranging from 20 – 200 nm in diameter[70], observed to be released constitutively from Gram-negative

bacterial outer membranes during the growth cycle. OMVs are observed to be composed of the same materials that compose the bacterial outer membrane: lipids, lipopolysaccharides, and proteins[70]. There are two different identified species of OMVs: larger OMVs, associated with fimbriae, pili, and other proteins; slightly smaller OMVs with more LPS compared to protein content[71]. Each species of OMV is identified to associate with either high density or low density biofilms, respectively[71]. During production, OMVs are decorated with outer membrane proteins and lipopolysaccharides, while also being filled with periplasmic content, including proteins and nucleic acid polymers[39], from their progenitor cells. OMV production rates and composition have been shown to vary due to environmental and cellular conditions. A series of genetic experiments, spanning a number of bacterial species, have revealed a number of OMV production mechanisms: maintenance of outer membrane leaflet asymmetry by the Yrb/VacJ ABC system[73, 74, 75]; peptide mediators of cell wall and outer membrane crosslinking (YnhG[76], YcbB[76], NlpA[77], OmpA[76]), endopeptidase (MepA, DacB, PbpG[78]), and lipoprotein (Lpp[76]) regulators of covalent crosslinking of the cell wall to the outer membrane[50, 51]; accumulation of peptidoglycan fragments[76] and toxic-misfolded proteins[81] in the periplasm; accumulation of quorum sensing and signaling molecules in the outer leaflet[82, 83, 84]. OMVs are similar to Swiss Army knives in that they have a number of diverse functions. Vesicles have been observed to facilitate both inter- and intraspecies transformation of genetic material, at equal efficiencies of transformation[72, 85, 86]. A series of mechanisms for OMV-mediated horizontal gene transfer have been

observed: vesicle fusion with bacterial-acceptor membrane; lysis of OMVs in proximity or attached to host-cell membranes[87]; internalization of OMVs by acceptor bacteria and subsequent lysis in the lumen[88]. Another example of interspecies OMV interaction is the transfer of proteins between bacteria and host cells[72, 89]. In *E. coli*, it has been established that OMVs can protect both *E. coli* and other Gram-negative organisms from antibiotic that specifically target the outer membrane like colistin and melittin[90]. The protective mechanism is facilitated by both OMV protease and peptidase cargo and saturation of the environment with outer membrane decoys. Additionally, OMVs from β-lactam-resistant *E. coli* can also increase survivability of antibiotic susceptible bacteria against β-lactam antibiotics[91]. The *E. coli* OmpT protease has an interesting relationship with *E. coli* OMV production, in that, in *ompT* mutants authors observe a significant decrease in vesicle production, while also observing an increase in vesicle diameter and concentration of content[92]. Authors speculate that expression of OmpT alters OMV production and composition in response to different stimuli, allowing for intercellular communication. OMVs have been identified to act as a novel effector secretion system. *P. aeruginosa* OMVs have been shown to successfully translocate effector proteins and virulence factors including β-lactamase, alkaline phosphatase, and hemolytic proteins directly into the host cytoplasm via vesicle and host-membrane fusion[93, 94]. The OMV-secretion system has also been shown to function as a stress response mechanism, i.e. removal of toxic-misfolded proteins promoted by antimicrobials[72, 95]. OMVs have been observed to perform a number of functions in *V. cholerae*, including transport of

virulence factors[96], trafficking of functional proteins[54], and acting a bacteriophage decoys, increasing *V. cholerae* resistance to phage[97].

Heightened resistance to environmental and chemical stresses can be attributed to the complexity and various molecular mechanisms within the matrix, highlighting a need to further investigate these biofilm components.

Vibrio cholerae **Biofilms**

Vibrio cholerae uses biofilm to increase successful transmission between aquatic and host environments[15]. Biofilm formation occurs in a stepwise process: surface scanning/motility; initial attachment; formation of microcolonies and expression of matrix components[15]. Initial attachment to surfaces uses the toxin-coregulated pilus[98] and the type IV mannose-sensing hemagglutinin (MSHA) pilus[99]. *V cholerae* bears a single polar flagellum which is reported to facilitate initial colonization[100]. Finally, products of the biofilm matrix components discussed above lead to formation of mature biofilms. Similar to other organisms, biofilm enhances *V. cholerae* resistance to antimicrobial and chemical agents[101]. The biofilm cycle ends in detachment of biofilm clumps or single cells from the primary mass. The importance of biofilm in the infection cycle was highlighted in the decontamination of water with 40 μm filters, almost 20 times the size of a single *V. cholerae*[102]. Additionally, biofilm-associated *V. cholerae* were shown to be hyper-infectious, when compared to planktonic cells[103].

Conclusion

Vibrio cholerae is an important pathogen, in that it causes a disease that still ravages an untold number of people. Biofilm formation, and the mechanisms within that lead to increased bacterial resistance, is critical to the survival and turnover of the infection cycle. However, we still do not fully understand the contribution of a number of the matrix-associated components: outer membrane proteins and outer membrane vesicles. This work focuses on and works to fill in knowledge gaps regarding the critically important *Vibrio cholerae* biofilm and the functions of the outer membrane proteins and outer membrane vesicles found within.

CHAPTER 2: Outer Membrane Proteins Influence *Vibrio cholerae* Biofilm Architecture

William Garvey & Fitnat H. Yildiz

Introduction

Vibrio cholerae is the pathogen responsible for the disease cholera[1], which still affects approximately 2.9 million people annually, resulting in high levels of both morbidity and mortality[2]. Biofilm formation is critical for the *V. cholerae* infection cycle, increasing successful transmission to and from the host and aquatic environment[15]. Biofilm-associated *V. cholerae* cells are resistant to a number of antibiotics and disinfectants[104]. Residence in biofilm also results in a hyper-infectious state, when compared to planktonic cells[103]. The majority of what we understand regarding *V. cholerae* biofilm comes from strains with enhanced biofilm forming ability. These are rugose strains of *V. cholerae*, with more high-volume and distinctly patterned biofilms due to increased production of VPS and the major biofilm matrix proteins. In this study, we use an A1552 *V. cholerae* rugose variant strain, which attributes its enhanced biofilm phenotype to a point mutation in *vpvC*, called VpvC[105]. This mutation, via an unknown mechanism, increases intracellular levels of cyclic-di-GMP, which enhances expression of matrix components. Increased abundance of matrix components results in increased incidents of component interaction. Understanding molecular underpinnings, such as the complete protein and exopolysaccharide interactomes of critical matrix components, like the RbmA, Bap1, and RbmC matrix proteins, of *V. cholerae* biofilm formation is needed to develop enhanced techniques and treatments for combating biofilms.

Recently, proteomic analysis was performed on the extracellular material of the *V. cholerae* biofilm[90, 91]. The analysis revealed a number of proteins theretofore unknown to exist in the matrix, suggesting a function therein. Most curiously, a set of outer membrane proteins (OMPs) were observed to exist in the extracellular matrix. These OMPs were then confirmed to be present in OMVs as proteinaceous accessories[106, 107].

OMPs are proteins found in and/or on the outermost membrane of Gram-negative bacteria. OMPs are identified to come in two different flavors, integral and peripheral membrane proteins. Containing only one hydrophobic region, peripheral proteins are anchored into the membrane by, either, a hydrophobic tail or a post-translational modulation[108]. Some bind the bacterial membrane by adhering to additional proteins embedded in the membrane[109], attaching via a protein anchor and not the stitching pattern of the integral membrane proteins. Integral membrane proteins are amino acid polymeric chains which weave in and out of the membrane, allowing hydrophobic stretches of the protein sequence to sequester within the hydrophobic center of the bilayer membrane[110]. Adhesin proteins are common examples of integral membrane proteins. OMPs have been shown to be important in facilitating attachment and coaggregation between bacteria and various environmental surfaces. CdrA, a 150 kDa protein identified in *Pseudomonas aeruginosa*, has been identified to facilitate bacterial aggregation and biofilm formation via an adhesin protein mechanism[50]. CdrA has been shown to be secreted into the extracellular space via CdrB, an outer

membrane transporter encoded in the same operon as CdrA. OMPs, more specifically porin proteins or porin complexes, are one of the primary ways in which bacteria are able to interact with and gain information about their environment[9]. Through multiple passages of the protein through the membrane and/or protein polymerization within the membrane, porin proteins form channels in the membrane. The primary function of these passages allows for the transportation of a number of molecular cargos, ions, or proteins.

The outer membrane proteins of interest, identified in the aforementioned proteomic analyses, and discussed in this project, are listed in Table 2.1.

Table 2.1. Select Proteins Identified in Proteomic Analysis of *V. cholerae* Biofilm and Outer Membrane Vesicles

Gene ID	Annotation	Known Localization	Function	Abundance in *V. cholerae* Biofilm Matrix (i)	Abundance in *V. cholerae* OMVs (ii)	Presence in *V. cholerae* Biofilm Matrix (iii)
VC0633	OmpU	OM	Porin Transporter Activity	6055	691	X
VC2213	OmpA	OM	Porin Transporter Activity	445	43	X
VC1854	OmpT	OM	Porin Transporter Activity	1854	27	X
VCA0867	OmpW	OM	Porin Transporter Activity	11	12	-
VC1318	OmpV	OM	Porin Transporter Activity	-	16	-

Table 2.1. Select Outer Membrane Proteins Identified in Proteomic Analysis of *V. cholerae* Biofilm and Outer Membrane Vesicles. Bioinformatic analysis of selected outer membrane proteins. (i) Spectral count of select proteins from mass spectrometry analysis of *V. cholerae* A1552 rugose variant extracellular matrix (Yildiz, Unpublished). (ii) Abundance of select proteins via liquid chromatography-mass spectrometry of outer membrane vesicles from *V. cholerae* El Tor C6706 extracellular matrix (Mekalanos, 2014). (iii) Presence of select proteins, identified via proteomic analysis by mass spectrometry, in *V. cholerae* MO10 extracellular matrix (Watnick, 2011).

VC2213 (OmpA)

Outer Membrane Protein A, or OmpA, has been identified in many bacterial species: *Vibrio cholerae*, *Yersinia enterica*, *Acinetobacter baumannii*, and thousands more (http://eggnogdb.embl.de/#/app/results#COG2885_datamenu). OmpA is an integral outer membrane porin observed to have two domains; the first is a hydrophobic β-barrel domain, imbedded in the outer membrane and a periplasmic domain, which, via perhaps two conserved residues, functions in linking the peptidoglycan cell wall to the outer membrane; the second domain is a globular periplasmic C terminal domain[111]. Dimerization of OmpA has been shown to alter interaction with the peptidoglycan cell wall modulating outer membrane rigidity. Initially identified as "outer membrane protein 38" in *Acinetobacter baumannii*, electron microscopy revealed that OmpA is essential for outer membrane stability, evidenced by an increase in vesicle-like structures on an *ompA* deficient *A. baumannii* mutant cell surface[112]. *A. baumannii* OmpA has been shown to be essential for adhesion to the pili of *Candida albicans*, an opportunistic pathogenic yeast species common to human gut flora, and A549 human alveolar epithelial cells, a common facet of *Acinetobacter* nosocomial infection[112], suggesting a role of OmpA during infection. In *E. coli*, specifically the K12 strain, OmpA has been shown to bind colicin, a bacteriocin[113], brain microvascular endothelial cells[114], and bacterial F conjugation partners[115]. *ompA* deficient *E. coli* mutants were observed to be more sensitive to environmental stresses, such as: acidity, osmolarity, and human serum[116]; suggesting OmpA, as an outer membrane accessory, is also an important stress response factor.

Additionally, *ompA* deficient *A. baumannii*[117], *V. cholerae*[118], and *E. coli*[119] strains have been shown to produce altered biofilms.

VC1854 (OmpT)

OmpT, an outer membrane aspartyl protease important for the cleavage of extracellular peptides, is a virulence factor common to most uropathogenic *E. coli*[120]. Analysis of *ompT* deficient mutants revealed that the outer membrane protein is important for: adhesion to human epithelial cells and human extracellular matrix components[120]; invasion of human bladder epithelial cells (cell line 5637)[120]. *Vibrio ichthyoenteri* OmpT functions as a pore, facilitating transport of amino acids, peptides, and antibiotics[121]. Interestingly, *V. cholerae* OmpT, presented to the matrix via OMV transport, was observed to associate with Bap1, enhancing *V. cholerae* resistance to Polymyxin B through binding and seclusion of the antimicrobial compound[54]. In *V. cholerae*, expression of OmpT is regulated by ToxR, a transcriptional regulator highly associated with expression of virulence factors, like cholera toxin[122]. In the presence of bile salt, ToxR down regulates expression of OmpT, suggesting an inverse relationship between OmpT, infection, and sensitivity to bile salts[123].

VC0633 (OmpU)

One of the most abundant outer membrane proteins, OmpU is noted for its role in facilitating passage of hydrophobic solutes and select cationic ions[124]. Similar to OmpT, in *V. cholerae*, expression of OmpU is regulated by the virulence regulator ToxR[122], mediating resistance to bile and anionic detergents such as sodium dodecyl sulfate[125]. In the presence of bile salt, ToxR up regulates expression of OmpU, suggesting a direct relationship between OmpU, infection, and resistance to bile salts[123]. OmpU has also been implicated to function in a fascinating regulatory pathway, promoting resistance to Polymyxin B and P2, two human defense peptides. Both Polymyxin B and P2 increase the permeability of bacterial outer membranes through interaction with LPS and membrane lipids[126]. This manipulation of the outer membrane results in an OmpU confirmation change, exposing a DegS binding site on the RseA anti-σ factor[127]. OMP induced cleavage of RseA results in alteration of the bacterial transcriptome through freeing of the RseB σ factor. OmpU is also a major immunostimulant, with OmpU having been noted to interact with host toll-like receptor 2 when present in cholera vaccines[128, 129]. Additionally, *V. cholerae* lacking *ompU* induce decreased IL-8 expression and adherence to HT-29 intestinal epithelial cells compared to the parental strain[130]. In *Vibrio anguillarum*, ToxR-mediated expression of OmpU is also shown to be upregulated in the presence of bile salt, suggesting a role of OmpU in response to conditional stresses[131]. Additionally, in *V. anguillarum,* OmpU expression increased in the presence of high salinity, suggesting a role in NaCl transport or resistance[132]. As a porin, OmpU has been identified to promote resistance to bile acids and antimicrobial peptides while also increasing

success of host invasion through observed adhesin activity in *Vibrio spendidus* and *Vibrio vulnificus*[113, 114, 115].

VC1318 (OmpV)

In *Vibrio cholerae*, OmpV is observed to be a peptidoglycan-associated porin-like protein[136]. OmpV has also been shown to be a critical osmoregulatory mechanism in a number of *Vibrio* bacteria. *Vibrio parahaemolyticus*[137], *Vibrio anguillarum*[132], and *Vibrio alginolyticus*[138] have all be shown to utilize OmpV in resistance to osmolarity stress. *V. parahaemolyticus* OmpV, acting as an efflux pump, is one of the mechanisms by which the organism attenuates the effect of antimicrobial peptides[139]. Additionally, in *V. anguillareum,* the OmpV homologue (96% similarity to *V. cholerae* OmpV) functions in response to low salinity[132].

VCA0867 (OmpW)

OmpW is noted to be an important asset in the *E. coli* resistome. OmpW has been shown to work in concert with EmrE, an inner membrane multidrug resistance efflux pump[140]. EmrE and OmpW work together to export a broad range of bactericidal quaternary cationic compounds, like surfactants and antiseptics, from the cytoplasm into the periplasm and finally into the extracellular space[140]. OmpW-mediated movement of quaternary cationic compounds has also been shown to mediate osmotic

stress[138]. Additionally, OmpW has been observed to be required for resistance to phagocytosis. An *ompW* deficient *E. coli* K12 strain displayed an increased rate of uptake during phagocytosis by macrophages[141]. OmpW has been suggested to be a vaccine target with inhibition of OmpW resulting in an increased ability of host macrophages to fight infection. Additionally, in *V. anguillarum,* OmpW expression increased in the presence of increased salinity, further suggesting a role in NaCl transport, resistance, or modulation of osmolarity[132].

The goal of this study was to determine if these outer membrane proteins play a role in *V. cholerae* biofilm formation. Our data has shown that, via unknown mechanism(s), these outer membrane proteins indeed function in biofilm architecture.

Materials and Methods

Bacterial strains, plasmids, and culture conditions

Bacterial strains and plasmids used in this study are listed in Table 2.2. *Escherichia coli* CC118λpir, DH5αλpir, and *E. coli* SM10λpir were used for DNA and plasmid construction and manipulation. *E. coli* S17λpir was used for conjugation with *V. cholerae*. *E. coli* and *V. cholerae* strains were grown aerobically at 30°C and 37°C, respectively. Cultures were grown in Luria-Bertani (LB) broth (1% Tryptone, 0.5% Yeast Extract, 1% NaCl), pH 7.5. Strain colonies were grown on LB agar medium,

containing 1.5% (wt/vol) granulated agar. Antibiotics were used at the following concentration: ampicillin 100 µg/ml; rifampicin 100 µg/ml; gentamicin 50 µg/ml; polymyxin B 12.5 µg/ml.

Generation of in-frame deletion and Tn7 complementation strains

5' (500 bp) and 3' (500 bp) regions of the respective genes, including start and stop codons, were amplified by PCR with the appropriate primers, A and B, C and D, respectively. The amplified 503-bp deletion fragments were cloned into pGP704-sacB28 via Gibson Assembly (NEB E2611L). Recombinant "deletion" plasmids were transformed into any of the three aforementioned *E. coli* strains. Deletion constructs were purified and sequenced (UC Berkeley DNA Sequencing Facility, Berkeley CA). Successful constructs were transformed into the appropriate *E. coli* strain. Transformants were then conjugated with *V. cholerae*. Trans-conjugants were selected on LB agar medium containing ampicillin (100 µg/ml) and rifampin (100 µg/ml). Sucrose-based selection was used to select *V. cholerae* deletion clones that had undergone homologous recombination between the wild-type chromosomal copy of the gene and rejected the plasmid. Briefly, independent ampicillin and rifampin-resistant trans-conjugants were randomly selected, streaked on LB agar plates containing of ampicillin (100 µg/ml) and rifampin (100 µg/ml), and incubated at 37°C. Single colonies were then inoculated into liquid LB and incubated over day at 37°C, shaking (200 rpm). From liquid culture, approximately 10 µl was streaked on LB agar plates containing 6% (wt/vol) sucrose without NaCl, pH 6.8-6.9 to test for sucrose sensitivity. Sucrose plates were incubated at room temperature over the

course of 48 hours. Single colonies were selected from sucrose plates and were patched on two LB agar plates, one containing ampicillin (100 µg/ml) and one not containing ampicillin. After incubation overnight at 37°C, presence of the deletion was verified by PCR. Deletion mutants were stored at -80°C. Complementation plasmids were constructed by cloning an amplified multi-kilobase pair fragment of the respective gene (including 500 bp upstream of the predicted open reading frame thought to contain the native promoter for each respective gene), using the appropriate primers, into pPG704Tn7 via NotI sites. Accuracy of complementation constructs were verified by sequencing (UC Berkeley DNA Sequencing Facility, Berkeley CA). Successful plasmids were transformed into appropriate *E. coli* strains, then purified for transformation of conjugational *E. coli*. Construct-positive *E. coli* and helper *E. coli* S17λpir cells harboring pUX-BF13 containing the Tn7 transposase gene, was then conjugated with *V. cholerae*. Trans-conjugants were selected on LB agar medium containing rifampicin (100 µg/ml) and gentamicin (15 µg/ml). Plates were incubated at 37°C overnight. Single colonies were selected from rifampicin and gentamicin plates and were patched on rifampicin and gentamycin LB agar plates. After incubation overnight at 37°C, presence of the complementation was verified by PCR. Complementation mutants of the respective genes generated in mutant backgrounds were stored at -80°C.

Table 2.2. Bacterial Strains

***E. coli* Strain**	**Relevant Genotype**	**Source**
CC118λpir	Δ(*ara-leu*) araD Δ*lacX74* galE galK phoA20 thi-1 rpsE rpoB argE(Am) recA1 λpir	Herrero *et al*. (1990)
S17λpir	Tp^r Sm^r *recA thi pro* r^-_Km^-_K RP4 : : 2-Tc : : MuKm Tn7 λpir	Herrero *et al*. (1990)
DH5α	F' *endA1 hsdR17 supE44 thi-1 recA1 gyrA96 relA1* Δ(*argF-lacZYA*) *U169* (ϕ80d*lac*Δ*M15*)	Promega
***V. cholerae* Strains**	**Relevant Genotype**	**Source**
FY_Vc_2	*V. cholerae* O1 El Tor A1552, rugose wild-type variant, Rif^r	Yildiz & Schoolnik (1999)
FY_Vc_222	Rugose mTn7-*gfp*, Rif^r Gm^r	Fong *et al*. (2005)
FY_Vc_240	Rugose-*gfp*, V. cholerae O1 El Tor A1552, rugose variant, Rif^r Gm^r	Beyhan & Yildiz (2007)
FY_Vc_4327	RΔ*vps*-IΔ*vps*-II, rugose variant with deletion of *vpsA-K* and *vpsL-Q*, Rif^r	Fong & Yildiz (2010)
FY_Vc_6431	Rugose *rbmA* (Myc tag), *rbmC* (3xFLAG tag), *bap1* (3xHA tag), Rif^r	Fong & Yildiz (2012)
FY_Vc_10559	Rugose Δ*rbmA*Δ*bap1*Δ*rbmC* Δ*vps-opI//opII*, Rif^r	Yildiz (unpublished) (2009)
FY_Vc_9250	Rugose Δ*toxR*, Rif^r	This Study
FY_Vc_9286	Rugose Δ*toxR::Tn7_GFP* (488nm), Rif^r Gm^r	This Study
FY_Vc_9935	Rugose Δ*hapA* Rif^r	Yildiz (unpublished) (2009)
FY_Vc_9949	Rugose Δ*hapA,* Δ*prtV,* Δ*vesB* Rif^r	Fong & Yildiz (2015)
FY_Vc_15181	Rugose Δ*ompA*, Rif^r	This Study
FY_Vc_15182	Rugose Δ*ompA::Tn7_GFP* (488nm), Rif^r Gm^r	This Study
FY_Vc_15183	Rugose Δ*ompA::Tn7_ompA_1D4*, Rif^r Gm^r	This Study
FY_Vc_15184	Rugose Δ*ompT*, Rif^r	This Study
FY_Vc_15185	Rugose Δ*ompT::Tn7_GFP* (488nm), Rif^r Gm^r	This Study
FY_Vc_15186	Rugose Δ*ompT::Tn7_ompT_1D4*, Rif^r Gm^r	This Study
FY_Vc_15187	Rugose Δ*ompU*, Rif^r	This Study
FY_Vc_15188	Rugose Δ*ompU::Tn7_GFP* (488nm), Rif^r Gm^r	This Study
FY_Vc_15189	Rugose Δ*ompU::Tn7_ompU_1D4*, Rif^r Gm^r	This Study

FY_Vc_15190	Rugose Δ*ompU*Δ*ompT*, Rif^r	This Study
FY_Vc_15191	Rugose Δ*ompU*Δ*ompT::Tn7_GFP* (488nm), Rif^r Gm^r	This Study
FY_Vc_15192	Rugose Δ*ompU*Δ*ompT::Tn7_ompT_1D4*, Rif^r Gm^r	This Study
FY_Vc_15193	Rugose Δ*ompV*, Rif^r	This Study
FY_Vc_15194	Rugose Δ*ompV::Tn7_GFP* (488nm), Rif^r Gm^r	This Study
FY_Vc_15195	Rugose Δ*ompV::Tn7_ompV_1D4*, Rif^r Gm^r	This Study
FY_Vc_15196	Rugose Δ*ompW*, Rif^r	This Study
FY_Vc_15197	Rugose Δ*ompW::Tn7_GFP* (488nm), Rif^r Gm^r	This Study
FY_Vc_15198	Rugose Δ*ompW::Tn7_ompW_1D4*, Rif^r Gm^r	This Study
FY_Vc_15199	Rugose Δ*ompA*::Tn7_*ompA*, Rif^r Gm^r	This Study
FY_Vc_15200	Rugose Δ*ompT::Tn7_ompT*, Rif^r Gm^r	This Study
FY_Vc_15201	Rugose Δ*ompU::Tn7_ompU*, Rif^r Gm^r	This Study
FY_Vc_15202	Rugose Δ*ompV::Tn7_ompV*, Rif^r Gm^r	This Study
FY_Vc_15203	Rugose Δ*ompW::Tn7_ompW*, Rif^r Gm^r	This Study
FY_Vc_15204	Rugose *rbmA* (Myc tag), *rbmC* (3xFLAG tag), *bap1* (3xHA tag), Δ*ompA* Rif^r	This Study
FY_Vc_15205	Rugose *rbmA* (Myc tag), *rbmC* (3xFLAG tag), *bap1* (3xHA tag), Δ*ompA::Tn7_GFP* (488nm) Rif^r Gm^r	This Study
FY_Vc_15206	Rugose *rbmA* (Myc tag), *rbmC* (3xFLAG tag), *bap1* (3xHA tag), Δ*ompA::Tn7_ompA_1D4* Rif^r Gm^r	This Study
FY_Vc_15207	Rugose *rbmA* (Myc tag), *rbmC* (3xFLAG tag), *bap1* (3xHA tag), Δ*ompT* Rif^r	This Study
FY_Vc_15208	Rugose *rbmA* (Myc tag), *rbmC* (3xFLAG tag), *bap1* (3xHA tag), Δ*ompT::Tn7_GFP* (488nm) Rif^r Gm^r	This Study
FY_Vc_15209	Rugose *rbmA* (Myc tag), *rbmC* (3xFLAG tag), *bap1* (3xHA tag), Δ*ompT::Tn7_ompT_1D4* Rif^r Gm^r	This Study
FY_Vc_15210	Rugose *rbmA* (Myc tag), *rbmC* (3xFLAG tag), *bap1* (3xHA tag), Δ*ompU* Rif^r	This Study
FY_Vc_15211	Rugose *rbmA* (Myc tag), *rbmC* (3xFLAG tag), *bap1* (3xHA tag), Δ*ompU::Tn7_GFP* Rif^r Gm^r	This Study
FY_Vc_15212	Rugose *rbmA* (Myc tag), *rbmC* (3xFLAG tag), *bap1* (3xHA tag), Δ*ompU::Tn7_ompU_1D4* Rif^r Gm^r	This Study
FY_Vc_15213	Rugose *rbmA* (Myc tag), *rbmC* (3xFLAG tag), *bap1* (3xHA tag), Δ*ompV* Rif^r	This Study
FY_Vc_15214	Rugose *rbmA* (Myc tag), *rbmC* (3xFLAG tag), *bap1* (3xHA tag), Δ*ompV::Tn7_GFP* (488nm) Rif^r Gm^r	This Study
FY_Vc_15215	Rugose *rbmA* (Myc tag), *rbmC* (3xFLAG tag), *bap1* (3xHA tag), Δ*ompV::Tn7_ompV_1D4* Rif^r Gm^r	This Study
FY_Vc_15216	Rugose *rbmA* (Myc tag), *rbmC* (3xFLAG tag), *bap1* (3xHA tag), Δ*ompW* Rif^r	This Study

FY_Vc_15217	Rugose *rbmA* (Myc tag), *rbmC* (3xFLAG tag), *bap1* (3xHA tag), Δ*ompW::Tn7_GFP* (488nm) Rif^r Gm^r	This Study
FY_Vc_15218	Rugose *rbmA* (Myc tag), *rbmC* (3xFLAG tag), *bap1* (3xHA tag), Δ*ompW::Tn7_ompW_1D4* Rif^r Gm^r	This Study
FY_Vc_15219	Rugose Δ*VC2519*, Rif^r	This Study
FY_Vc_15220	Rugose Δ*rbmA*Δ*bap1*Δ*rbmC* Δ*vps-opI//opII, ΔVC2519*, Rif^r	This Study

Table 2.3. Plasmids

pGP704sacB28	pGP704 derivative, *mob/oriT sacB*, Ap^r	G. Schoolnik
pGP704::Tn7-GFP	Mini-Tn7 vector harboring a constitutively expressed gfp cassette	G. Schoolnik
pUX-BF13	Helper plasmid containing transposase gene for mini-Tn7	G. Schoolnik
pMCM11	pGP704::mTn7-*gfp*, Gm^r Ap^r	M. Miller/ G. Schoolnik
pGP704sacB28	pGP704SacB-Δ*ompA,* Ap^r	This Study
pGP704sacB28	pGP704SacB-Δ*ompT,* Ap^r	This Study
pGP704sacB28	pGP704SacB-Δ*ompU,* Ap^r	This Study
pGP704sacB28	pGP704SacB-Δ*ompV,* Ap^r	This Study
pGP704sacB28	pGP704SacB-Δ*ompW,* Ap^r	This Study
pGP704sacB28	pGP704SacB-Δ*toxR,* Ap^r	This Study
pGP704sacB28	pGP704SacB-Δ*2519,* Ap^r	This Study
pGP704::Tn7	pTn7::*ompA,* Ap^r, Gm^r	This Study
pGP704::Tn7	pTn7::*ompT,* Ap^r, Gm^r	This Study
pGP704::Tn7	pTn7::*ompU,* Ap^r, Gm^r	This Study
pGP704::Tn7	pTn7::*ompV,* Ap^r, Gm^r	This Study
pGP704::Tn7	pTn7::*ompW,* Ap^r, Gm^r	This Study
pBAD myc-His A	pBAD myc-His A	Invitrogen
pBAD myc-His A	pBAD myc-His A_8Gly-1D4	This Study
pBAD myc-His A	pBAD myc-His A_*ompA*-8Gly-1D4	This Study
pBAD myc-His A	pBAD myc-His A_*ompT*-8Gly-1D4	This Study
pBAD myc-His A	pBAD myc-His A_*ompU*-8Gly-1D4	This Study
pBAD myc-His A	pBAD myc-His A_*ompV*-8Gly-1D4	This Study
pBAD myc-His A	pBAD myc-His A_*ompW*-8Gly-1D4	This Study
pGP704::Tn7	pTn7::*ompA_8Gly-1D4,* Ap^r, Gm^r	This Study
pGP704::Tn7	pTn7::*ompT_8Gly-1D4,* Ap^r, Gm^r	This Study
pGP704::Tn7	pTn7::*ompU_8Gly-1D4,* Ap^r, Gm^r	This Study
pGP704::Tn7	pTn7::*ompV_8Gly-1D4,* Ap^r, Gm^r	This Study
pGP704::Tn7	pTn7::*ompW_8Gly-1D4,* Ap^r, Gm^r	This Study

Table 2.4. Primers

Deletion	
VC2213_del_A	atccacgaagcttcccatggaggttttacatcgctcag
VC2213_del_B	aaataccatgtaatttacggtaatcatcaagattc
VC2213_del_C	ccgtaaattacatggtatttccttttttctttatgattattg
VC2213_del_D	actagagggtaccagagctcagcactgcatcac
VC1854_del_A	atccacgaagcttcccatggcaattgattttgtagattttgataac
VC1854_del_B	cgagatcttacaactctttgtttggtcac
VC1854_del_C	caaagagttgtaagatctcgaacacgtttattg
VC1854_del_D	actagagggtaccagagctccgacagattgccctttttc
VC0633_del_A	atccacgaagcttcccatggccagccacaaatcgcc
VC0633_del_B	caaatttatgtaattgttgacttcaggtcacacg
VC0633_del_C	tcaacaattacataaatttgatttttgtgcg
VC0633_del_D	actagagggtaccagagctcttggacaataaaaaatttccc
VC1318_del_A	ctagccatggtctgcatcgccatacacg
VC1318_del_B	aatgagcgattagagcgttgcctgcgat
VC1318_del_C	caacgctctaatcgctcattcacccatc
VC1318_del_D	ctattctagacgtgttgaaacaggacc
VCA0867_del_A	atccacgaagcttcccatggatttgtgccgcatagagag
VCA0867_del_B	aaacgtcatgtaacgccctatttcgaaaataaag
VCA0867_del_C	tagggcgttacatgacgttttccttttttg
VCA0867_del_D	actagagggtaccagagctccctctacttaactacggtc
Complementation	
VC2213_tn7_F	ggatccacgcgtcttaaggcagcactgcatcacgtgatc
VC2213_tn7_R	cccgacgggcccggtaccgcttattcagtaacttggtactggaattc
VC1854_tn7_F	ggatccacgcgtcttaaggccaattgattttgtagattttgataac
VC1854_tn7_R	cccgacgggcccggtaccgcttaccagtagatacgagc
VC0633_tn7_F	ggatccacgcgtcttaaggcttggacaataaaaaatttccc
VC0633_tn7_R	cccgacgggcccggtaccgcttagaagtcgtaacgtagac
VC1318_tn7_F	ggatccacgcgtcttaaggcattgaagcgagtaccgtc
VC1318_tn7_R	cccgacgggcccggtaccgcctagaagtggtaagcgac
VCA0867_tn7_F	ggatccacgcgtcttaaggccctctacttaactacggtc

VCA0867_tn7_R	cccgacgggcccggtaccgcttagaacttataaccacccg
Tagging	
pBADMycHisA-Gly(8)1D4 F	gagaccagccaagtggcgcctgcctaattcgaagcttgggcccga
pBADMycHisA-Gly(8)1D4 R	tgtacctccgccacctccgccacctcctcccatatggtaccagctgc
Lin-pBAD1D4MycHisA F	ggaggtggcggaggtggcg
Lin-pBAD1D4MycHisA R	tcccatatggtaccagctgcagatctcg
pBAD1D4MHA Seq F	ttttgggctaacaggaggaa
pBAD1D4MHA Seq R	atcttctctcatccgccaaa
pBAD1D4MHA_ompA_in F	gcagctggtaccatatgggaagcactgcatcacgtgatc
pBAD1D4MHA_ompA_in R	ccgccacctccgccacctccttcagtaacttggtactggaattc
pBAD1D4MHA_ompU_in F	gcagctggtaccatatgggattggacaataaaaaatttccc
pBAD1D4MHA_ompU_in R	ccgccacctccgccacctccgaagtcgtaacgtagacc
pBAD1D4MHA_ompW_in F	gcagctggtaccatatgggacctctacttaactacggtc
pBAD1D4MHA_ompW_in R	ccgccacctccgccacctccgaacttataaccacccgc
pBAD1D4MHA_ompT_in F	gcagctggtaccatatgggacaattgattttgtagattttgataactg
pBAD1D4MHA_ompT_in R	ccgccacctccgccacctccccagtagatacgagcacc
Tn7_ompA1D4_Insert F	ggatccacgcgtcttaaggcagcactgcatcacgtgatc
Tn7_ompU1D4_Insert F	ggatccacgcgtcttaaggcttggacaataaaaaatttcccaacatcc
Tn7_ompW1D4_Insert F	ggatccacgcgtcttaaggccctctacttaactacggtcactattaatgg
Tn7_ompT1D4_Insert F	ggatccacgcgtcttaaggccaattgattttgtagattttgataactgttgcg
Tn7_[X]1D4_Insert R	cccgacgggcccggtaccgcttaggcaggcgccacttg

Colony Biofilm Morphology Analysis

For analysis of corrugated colony morphology development, cultures grown overnight at 30ºC shaking (200 rpm) were serially diluted (10^{-1}-10^{-8}) with LB medium and 100 µl aliquots of the 10^{-8} dilution were plated onto 20 ml LB agar medium. Samples were then incubated at 30ºC for 120 hours before imaging.

Spot Biofilm Morphology Analysis

For analysis of corrugated colony morphology development, cultures grown overnight at 30ºC shaking (200 rpm), then 3 µl of diluted (1:200) culture were plated onto LB agar medium (20 ml). Samples were then incubated at 30ºC for 120 hours before imaging.

Pellicle Morphology, Stability, and Hydrophobicity

For analysis of pellicle morphology development, cultures grown overnight at 30ºC shaking (200 rpm), then 25 µl of overnight culture were added to 4.975 mL of LB media in either sterile 18mmx150mm test tubes or 24-well plate. Images were taken after 5 days of growth, at which time pellicles were either vortexed briefly at 1,000xg or removed from their culture and transplanted into a dish of deionized H_2O to assess hydrophobicity.

Microbial adhesion to hydrocarbon (MATH) test

For analysis of *V. cholerae* strain hydrophobicity, 2.5 ml of overnight culture was pelleted at 4,000xg at 4°C for 10 minutes and resuspended in 5 ml of 25 mM PBS

(5/2x PBS), this was repeated twice. Pellets were resuspended in 9 ml 25 mM PBS. Samples were adjusted to OD_{600} 0.6-0.7. 1.5 ml of culture suspension were mixed various volumes (0, 100, 200, 300, 400, 500 µl) of hexadecane in test tubes, then vortexed for 30 seconds at 2,500xg. OD_{600} of the aqueous phase was measured after 30 minutes of equilibration at room temperature. Adherence to hexadecane was determined as follows: $(OD_{600Final}/OD_{600Initial})x100$

Flow cells and confocal scanning laser microscopy (CSLM)

Cultures grown overnight at 30ºC shaking (200 rpm) were diluted to OD_{600} of 0.02 using 2% LB (0.2 g/liter tryptone, 0.1 g/liter yeast extract, 10 g/liter NaCl), and 150 µl aliquots were inoculated into flow cell chambers (Ibidi #80601). After inoculation, the chambers rested for 1 hour, with no flow, at room temperature to allow for initial cell attachment. Flow was resumed at a rate of 0.14 ml/min with chambers remaining at room temperature. Confocal images of biofilms that formed in flow cell chambers were captured with an LSM 5 PASCAL system (Zeiss) at 488-nm excitation. Three-dimensional images of the biofilms were reconstructed using Imaris software (Bitplane) and quantified using COMSTAT[142].

Western Blot Analysis

Biofilms were grown for 24 hours at 30ºC, as described above (Spot Biofilm Morphology Analysis) then harvested and resuspended in 400 µl protease inhibitor (Sigma S8820) water. When samples were sufficiently suspended, 100 µl of 10% SDS was added and samples were heated at 91ºC for 10 minutes. Protein

concentrations were determined using a bicinchoninic acid assay (Pierce). Before loading samples for SDS-polyacrylamide gel electrophoresis (SDS-PAGE), β-mercaptoethanol was added to a final concentration of 5% (vol/vol). 85 µg of protein was loaded into 12% SDS-PAGE, before protein was transferred to nitrocellulose membrane with a Mini Trans-Blot Cell (Bio-Rad) apparatus in transfer buffer containing 25 mM Tris (pH 8.3), 192 mM glycine, 20% (vol/vol) methanol, and 0.1% (wt/vol) SDS. The blot was blocked with 5% (wt/vol) milk and washed with PBS buffer containing 250 mM NaCl and 0.1% (vol/vol) Tween 20. Rabbit monoclonal antibody against the Myc epitope and mouse polyclonal antisera against *V. cholerae* RNA polymerase were used to detect RbmA-Myc and RnaP, respectively. RNA polymerase was used as a loading control. Horseradish peroxidase-conjugated goat anti-rabbit and anti-mouse secondary antibodies (Santa Cruz Biotechnology) were used at a dilution of 1:2,500. Immunoblots were developed with a SuperSignal West Pico chemiluminescent kit (Pierce). Immunoblot analyses were conducted using two biological replicates and two technical replicates.

VPS immunoblot assays

Isolation of purified VPS from *V. cholerae* strains and immunoblot analyses of the extracted VPS were carried out according to a protocol similar to those previously published (Enos-Berlage & McCarter, 2000; Fong & Yildiz, 2007; Yildiz & Schoolnik, 1999). Briefly, overnight-grown cultures on LB agar medium, overlaid with a sterile dialysis membrane, were harvested and resuspended in 10 mM Tris (pH 8.0). Normalization was carried out by adjusting each culture to within one OD_{600}

unit. Equal volumes of cultures were pipetted into 2 ml Eppendorf tubes and the suspension was mixed at 4ºC, constantly rotated for 5 hours. Crude VPS supernatant was separated from the bacterial cells and debris by centrifugation twice at 15,000x g for 30 min at 4ºC and the supernatant was precipitated with 3x volumes of 100% ethanol at -20ºC overnight. Crude VPS was pelleted twice by centrifugation at 15,000x g for 30 min at 4ºC, intermittently resuspended with 70% ethanol. Pellets were then air-dried and resuspended in 500 ml water. Purified VPS was isolated as described above with additional purification steps published previously (Fong & Yildiz, 2007). Briefly, crude VPS pellet was resuspended in nuclease buffer (40 mM Tris/HCl pH 8.0, 10 mM $MgCl_2$, 2 mM $CaCl_2$, 0.05% NaN_3). DNase I and RNase A were added to the VPS suspension at final concentrations of 2 units/ml and 0.25 units/ml, respectively, followed by incubation at 37ºC shaking for at least 3 hours. Proteinase K was then added at a final concentration of 2 mg/ml, and the suspension was further incubated shaking overnight at 37ºC. 1:1 Phenol/chloroform extractions were carried out in triplicate, followed by an overnight precipitation with 3x volumes of 100% ethanol at -20ºC. VPS was pelleted twice by centrifugation at 15,000xg for 30 min at 4ºC, intermittently resuspended with 70% ethanol. Pellets were then air-dried and resuspended in 100-200 µl water. Stored short-term at 4ºC or long-term at -20ºC. 3 µl of serial diluted purified VPS (1-1/32) was spotted onto nitrocellulose membranes and immunoblot analyses were carried out using anti-VPS antiserum and goat anti-rabbit horseradish-peroxidase-conjugated antibody. The immunoblots were developed with the SuperSignal West Pico chemiluminescent kit (Pierce) and

quantified using ImageQuant 5.2 software (Molecular Dynamics). VPS immunoblot analyses were carried out with two different biological replicates and at least two technical replicates. It should be noted that the VPS antibody used in this study is polyclonal, with undefined epitopes. VPS was quantified via densitometry through ImageJ.

Results

Outer membrane proteins impact *V. cholerae* biofilm morphology

The presence of outer membrane proteins within both the biofilm matrix and OMV proteomes prompted us to ask whether these proteins are involved in biofilm formation. We first generated strains lacking *ompA*, *ompT*, *ompU*, *ompV*, or *ompW* in the rugose genetic background, as this strain has enhanced matrix production and alterations in biofilm formation are reflected in colony corrugation patterns. We next examined how the loss of each OMP affected biofilm formation by measuring rugosity when bacteria were grown at an air-solid surface interface. This assessment was done in two ways: by examining the rugosity of single colony biofilms and spot biofilms resulting from growth of a diluted cell suspensions. We used both of these assays to assess biofilm formation as some of the phenotypes are apparent in either colony or spot biofilms.

Δ*ompA* was observed to have a decrease in corrugation in the single colony biofilm assay, with traditional rugose wrinkles being less pronounced, when compared to the

parent (Fig. 2.1). The absence of OmpA showed little to no phenotype in the spot biofilm (Fig. 2.2) Complementation of Δ*ompA* recovered rugose-like biofilm morphology. Δ*ompT* lost almost all traditional corrugation in the single colony assay, with the exception of the center of the colony, when compared to the parent (Fig. 2.1). The spot biofilm lacking OmpT showed a similar phenotype as the colony biofilm, in that the spot suffered from a decrease in defined corrugation (Fig. 2.2). The Δ*ompT* phenotype was recovered with complementation. Δ*ompU* was unusual in that it was the only strain to become more rugose in both of the assays. The colony biofilm was greater in diameter, when compared to the parent, and was more corrugated, displaying more defined and an increased number of ridges (Fig. 2.1). The Δ*ompU* spot biofilm similarly exhibited an increase in overall apparent matrix material compared to the rugose strain. The complementation of Δ*ompU* only partially recovered the phenotypes of Δ*ompU*, interestingly, the complement became less corrugated than the parent strain in both assays. Δ*ompV* also had a unique phenotype in that it retained corrugation, but the wrinkles lost definition, as if they were unable to maintain parent-like structure and rigidity (Fig. 2.1). The spot phenotype was less drastic, however in the absence of *ompV*, there still remained a loss in corrugation structure (Fig. 2.2). Complementation of the Δ*ompV* strain recovered to parent strain morphology. Δ*ompW*, similar to Δ*ompT*, lost corrugation at the periphery, while retaining moderate corrugation at the center (Fig. 2.1). The absence of OmpW showed little to no phenotype in the spot biofilm (Fig. 2.2). The Δ*ompW* phenotype is recovered with complementation in the colony biofilm.

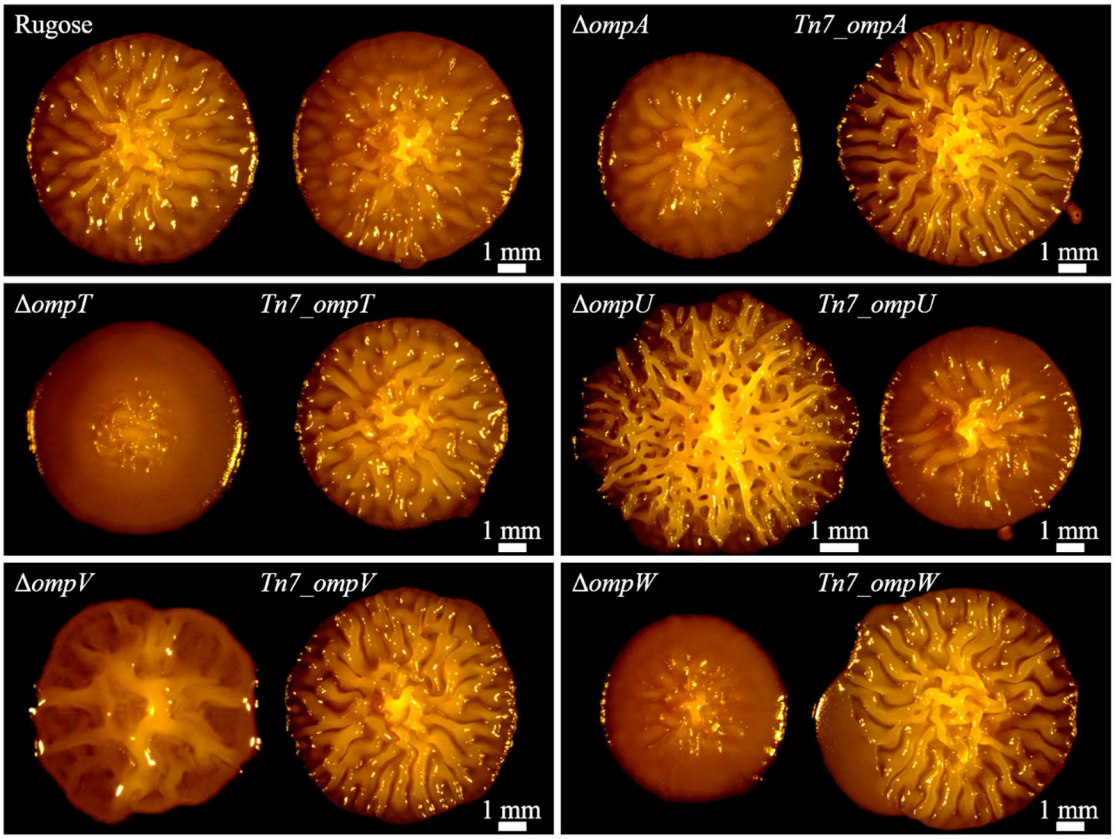
Rugose
1 mm
ΔompA
Tn7_ompA
1 mm
ΔompT
Tn7_ompT
1 mm
ΔompU
Tn7_ompU
1 mm
1 mm
ΔompV
Tn7_ompV
1 mm
ΔompW
Tn7_ompW
1 mm

Figure 2.1. Outer Membrane Proteins Participate in *V. cholerae* Colony Morphology Development at Solid-Air Interface. Biofilm morphologies, formed from single cells, of strains lacking and complemented for target outer membrane proteins. 100 µl of serially diluted overnight culture (final dilution of 10^{-9}) was plated on 20 ml LB agar plates. Biofilms were grown at 30°C and imaged after 120 hours. The experiment was repeated in two biological replicates and two technical replicates.

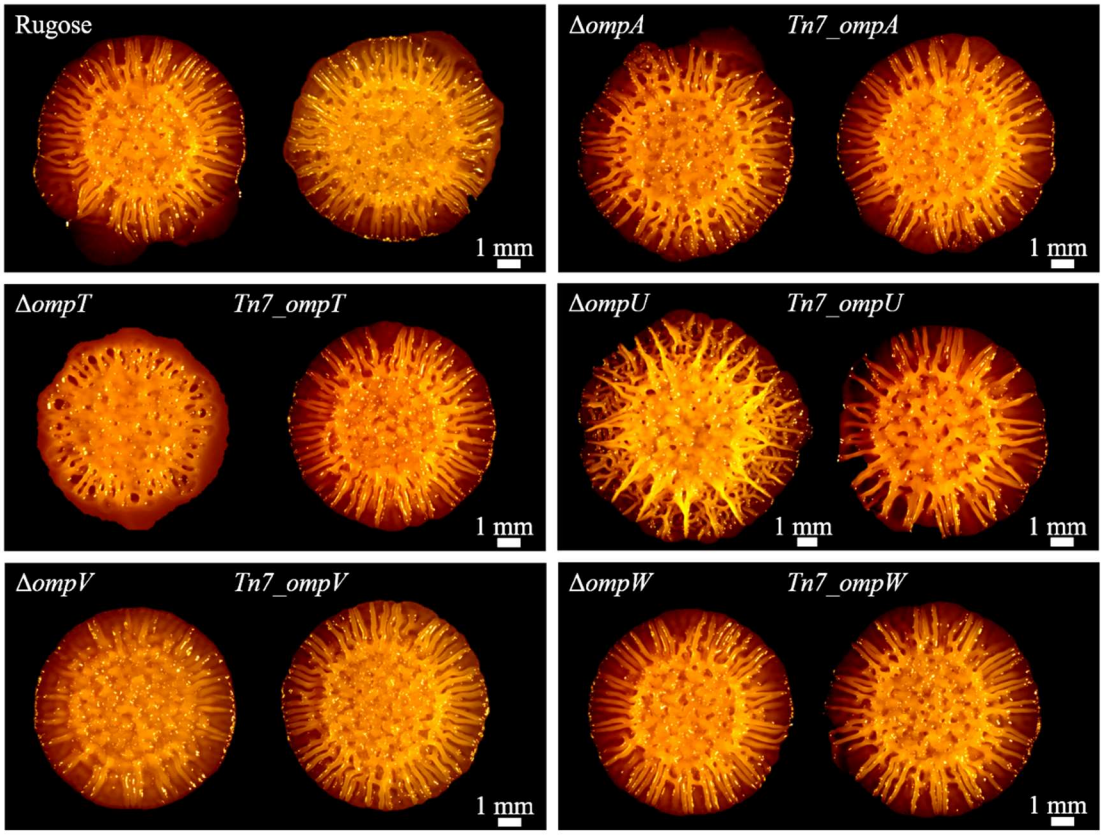
Rugose
1 mm
ΔompA
Tn7_ompA
1 mm
ΔompT
Tn7_ompT
1 mm
ΔompU
Tn7_ompU
1 mm
1 mm
ΔompV
Tn7_ompV
1 mm
ΔompW
Tn7_ompW
1 mm

Figure 2.2. Outer Membrane Proteins Contribute to the Development of *V. cholerae* Biofilm Structure at Solid-Air Interface. Biofilm morphologies, formed from dilute overnight cultures, of strains lacking and complemented for target outer membrane proteins. 3 µl of diluted overnight culture (1:200) was plated in triplicate on 20 ml LB agar plates. Biofilms were grown at 30°C and imaged after 120 hours. The experiment was repeated in two biological replicates and two technical replicates.

Regulation of outer membrane proteins impacts *V. cholerae* biofilm morphology

Having determined that outer membrane proteins influence biofilm morphology and that OmpT and OmpU are inversely regulated by ToxR[122, 131], we wanted to explore these relationships in the context of biofilm morphology. In summary of what is described above (Fig. 2.1. and 2.2), Δ*ompT* lost almost all corrugation in the single colony and spot assays, to varying degrees. Both the single colony and spot biofilms formed by Δ*ompU* were observed to be more rugose and larger in diameter, when compared to the parent morphologies. The biofilm formed by Δ*ompT*Δ*ompU* single colonies showed traits similar to those of both Δ*ompT* and Δ*ompU*, in that Δ*ompT*Δ*ompU* has an obvious increase in rugosity, when compared to the parent, but loses peripheral colony corrugation, similar to Δ*ompT*, but dissimilar to Δ*ompU* (Fig. 2.3). The spot biofilm formed by Δ*ompT*Δ*ompU* is strikingly similar to the spot biofilm formed by Δ*ompU* (Fig. 2.4). Similarly, biofilms formed by Δ*toxR*, in both assays, are similar to the single Δ*ompU* mutant biofilms. Δ*toxR* single colony biofilms are more corrugated and larger in diameter, when compared to the parent strain (Fig. 2.3). This phenotypic trend is also observed in the spot biofilm (Fig. 2.4), enhanced corrugation and diameter. However, the enhanced rugosity of Δ*toxR* is dissimilar to both Δ*ompU* and Δ*ompT*Δ*ompU*, with the wrinkles of Δ*toxR* being larger and in fewer number when compared to biofilms lacking OmpU. This suggests that there exists a balanced or additive role of outer membrane proteins in *V. cholerae* biofilm structure and formation, with the absence of an OMP having a different affect when compared to its decreased expression.

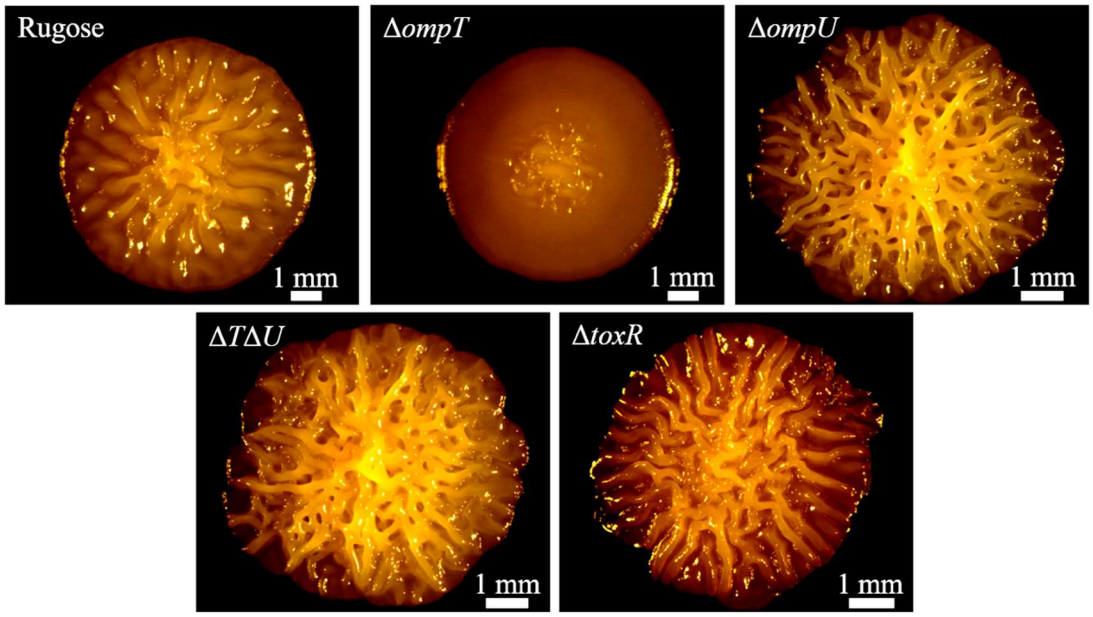
Rugose
1 mm
ΔompT
1 mm
ΔompU
1 mm
ΔTΔU
1 mm
ΔtoxR
1 mm

Figure 2.3. Regulation of Outer Membrane Proteins Participates in *V. cholerae* Colony Morphology Development at Solid-Air Interface. Biofilm morphologies, formed from single cells, of strains lacking and complemented for target outer membrane proteins. 100 µl of serially diluted overnight culture (final dilution of 10^{-9}) was plated on 20 ml LB agar plates. Biofilms were grown at 30°C and imaged after 120 hours. The experiment was repeated in two biological replicates and two technical replicates.

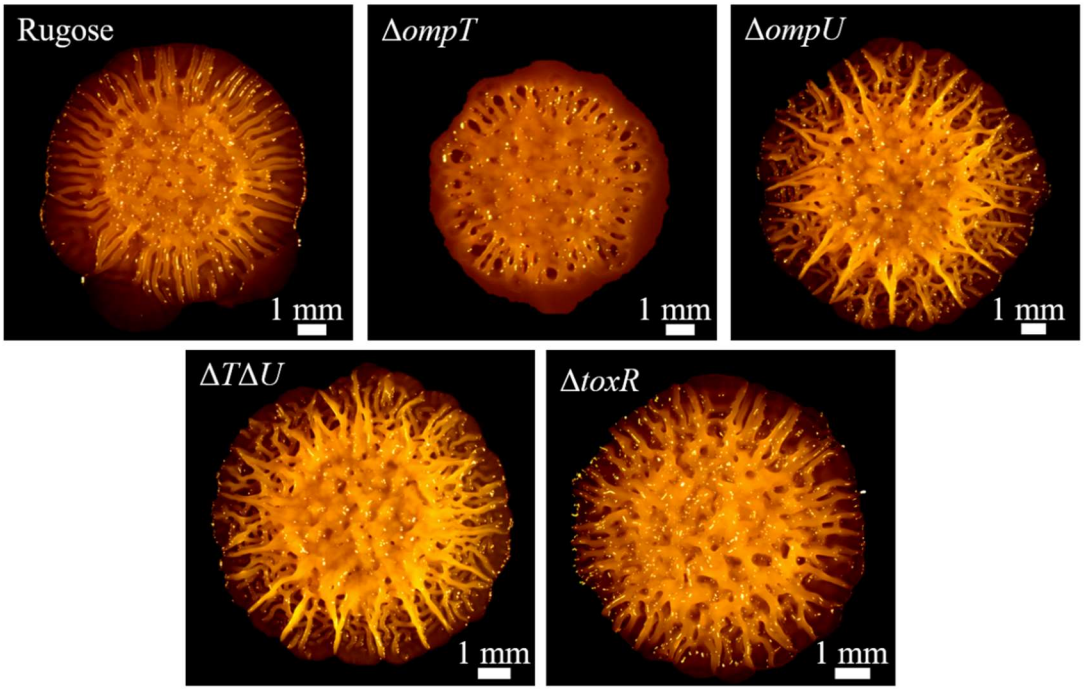
Rugose
1 mm
ΔompT
1 mm
ΔompU
1 mm
ΔTΔU
1 mm
ΔtoxR
1 mm

Figure 2.4. Regulation of Outer Membrane Proteins Contributes to the Development of *V. cholerae* Biofilm Structure at Solid-Air Interface. Biofilm morphologies, formed from dilute overnight culture, of strains lacking and complemented for target outer membrane proteins. 3 µl of diluted overnight culture (1:200) was plated in triplicate on 20 ml LB agar plates. Biofilms were grown at 30°C and imaged after 120 hours. The experiment was repeated in two biological replicates and two technical replicates.

Outer membrane proteins impact *Vibrio cholerae* pellicle biofilm formation

Previous work has established that our *V. cholerae* rugose variant forms a stable hydrophobic pellicle[56], a biofilm formed at a liquid-air interface. When cultures are grown statically, the parent rugose strain forms an evenly corrugated biofilm, a few millimeters tall (Fig. 2.5). This rugose pellicle breaks into a few pieces when disturbed but maintained connection to the vial, and when transferred to a dish of water, the sample spreads flat, indicative of a hydrophilic characteristic. Given this extensive information, we next compared our OMP mutants to the rugose parent using this pellicle assay. Δ*ompA* formed a similarly tall and stable pellicle, but had lost defined corrugation on the air-exposed surface (Fig. 2.5). The pellicle without OmpA was similarly as stable as the parent, breaking into a few pieces but retaining its connection to the test tube. There was no observable variation in the hydrophobicity of the sample. Δ*ompT* and Δ*ompV* formed pellicles very similar in height and corrugation to the parent, with the exception, perhaps, of the decreased corrugation within the vertical, wall-associated biofilm growth (Fig. 2.5). The pellicles broke into a few pieces when disturbed but maintained connection to the vial. Neither pellicle showed variation in hydrophobicity. Δ*ompW* showed an increase in "climbing", having formed a taller, but similarly corrugated biofilm, when compared to the parent (Fig. 2.5). Most notably, Δ*ompW* showed an increase in pellicle stability, remaining as one intact pellicle while retaining much of its connection to the sides of the vials. Overall, these data suggest that OMPs do not necessarily participate in biofilms formed at the liquid-air interface.

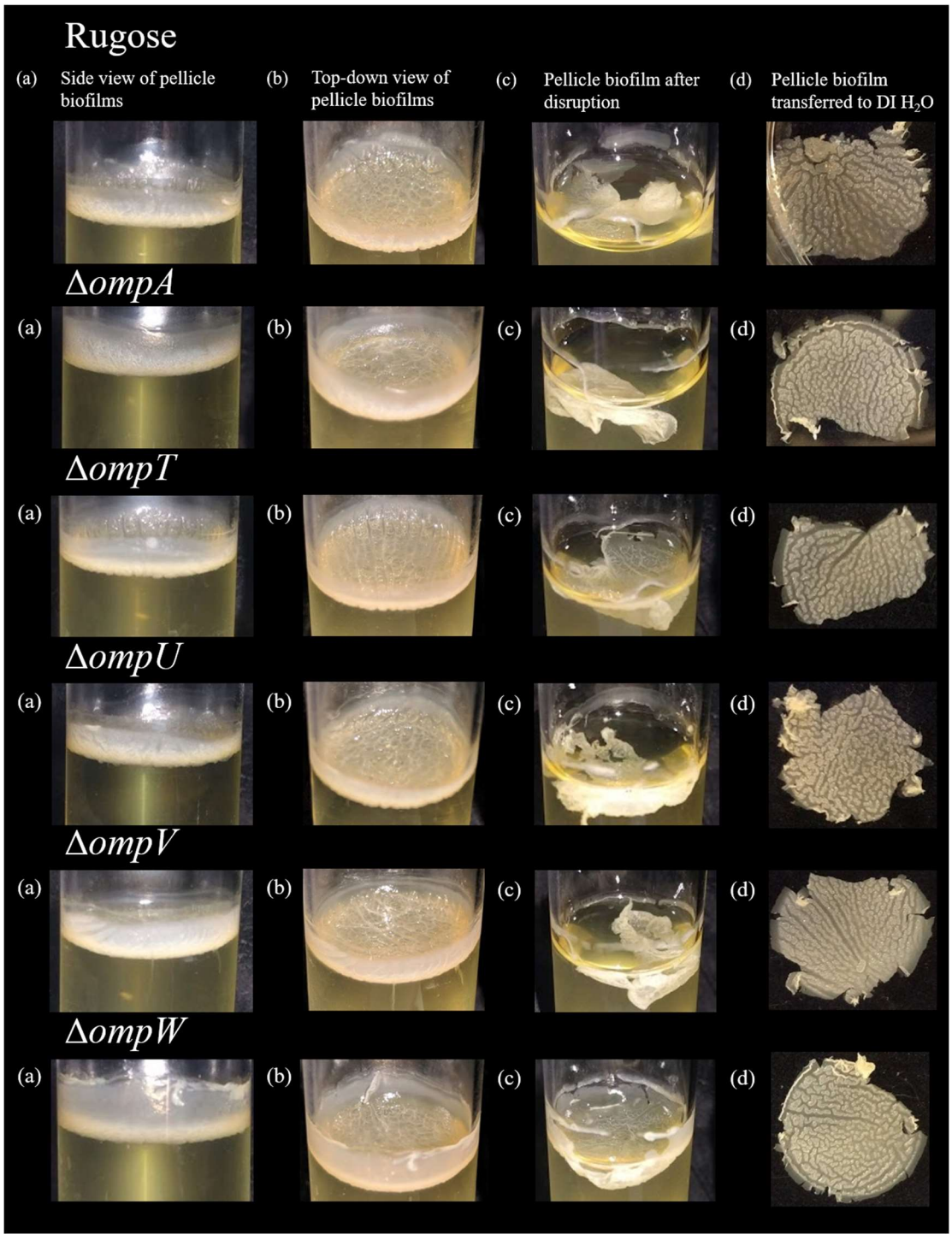
Rugose
(a) Side view of pellicle biofilms
(b) Top-down view of pellicle biofilms
(c) Pellicle biofilm after disruption
(d) Pellicle biofilm transferred to DI H_2O
ΔompA
(a)
(b)
(c)
(d)
ΔompT
(a)
(b)
(c)
(d)
ΔompU
(a)
(b)
(c)
(d)
ΔompV
(a)
(b)
(c)
(d)
ΔompW
(a)
(b)
(c)
(d)

Figure 2.5. Outer Membrane Proteins Participate in *V. cholerae* Pellicle Morphology and Stability. Overnight culture was added to either sterile 18 mm x 150 mm test tubes or a 24-well plate at a final dilution of 1:200. Images were taken after 5 days of growth (a, b), at which time pellicles were either vortex briefly at 1,000xg (c) or removed from their culture well and transplanted into a dish of deionized H_2O to assess pellicle hydrophobicity (d). Biofilms were grown at 30°C and imaged after 120 hours. The experiment was repeated in two biological replicates.

V. cholerae lacking outer membrane proteins are more hydrophilic

Previously, our lab has shown that changes in pellicle morphology can be attributed to variation in strain hydrophobicity, an observation based on the *bap1* mutant[143]. Bap1, one of the foundation matrix proteins, contributes to the hydrophobicity and mechanical stability of *V. cholerae* pellicle biofilms[143]. VPS, and over production thereof by rugose *V. cholerae*, also contributes to strain hydrophobicity[144]. So, we also examined the pellicle growth for variation in hydrophobicity between rugose parent and mutant pellicles. There was no observed change in the hydrophobicity of any of the pellicles when compared to the rugose parents (Fig. 2.5.d). Varied resilience of OMP mutant pellicles against "detachment by sheer" prompted us to further characterize strains. OMP mutant hydrophobicity/hydrophilicity was determined using microbial adhesion to hydrocarbon (MATH) test. Mutants showed increases in hydrophilicity, perhaps with the exception of Δ*ompV*, which showed rugose-like levels of adherence at lower volumes of hexadecane (Fig. 2.6). These observations suggest that some of the OMPs, as membrane accessories, influence hydrophobic character of the cellular outer membrane.

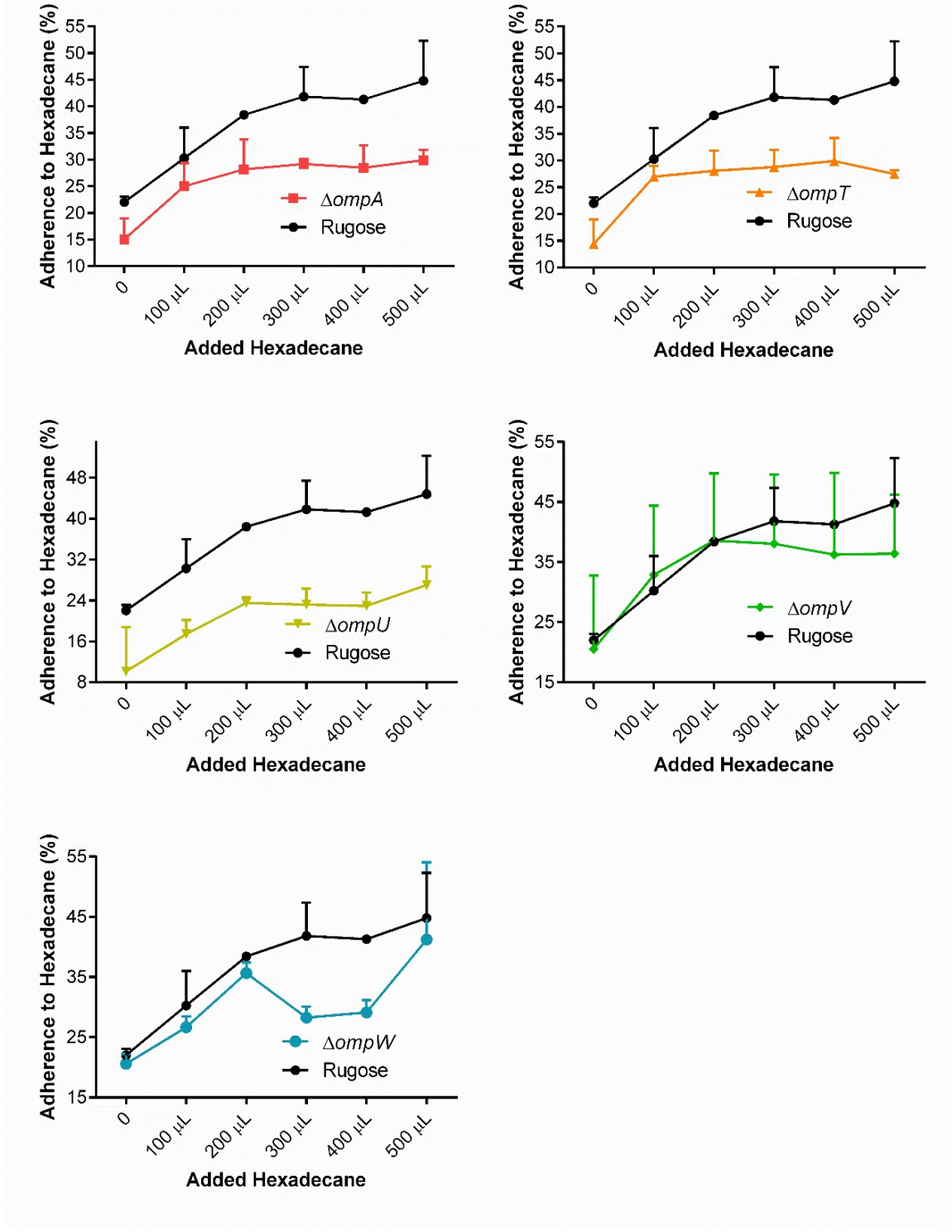
Adherence to Hexadecane (%)
55
50
45
40
35
30
25
20
15
10
ΔompA
Rugose
0
100 µL
200 µL
300 µL
400 µL
500 µL
Added Hexadecane
Adherence to Hexadecane (%)
55
50
45
40
35
30
25
20
15
10
ΔompT
Rugose
0
100 µL
200 µL
300 µL
400 µL
500 µL
Added Hexadecane
Adherence to Hexadecane (%)
48
40
32
24
16
8
ΔompU
Rugose
0
100 µL
200 µL
300 µL
400 µL
500 µL
Added Hexadecane
Adherence to Hexadecane (%)
55
45
35
25
15
ΔompV
Rugose
0
100 µL
200 µL
300 µL
400 µL
500 µL
Added Hexadecane
Adherence to Hexadecane (%)
55
45
35
25
15
ΔompW
Rugose
0
100 µL
200 µL
300 µL
400 µL
500 µL
Added Hexadecane

Figure 2.6. Absence of Outer Membrane Proteins Increase *V. cholerae* Hydrophilicity. 2.5 ml of overnight culture was pelleted and resuspended in 5 ml of 25 mM PBS (pH 7.4), this was repeated twice. Pellets were resuspended in 9 ml 25 mM PBS. Sample OD_{600} were adjusted to 0.6-0.7. 1.5 ml of culture suspension was mixed volumes (0, 100, 200, 300, 400, 500 uL) of hexadecane in test tubes. Solutions were vortexed. OD_{600} of the aqueous phase was measured after 30 minutes of solution equilibration at room temperature. Adherence to hexadecane (%) was determined as follows: $(OD_{600Final}/OD_{600Initial}) \times 100$

Absence of outer membrane proteins does not impact abundance of *Vibrio* polysaccharide or the RbmA matrix protein

Alteration in biofilm structure and function can be indicative of reorganization of matrix components. We then asked whether altered corrugation, in the absence of OMPs, could be the result of variation in the quantity of established matrix components. Matrix-associated VPS was quantified via immunoblotting for VPS isolates from each of the OMP deletion mutants. Quantification by densitometry showed no observable change in VPS in any of the mutant strains (Fig. 2.7). Signal in the whole-cell Δ*vps*-IΔ*vps*-II sample is believed to be from non-specific binding of the anti-VPS antiserum to LPS or other cell-associated carbohydrate molecules. Lack of variation in VPS detected between the parent and mutant strains suggests that VPS abundance is not responsible for observed morphology phenotypes. In addition to VPS, we also quantified RbmA in OMP-mutant biofilms. Total protein was harvested from colony biofilms grown at 30ºC for 24 hours, a time point chosen to minimize HapA-mediated RbmA proteolysis[37]. There was no observed variation in RbmA in these OMP mutants (Fig. 2.8), suggesting biofilm phenotypes are not the result of altered matrix protein levels. Bap1 and RbmC were unable to be quantified as they were below the detection limit, presumably due to HapA-dependent proteolysis. Overall, these results suggest that these OMPs neither affect biofilm VPS levels nor abundance of RbmA matrix protein.

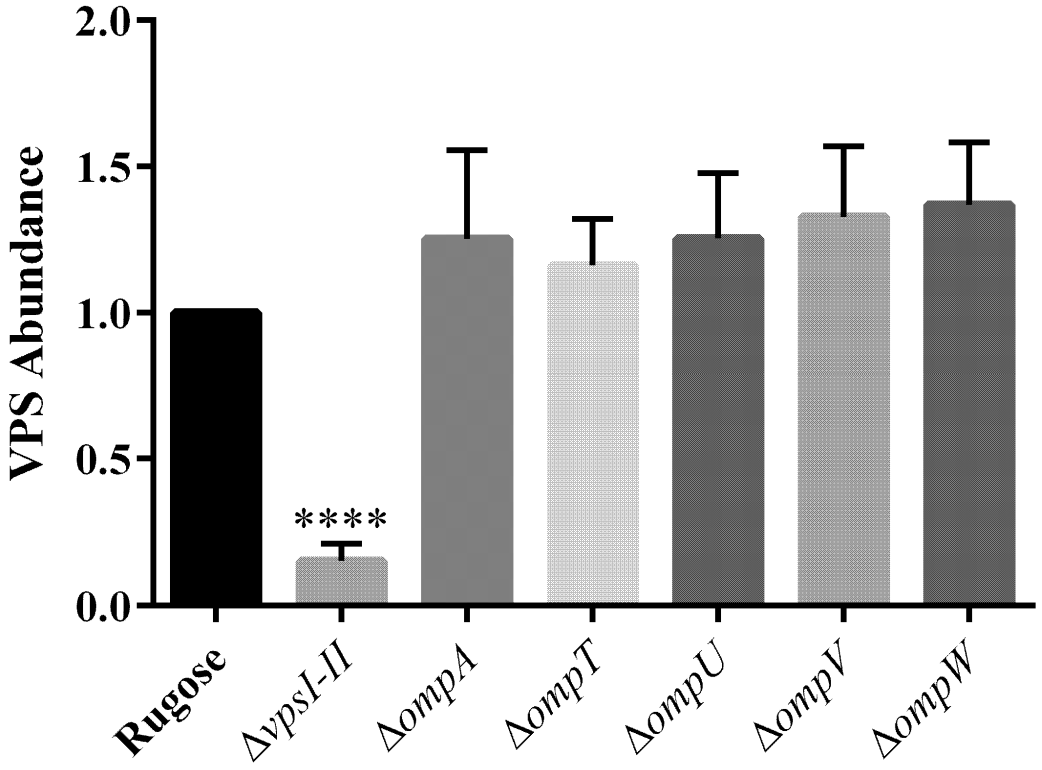
VPS Abundance
2.0
1.5
1.0
0.5
0.0
****
Rugose
ΔvpsI-II
ΔompA
ΔompT
ΔompU
ΔompV
ΔompW

Figure 2.7. Abundance of *Vibrio* Polysaccharide in *V. cholerae* Biofilms Lacking Outer Membrane Proteins. 100 µl of overnight culture was plated on 20 ml LB agar plates overlaid with a single layer of sterile dialysis tubing. Biofilms were grown at 30°C, harvested after 24 hours, and resuspended in 1xPBS. Cells were removed via centrifugation. VPS was purified via ethanol precipitations and phenol chloroform extractions. Abundance of VPS in purified samples was determined using immunostaining and subsequently quantified using ImageJ software. The experiment was repeated in two biological replicates and two technical replicates. Presented values are the mean of these four trials.

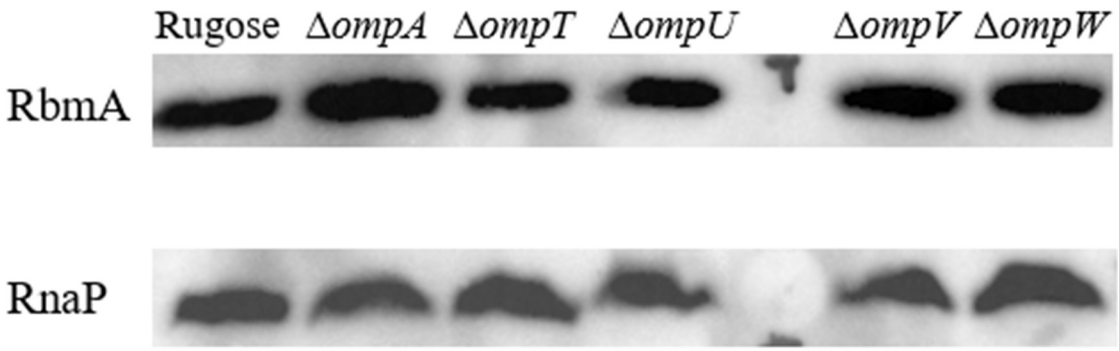
Rugose
ΔompA
ΔompT
ΔompU
ΔompV
ΔompW
RbmA
RnaP

Figure 2.8. Abundance of the RbmA Matrix Protein in *V. cholerae* Biofilms Lacking Outer Membrane Proteins. 5 µl of diluted overnight culture (1:200) was plated in triplicate on 20 ml LB agar plates Biofilms were grown at 30°C, harvested after 24 hours, and resuspended in sterile H_2O. Samples were boiled after the addition of 10% SDS, to a final concentration of 2% SDS. RbmA was analyzed via immunostaining. RnaP is used as a sample loading control. The experiment was repeated in two biological replicates and two technical replicates.

Conclusion

Overall, we can conclude that OMPs and their regulation do, in fact, play a role in *V. cholerae* biofilm architecture. Absence of each of the OMPs influenced development and mature morphology both air-solid and sir-liquid interface biofilms. Additionally, OMPs increase *V. cholerae* cell hydrophobicity, to an unknown purpose, suggesting a larger role in defining the character of the outer membrane. The role of these OMPs, however, does not influence abundance of VPS or RbmA. Traditionally, the functions of outer membrane proteins are considered to be passage of water, small hydrophilic molecules, and nutrients through the conserved β-barrel structure[145], while also facilitating secretion of a number of macromolecules, like LPS[146], matrix components[147], proteins[148], and self-peptide chains[149]. Additional canonical functions of OMPs include protein hydrolysis[150] and virulence[151]. This and other recent studies have worked to establish roles for OMPs in biofilms. While we have yet to establish a mechanism for OMP participation in *V. cholerae* biofilms we hypothesize that OMPs possess a larger interactome than what is currently established, giving OMPs the potential to alter interaction and localization of critical biofilm components. We will continue to explore a number of possibilities, including outer membrane protein-protein interaction, production of outer membrane vesicles, and localization of biofilm components within the matrix.

CHAPTER 3: Outer Membrane Vesicles are Present and Participate in *Vibrio cholerae* Biofilm

William Garvey & Fitnat H. Yildiz

Introduction

Outer membrane vesicles (OMVs) are composed of lipids, lipopolysaccharides, and proteins[70]. OMVs are observed to be released constitutively from Gram negative bacterial outer membranes during the growth cycle[70]. Production mechanisms include: maintenance of outer membrane leaflet asymmetry by the Yrb/VacJ ABC system[73, 74, 75]; peptide linkages between the outer membrane and cell wall (YnhG[76], YcbB[76], NlpA[77], OmpA[76]), endopeptidase (MepA, DacB, PbpG[78]), and lipoprotein (Lpp[76]) regulators of covalent crosslinking of the cell wall to the outer membrane[50, 51]; accumulation of peptidoglycan fragments[76] and toxic-misfolded proteins[81] in the periplasm; accumulation of quorum sensing and signaling molecules in the outer leaflet[82, 83, 84]. OMVs possess lipopolysaccharides on their exterior and during production, are filled with periplasmic content, including proteins and nucleic acid polymers[39], from their progenitor cells. OMVs have been observed to perform a number of functions in *V. cholerae*, including transport of virulence factors[96], trafficking of functional proteins[54], and acting as bacteriophage decoys, increasing *V. cholerae* resistance to phage[97]. More than 50% of biofilm lipid composition has been identified to be OMV-associate[152], suggesting OMVs have a role in the function and structure of biofilm formation. Many investigators have speculated that the charged lipopolysaccharides of OMVs may facilitate interaction with eDNA, which acts as a scaffold for additional extracellular polysaccharides, resulting in a more robust biofilm[71, 153]. A study in *H. pylori* showed that addition of OMVs to liquid culture prompted biofilm formation, establishing OMVs as a nucleation point for biofilm

formation[154]. OMVs have yet to be identified to play a role, or even observed, in *V. cholerae* biofilms. However, the observation that OMV-associated OmpT associates with Bap1[54], could suggest a greater role for OMVs in *V. cholerae* biofilm architecture. In this study we investigate the role of outer membrane vesicles in *V. cholerae* biofilm formation and structure. We found that, not only do OMVs exist in *V. cholerae* biofilm, but that they play a distinct role in matrix formation and morphology.

Materials and Methods

Bacterial strains, plasmids, and culture conditions

Bacterial strains and plasmids used in this study are listed in Table 2.2. *Escherichia coli* CC118λpir, DH5αλpir, and *E. coli* SM10λpir were used for DNA and plasmid construction and manipulation. *E. coli* S17λpir was used for conjugation with *V. cholerae*. *E. coli* and *V. cholerae* strains were grown aerobically at 30°C and 37°C, respectively. Cultures were grown in Luria-Bertani (LB) broth (1% Tryptone, 0.5% Yeast Extract, 1% NaCl), pH 7.5. Strain colonies were grown on LB agar medium, containing 1.5% (wt/vol) granulated agar. Antibiotics were used at the following concentration: ampicillin 100 μg/ml; rifampicin 100 μg/ml; gentamicin 50 μg/ml; polymyxin B 12.5 μg/ml.

Scanning Electron Microscopy

100 µl from overnight grown cultures, 30ºC shaking (200 rpm), were spread onto 20 ml LB plates (+/- 12.5 µg/ml) overlaid with a sterile dialysis membrane (FisherBrand #21-152), using a sterile cell spreader. Samples were grown over 24 hours at 30ºC. Sterile forceps were used to place sterile 12mm diameter cover slips (Chemglass #CLS-1760-012) on the bacterial lawn. Slides were gently pressed onto the sample, then slides were lifted and placed into a dish containing 2.5% glutaraldehyde for 1 hour at room temperature. Samples were then transferred, sequentially, into dishes containing 30%, 50%, 70%, and 90% ethanol. Samples were stored in 100% ethanol at room temperature until imaging.

OMV Isolation

Cultures grown overnight at 30ºC shaking (200 rpm) were diluted to OD_{600} 0.1 and 500 µl were spread on 50 ml 150 mm x 15 mm LB agar medium plates, overlaid with sterile dialysis membrane, using a sterile spreader. Samples were grown at 30°C for 24 hours before biofilm was harvested and resuspended in 0.9% (wt/vol) NaCl. Normalization of samples were carried out by adjusting each sample to within one OD_{600} unit. Equal volumes of samples were transferred to new conical tubes and constantly rotated, at 4°C, for 1 hour. Crude extracellular matrix was separated from cells and debris by centrifugation twice at 10,000xg for 30 mins at 4°C. Supernatant was filtered through 0.45 µm membranes. Crude OMVs were pelleted via centrifugation at 150,000xg for 3 hours at 4°C. Pellets were resuspended in 50 mM HEPES (11.9 g/L) buffer (pH 6.8). Samples were adjusted to 45% Optiprep and fractionated using an Optiprep density gradient of the following percentages: 10%,

15%, 20%, 25%, 30%, and 35%. Samples were fractionated at 292,700xg for 3 hours at 4°C. Aliquots of equal volume were removed sequentially from the gradient and analyzed via SYPRO protein staining and immunostaining. OMV-positive fractions were pooled and separated from Optiprep via centrifugation at 200,000xg for 3 hours at 4°C. OMV pellets were resuspended in DPBS (10 mM Na_2HPO_4, 1.8 mM KH_2PO_4, 137 mM NaCl, 2.7 mM KCl).

Isolation of Extracellular Matrix

Cultures grown overnight at 30ºC shaking (200 rpm) were diluted to OD_{600} 0.1 and 500 µl were spread on 20 ml LB agar medium plates, overlaid with sterile dialysis membrane, using a sterile spreader. Samples were grown at 30°C for 24 hours before biofilms were harvested and resuspended in PBS (pH 7.4) containing EDTA-free protease inhibitor (Sigma S8830). Normalization of samples was carried out by adjusting each sample to within one OD_{600} unit. Equal volumes of samples were transferred to new conical tubes and constantly rotated, at 4°C, for 1 hour. Crude extracellular matrix was separated from cells and debris by centrifugation twice at 10,000xg for 30 mins at 4°C. Supernatant was filtered through 0.45 µm membranes. Samples were transferred to Eppendorf Safe-Lock Natural tubes (#022363352). Bovine serum albumin solution and sodium deoxycholate were added to each sample to final concentrations of 35 µg/ml and 0.02% respectively. Samples were vortexed to mix and incubated on ice for 1 hour. Trichloroacetic acid was added to each sample to a final concentration of 12.5%. Samples were vortexed to mix and incubated overnight, shaking, at 4°C. Samples were centrifuged at 21,130 xg for 1 hour at 4°C.

Supernatant was discarded and resulting pellets were resuspended in 1.5 ml of ice-cold acetone. Samples were centrifuged at 21,130 xg for 1 hour at 4°C. Supernatant was discarded and resulting pellets were allowed to dry in the fume hood for about 10 minutes. Samples were resuspended in 400 µl of 5% SDS/protease inhibitor cocktail/50 mM triethylammonium bicarbonate. Resuspended samples were boiled at 100°C for 45 mins, vortexing intermittently, ensuring the entirety of the sample is resuspended. Protein content was determined by BCA and 100-150 µg/µl aliquots were flash frozen in liquid nitrogen. Samples were stored at -80°C until shipment to the UC Davis Proteomics Core Center.

OMV Quantification

Aliquots of OMV samples were adjusted to a final protein concentration of between 0.08 and 0.32 µg/µl and a volume of 193.4 µl. 6.6 µl of 100 µg/ml FM4-64 lipophilic dye (Thermo Fisher Scientific #T-13320) was added to each 193.4 µl sample, to a final concentration of 3.3 µg/ml. Samples were loaded in triplicate into black walled 96-well plates (#3904). Plates were incubated for 10 minutes at 37°C. Sample fluorescence was measured via Perkin Elmer Victor X3 plate reader protocol. Mean sample values were adjusted for background fluorescence.

Analysis of Polymyxin B Sensitivity

A 50 ml culture was inoculated 1:200 from overnight grown cells at 30ºC shaking (200 rpm), polymyxin B was added to a final concentration of 12.5 µg/ml and cultures were again grown at 30ºC shaking (200 rpm). 1.5 ml aliquots were taken

hourly and used to measure OD_{600} and generate serial dilutions for colony forming unit (CFU) enumeration. Aliquots for serial dilutions were vortexed with glass beads for 30 seconds at 2,500xg before each subsequent dilution. Each dilution was vortexed at 2,500xg for an additional 15 seconds before plating. CFU/ml was determined after 24 hours of growth at 30ºC.

Static Biofilms formed at Solid-Liquid Interface

Cultures grown overnight at 30ºC shaking (200 rpm) were diluted (1:200) using LB. 1 ml aliquots were inoculated into dual well chambers (Ibidi #80287). After inoculation, the static biofilms were grown for 1, 2, and 6 hours, respectively, at 30ºC. A sterile spatula was used to remove pellicles formed at liquid-air interface. Remaining LB was removed from the chambers and biofilms were washed in triplicate with PBS (pH 7.4). Confocal images of biofilms that formed in flow cell chambers were captured with an LSM 5 PASCAL system (Zeiss) at 488-nm excitation. Three-dimensional images of the biofilms were reconstructed using Imaris software (Bitplane) and quantified using COMSTAT[142].

OMV-Biofilm Supplementation

A BSA protein quantification assay was used to determine protein content of the rugose parent (R) and Δ*rbmA*Δ*bap1*Δ*rbmC*Δ*vps-I*Δ*vps-II* (ΔABCΔ*VPSI-II*) OMV samples. 55 µg of *V. cholerae* OMVs were added to 1:200 dilutions of R and ΔABCΔ*VPSI-II* cultures. OMV supplemented samples were grown alongside R and ΔABC cultures supplemented with volumes of DPBS equal to that of the volume of

OMV sample added. Samples were grown as colony biofilms, on 20 mL LB agar plates, and pellicle biofilms, formed in 2 mL of LB media. Samples were grown, consistently at 30ºC, and imaged at 120 hours.

Results

Observation of outer membrane vesicles in *V. cholerae* biofilms

Vibrio cholerae is known to produce OMVs, with a number of functions in planktonic culture, however, OMVs have yet to be observed in biofilms. Our electron micrographs (Fig. 3.1) reveal, for the first time, the presence of OMVs in *V. cholerae* biofilm.

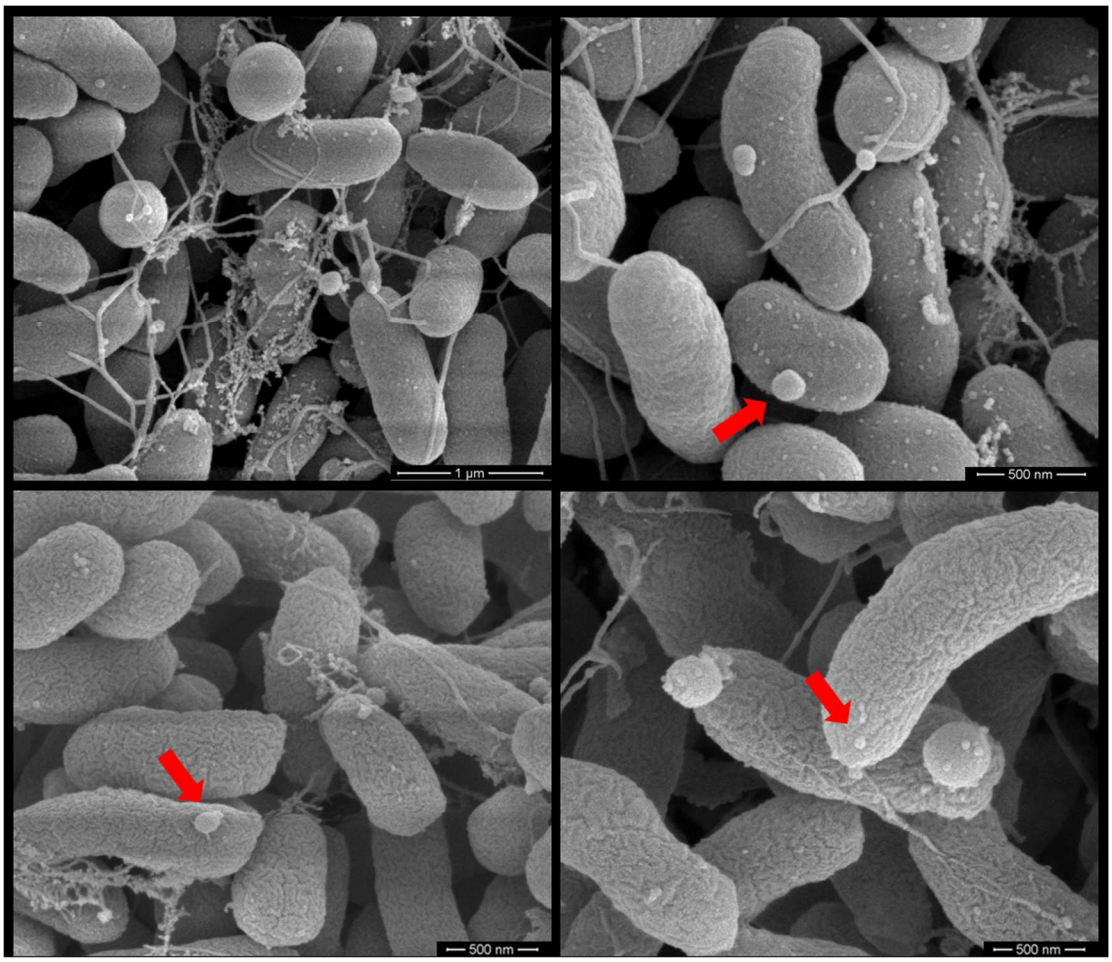
1 µm
500 nm
500 nm
500 nm

Figure 3.1. Observation of Outer Membrane Vesicles in *V. cholerae* Biofilms via Scanning Electron Microscopy. 100 µl of overnight culture was plated on 20 ml LB agar plates previously covered with a single layer of sterile dialysis membrane. Biofilms were grown at 30°C and samples were prepared after 24 hours. Sterile glass coverslips were pressed into the biofilm. Retrieved samples were fixed with 2.5% glutaraldehyde and serially dehydrated with increasing concentrations of ethanol. Red arrows indicate OMVs. The experiment was repeated in two biological replicates, images on the right are from one trial and images on the left from the other.

Outer membrane vesicles can be purified from *Vibrio cholerae* biofilms

Having identified OMVs in *V. cholerae* biofilms, we then wanted to further characterize their abundance, protein content, and effect on biofilm formation via a number of assays. We started by isolating OMVs from biofilm samples. Previous work has determined that ultracentrifugation of OMV samples are contaminated with extracellular components such as flagella[155]. So, I optimized a method for isolating clean OMVs from *V. cholerae* biofilm. Briefly, this method involves ultracentrifugation followed by density gradient separation and analysis of protein content in different fractions to identify OMV-positive samples without contaminants. Firstly, density fractions are run on a protein gel to determine successful fractionation by density gradient (Fig. 3.2.a). Next, fraction content was observed via immunostaining for known OMV and extracellular content (Fig. 3.2.b and c). OmpU is a known component of OMVs[106] and FlaA is the primary contaminant of concern in OMV preparations[155], therefore, each component is used as the marker for its respective fractions. Finally, purity of OMV samples was determined and confirmed via scanning electron microscopy (Fig. 3.3). Scanning electron micrographs reveal OMVs of varying size, while confirming purity of OMV samples.

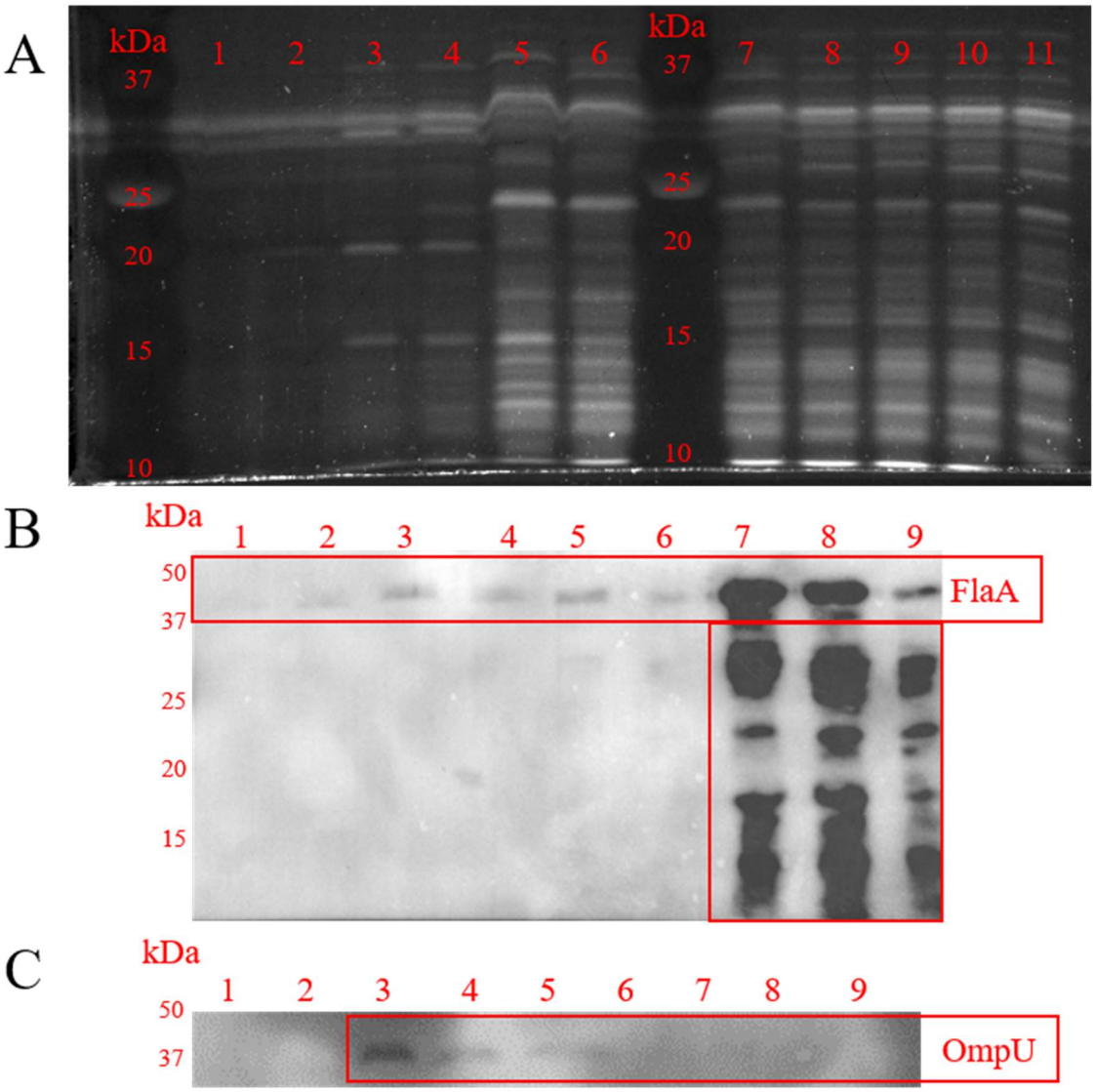
A
kDa
37
25
20
15
10
1
2
3
4
5
6
kDa
37
25
20
15
10
7
8
9
10
11
B
kDa
50
37
25
20
15
1
2
3
4
5
6
7
8
9
FlaA
C
kDa
50
37
1
2
3
4
5
6
7
8
9
OmpU

Figure 3.2. Sequential Assessment of Purity of Outer Membrane Vesicles Isolated from *V. cholerae* Biofilms. After isolation of crude OMVs from biofilms, samples were applied to a density gradient. Resulting fractions are assessed via SYPRO protein gel to determine separation of solution content (A). Fractions are also subject to immunostaining to determine OMV and non-OMV containing fractions, OmpU and FlaA, respectively (B, C). OMV positive fractions are pooled and centrifuged to concentrate samples.

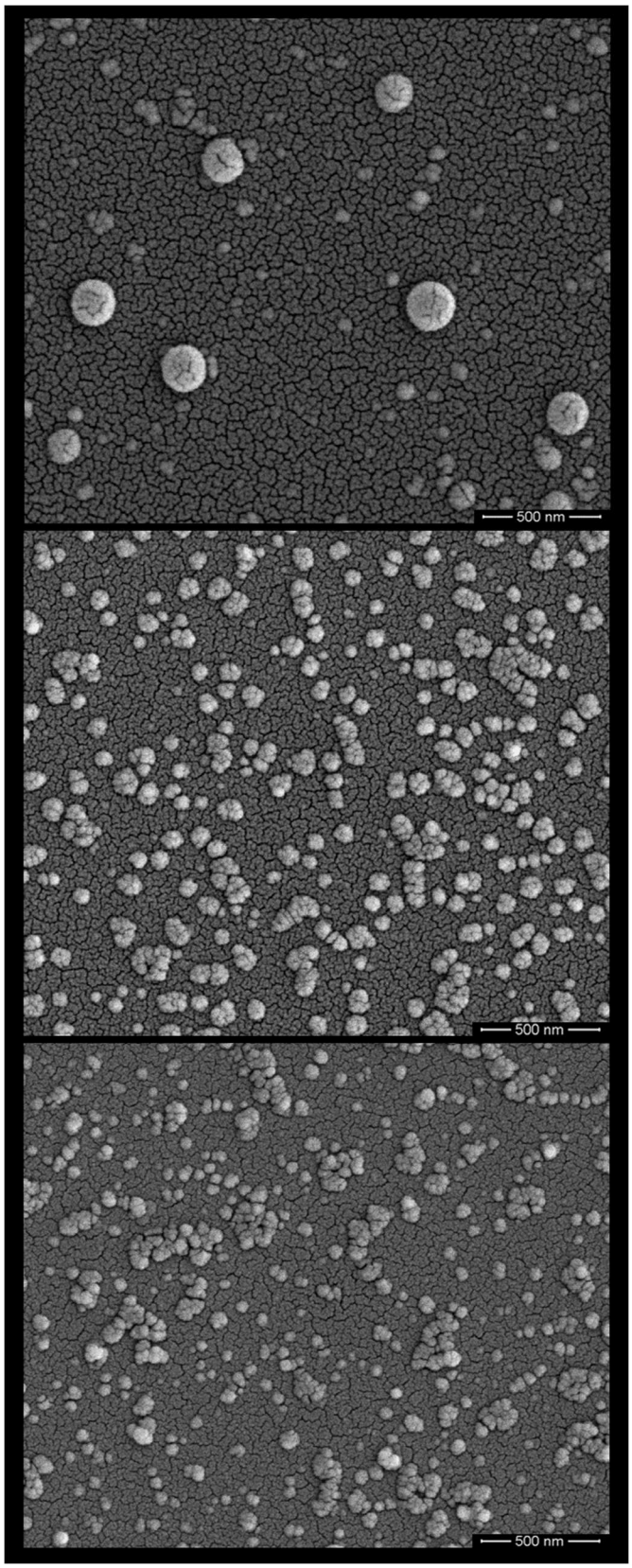
500 nm
500 nm
500 nm

Figure 3.3. Confirmation of OMV Sample Purity by Scanning Electron Microscopy. OMV samples were fixed with 2.5% glutaraldehyde and serially dehydrated with increasing concentrations of ethanol. The experiment was repeated in multiple (n=2) biological replicates, images presented are representative of isolated trials.

Comparison of outer membrane vesicle and biofilm matrix proteomes

Having established that OMVs are both present in and can be successfully isolated from *V. cholerae* biofilms we sought to characterize the role of OMVs in biofilm formation. We wanted to understand the extent to which OMVs contribute to the extracellular proteome of the *V. cholerae* biofilm. This was done by proteomic analysis of extracellular matrix and isolated OMVs such that we could establish two respective proteomes, determine enrichment and overlap of the OMV-associated proteins with the whole matrix proteome.

.

Variation in *V. cholerae* outer membrane and extracellular matrix composition effects abundance of outer membrane vesicles in biofilms

To further characterize biofilm-associated OMVs we wanted to understand if and how the composition of the outer membrane and extracellular matrix can affect abundance of OMVs. The method I adapted for our system utilizes the fluorescent FM4-64 lipophilic dye to quantify abundance of OMVs by sample lipid content. We do not observe a variation in the abundance of OMVs in biofilms produced by Δ*ompT*, Δ*ompT*Δ*ompU*, Δ*ompV*, Δ*ompW*, Δ*toxR* (Fig. 3.4). There is a small but statistically significant increase in abundance of OMVs in biofilm lacking OmpA (Fig. 3.4). Increased OMV production in the absence of OmpA has been observed in a number of bacteria and is believed to be the result of decreased cell-wall and outer membrane linkage[156]. Abundance of OMVs isolated from biofilms lacking OmpU showed a significant increase when compared to the parent (Fig. 3.4). Variation in abundance of biofilm-associated OMVs in the absence of OmpU, similar to its increased corrugated morphology (Fig. 2.2), distinguishes this mutant from the other OMP mutants. Overall, this suggests that manipulation of OMVs is a possible mechanism for OmpU participation in biofilm formation and architecture. However, the absence of increased abundance of OMVs in the Δ*ompT*Δ*ompU* and Δ*toxR* strains suggests, again, that OMP participation in biofilm formation is influenced by the role of other OMPs.

Additionally, we examined the abundance of OMV in biofilms formed in either an enhanced presence or absence of certain matrix components. There was no significant

change in abundance of OMVs isolated from biofilms formed by either Δ*hapA*, which results in increased accumulation of the three matrix proteins, or Δ*VPSI-II*, biofilms lacking the *Vibrio* polysaccharide, aside from a consistently decreased trend (Fig. 3.5). In the absence of matrix proteins RbmA, Bap1, and RbmC and the *Vibrio* polysaccharide, however, we observed an increase in OMV abundance when compared to the parent (Fig. 3.5). This data suggests a connection between the abundance of the *V. cholerae* matrix proteins and VPS and either the production or stability of biofilm-associated OMVs.

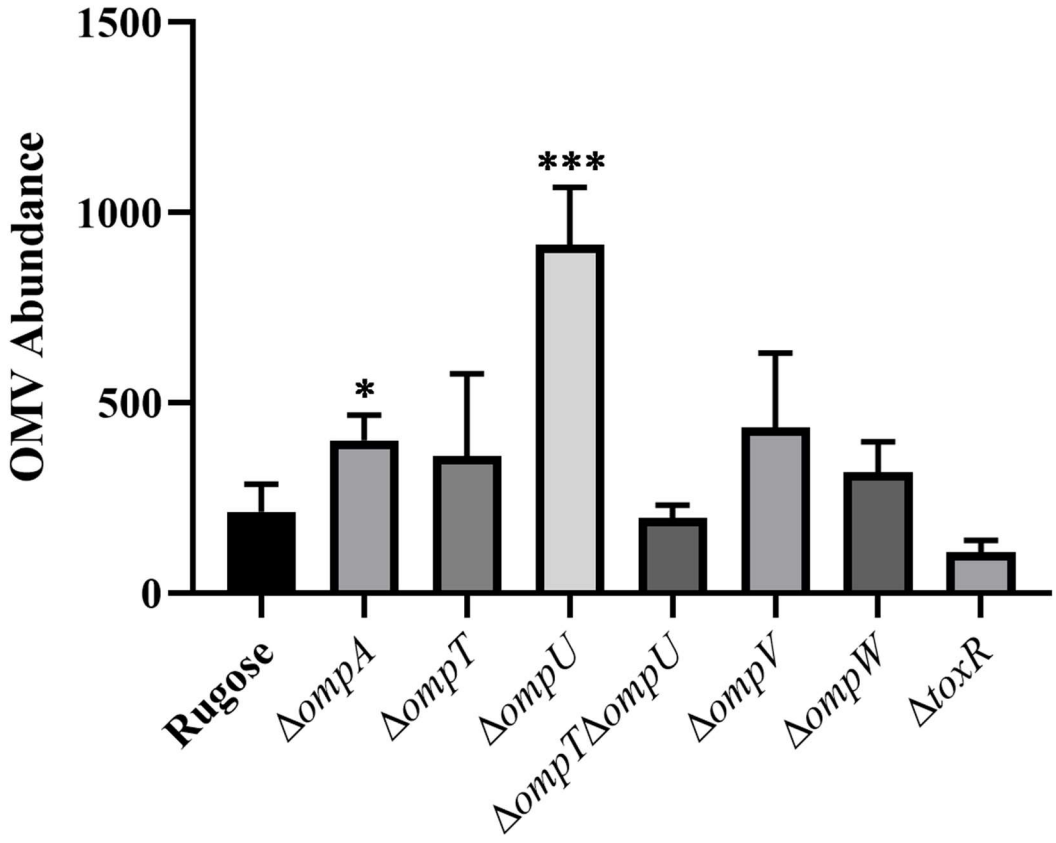
OMV Abundance
1500
1000
500
0
*
***
Rugose
ΔompA
ΔompT
ΔompU
ΔompTΔompU
ΔompV
ΔompW
ΔtoxR

Figure 3.4. Abundance of Outer Membrane Vesicles in Biofilms Lacking Outer Membrane Proteins or an Outer Membrane Protein Regulator. OMVs were isolated as previously discussed. Aliquots of OMV samples were adjusted to protein content 0.2 µg/µl in a final volume of 193.4 µl. 6.6 µl of 100 µg/ml FM4-64 dye was added to each sample. Sample were allowed to incubate at 37°C for 10 mins. Fluorescence was measured in triplicate per sample, then normalized to the rugose value. The experiment was repeated in two biological replicates.

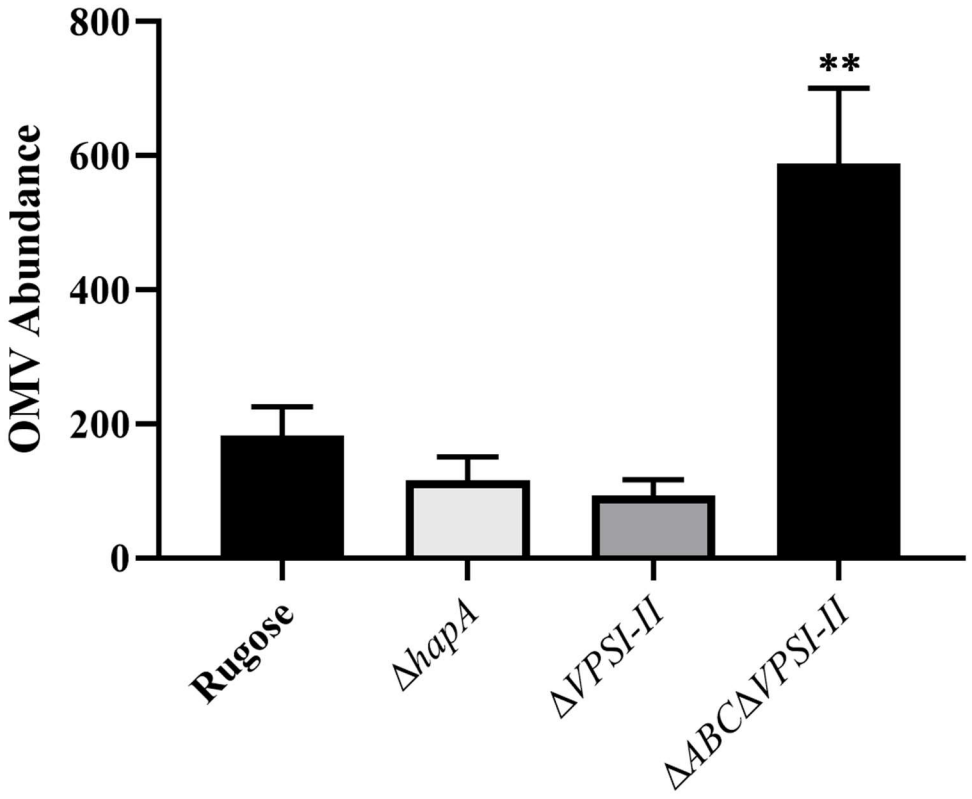
800
600
400
200
0
OMV Abundance
**
Rugose
ΔhapA
ΔVPSI-II
ΔABCΔVPSI-II

Figure 3.5. Abundance of Outer Membrane Vesicles in Biofilms Lacking or Enhanced for Matrix Components. OMVs were isolated as previously discussed. Aliquots of OMV samples were adjusted to protein content 0.2 µg/µl in a final volume of 193.4 µl. 6.6 µl of 100 µg/ml FM4-64 dye was added to each sample. Sample were allowed to incubate at 37°C for 10 mins. Fluorescence was measured in triplicate per sample, then normalized to the rugose value. The experiment was repeated in two biological replicates.

Variation in *V. cholerae* outer membrane and extracellular matrix composition effects abundance of *Vibrio* polysaccharide in biofilm-associated outer membrane vesicles

Having established that the absence of certain OMPs and matrix components can influence the abundance of OMVs in *V. cholerae* biofilm, we next turned to determine if the absence of OMPs or matrix components influences composition of OMVs. Abundance of VPS in OMV samples was quantified via immunoblotting and subsequent quantification by densitometry. Mean values of VPS were normalized to abundance of lipid content in respective OMV samples, such that abundance of VPS is representative of VPS signal per OMVs. OMVs isolated from biofilms lacking OmpT alone and OmpT and OmpU showed a slight, but non-significant, decrease in VPS abundance (Fig. 3.6). OMVs isolated in the absence of OmpV and OmpW show a decrease in abundance of VPS in OMV samples (Fig. 3.6). OmpA and OmpU stand apart from the other OMP mutants, OMVs isolated from Δ*ompA* and Δ*ompU* showed a significant decrease in VPS content when compared to OMVs isolated from rugose parent biofilm (Fig. 3.6). This variation may be, in part, a result of an increase in OMV abundance without an associated increase in VPS abundance, however, in the absence of HapA, which did not show an increase in OMV production (Fig. 3.5), we observe a decrease in abundance of OMV-associated VPS (Fig. 3.7). Together, this suggests that there may be an alternative mechanism for the decrease in OMV-associated VPS in the absence of OmpA and OmpU. Additionally, we observe a significant increase in OMV-associated VPS in the absence of ToxR (Fig. 3.6). The

relationship between OmpT, OmpU, ToxR-mediated expression, OMVs, and OMV cargo needs to be further explored to fully understand the system.

Not only is this the first example of VPS associating with OMVs, but we have also established that composition of OMVs affects relative association of OMV and biofilm components.

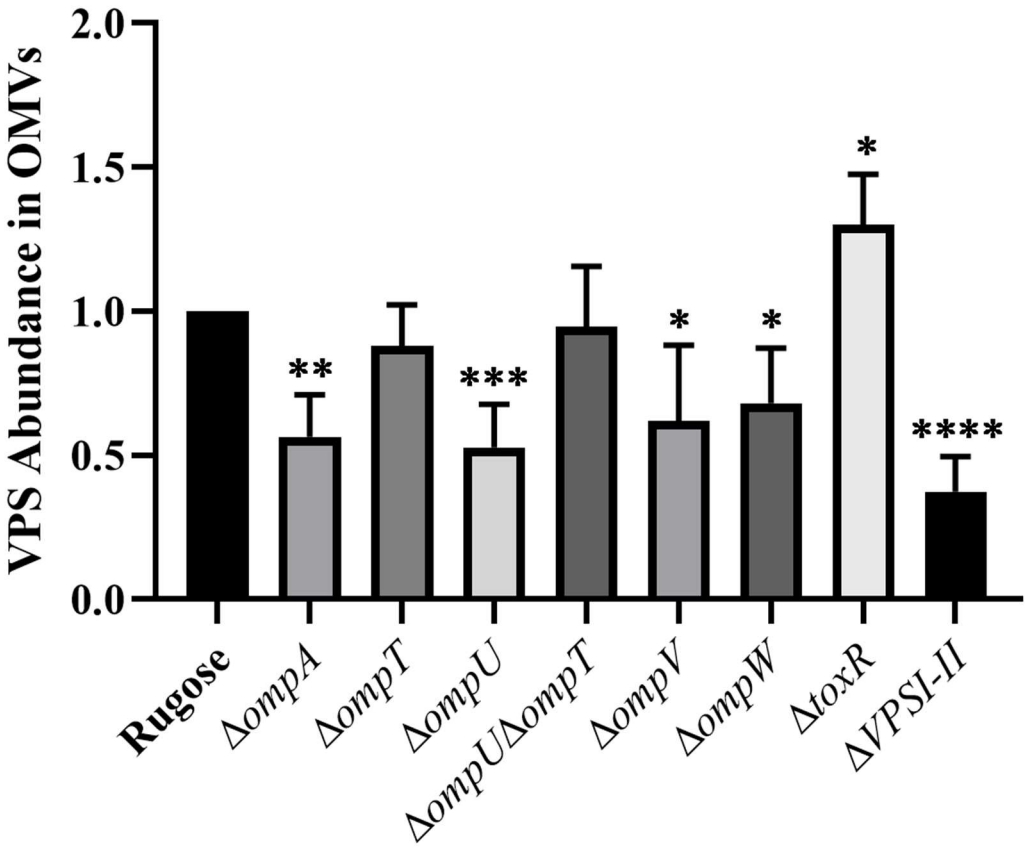
VPS Abundance in OMVs
2.0
1.5
1.0
0.5
0.0
**
***
*
*
*
****
Rugose
ΔompA
ΔompT
ΔompU
ΔompUΔompT
ΔompV
ΔompW
ΔtoxR
ΔVPSI-II

Figure 3.6. Abundance of *Vibrio* Polysaccharide in Outer Membrane Vesicles Isolated from Biofilms Lacking Outer Membrane Proteins or an Outer Membrane Protein Regulator. OMVs were isolated as previously discussed. Abundance of VPS in purified samples was determined using immunostaining and subsequently quantified using ImageJ software. The experiment was repeated in two biological replicates and two technical replicates. Presented values are the mean of these four trials.

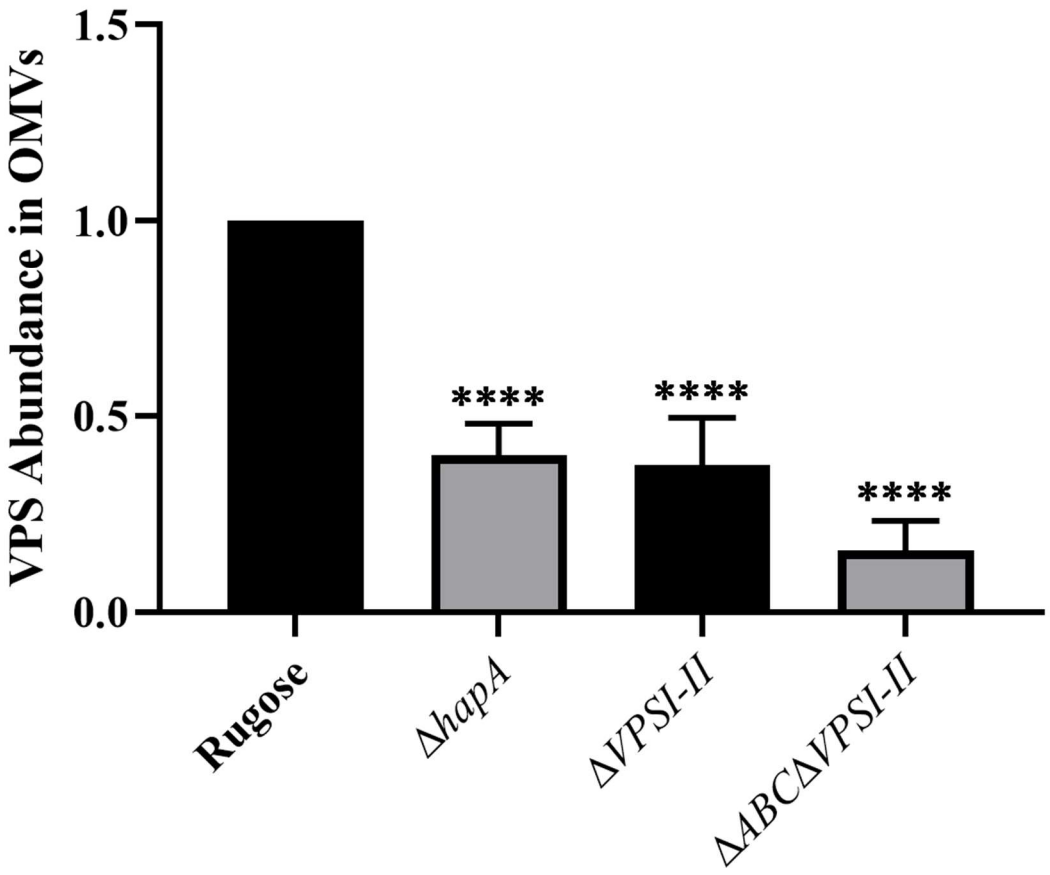
VPS Abundance in OMVs
1.5
1.0
0.5
0.0
****
****
****
Rugose
ΔhapA
ΔVPSI-II
ΔABCΔVPSI-II

Figure 3.7. Abundance of *Vibrio* Polysaccharide in Outer Membrane Vesicles Isolated from Biofilms Lacking or Enhanced for Matrix Components. OMVs were isolated as previously discussed. Abundance of VPS in purified samples was determined using immunostaining and subsequently quantified using ImageJ software. The experiment was repeated in two biological replicates and two technical replicates. Presented values are the mean of these four trials.

Variation in *V. cholerae* outer membrane and extracellular matrix composition effects abundance of matrix proteins in biofilm-associated outer membrane vesicles

In addition to VPS, we also looked at relative abundance of RbmA, as a representative of the matrix proteins, in OMVs isolated from biofilms lacking OMPs and matrix components. We observe a slight increase in abundance of a RbmA cleavage product, about 15.5 - 16 kilodaltons (kDa) in size, in OMVs isolated from Δ*ompW* and Δ*ompT* biofilms (Fig. 3.8). There is an increased abundance of a RbmA cleavage product, about 19 kDa in size, associated with Δ*ompV* OMVs (Fig. 3.8). RbmA could not be detected in OMVs from Δ*vpsI-II*, ΔABCΔ*vpsI-II*, or the Δ*hapA*Δ*prtV*Δ*vesB* triple protease deletion strain biofilms (Fig. 3.8). In the absence of OmpU, we observe a drastic increase in OMV-associated RbmA products. Additionally, the absence of OmpT and OmpU appears to have an additive effect on the increased abundance of OMV-associated RbmA products, apparent in the Δ*ompT*Δ*ompU* mutant (Fig. 3.8). Similar to previous observations, the absence of ToxR appears to result in a Δ*ompT* and Δ*ompU* intermediate phenotype, showing an increased abundance of RbmA, when compared to Δ*ompT*, but a decreased abundance, when compared to Δ*ompU*. ΔBCΔ*ompU* was run to see if the absence of Bap1 and RbmC could affect association of RbmA products with the Δ*ompU* OMVs. Abundance of RbmA in OMVs isolated from ΔBCΔ*ompU* biofilm is decreased when compared to the Δ*ompU* and *ΔompTΔompU* strains, however, more work needs to be done to characterize this interaction. Another conclusion we can make, from this data,

is that full length RbmA protein does not associate with OMVs, only differently sized cleavage products are seen.

The Bap1 matrix protein was successfully visualized in the triple protease deletion background at 75 kDa (Fig.3.8). OMVs isolated from Δ*ompT*, Δ*ompU*, and Δ*ompT*Δ*ompU* are observed to contain variable Bap1 degradation products of about 40 and 45 kDa size. In contrast to RbmA, it appears that full length Bap1 protein can associate with OMVs.

Overall, these results suggest that outer membrane protein profile can affect relative abundance of OMV-associated matrix proteins.

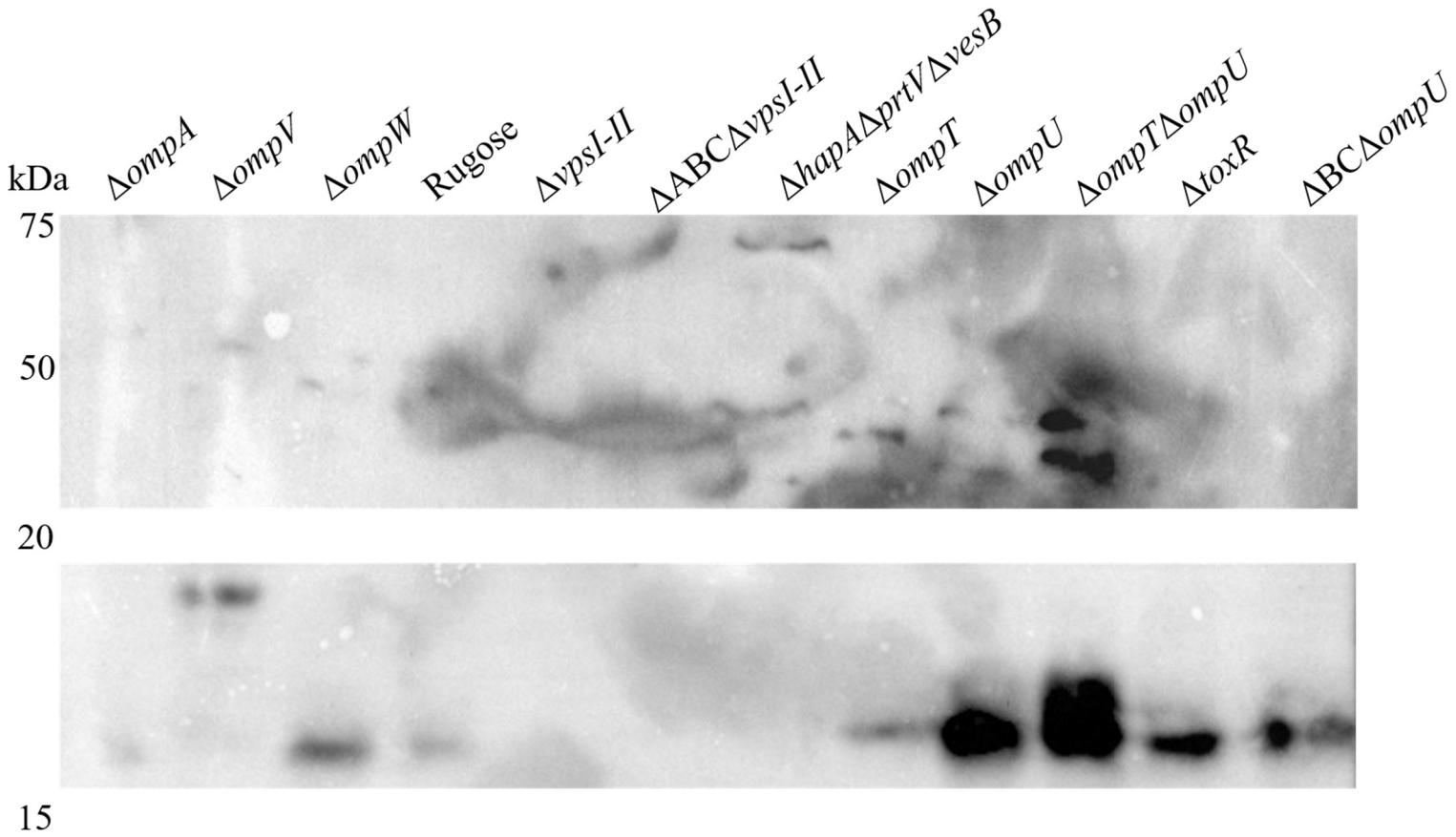
kDa
ΔompA
ΔompV
ΔompW
Rugose
ΔvpsI-II
ΔABCΔvpsI-II
ΔhapAΔprtVΔvesB
ΔompT
ΔompU
ΔompTΔompU
ΔtoxR
ΔBCΔompU
75
50
20
15

Figure 3.8. Abundance of *V. cholerae* RbmA and Bap1 in Outer Membrane Vesicles Isolated from Biofilms Lacking or Enhanced for Matrix Components or Outer Membrane Proteins. OMVs were isolated as previously discussed. RbmA, represented on the bottommost image, and Bap1, represented on the uppermost image, were analyzed via immunostaining. The experiment was repeated in two biological replicates and two technical replicates.

Increased presence of outer membrane vesicles, via genetic modification, affects *V. cholerae* biofilm morphology

To determine whether increased production of OMVs alters biofilm architecture, we first generated strains with altered ability to produce OMVs. The Yrb/VacJ ABC system is a highly conserved, Gram-negative phospholipid transport system which transfers phospholipids from the outer to the inner membrane in order to maintain membrane asymmetry[73, 74]. Previously, it was shown that disruption of this system results in an increase in OMV production in *H. influenzae*, *V. cholerae*, and *E. coli*[75]. Here, I generated a *V. cholerae* strain lacking the Yrb/VacJ system permease (YrbE/VC2519). Earlier studies showed that this mutation results in the accumulation of phospholipids in the outer membrane/periplasmic space without compromising outer membrane integrity[75], in an effort to synthesize a hypervesiculating stain of *V. cholerae*. First, we quantified abundance of OMVs isolated from Δ*yrbE* biofilms. We observed a significant increase in abundance of OMVs when compared to the rugose parent strain (Fig. 3.9). Biofilms produced by the Δ*yrbE* strain are larger and more corrugated, when compared to the parent strain (Figs. 3.10. and 3.11). Additionally, I observed an increased abundance of OMVs in SEM micrographs of Δ*yrbE* biofilms, when compared to the parent strain (Fig. 3.12). OMVs isolated from Δ*yrbE* showed a significant decrease in VPS content when compared to OMVs isolated from rugose parent biofilm (Fig. 3.13). This variation may be, in part, a result of an increase in OMV abundance without an associated increase in VPS abundance. From this data, we confirm that the *yrbE* deletion does significantly increase OMV production and

said OMV production affects biofilm formation. This strongly suggests a role for OMVs in *V. cholerae* biofilm formation.

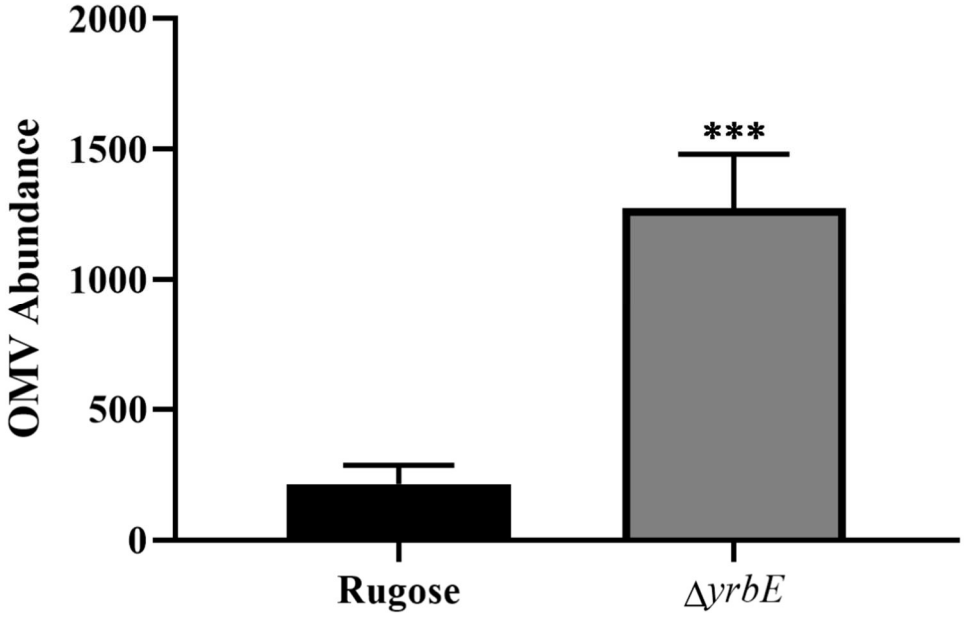
2000
1500
1000
500
0
OMV Abundance
***
Rugose
ΔyrbE

Figure 3.9. Abundance of Outer Membrane Vesicles in Biofilms Lacking YrbE. OMVs were isolated as previously discussed. Aliquots of OMV samples were adjusted to protein content 0.2 µg/µl in a final volume of 193.4 µl. 6.6 µl of 100 µg/ml FM4-64 dye was added to each sample. Sample were allowed to incubate at 37°C for 10 mins. Fluorescence was measured in triplicate per sample, then normalized to the rugose value. The experiment was repeated in two biological replicates.

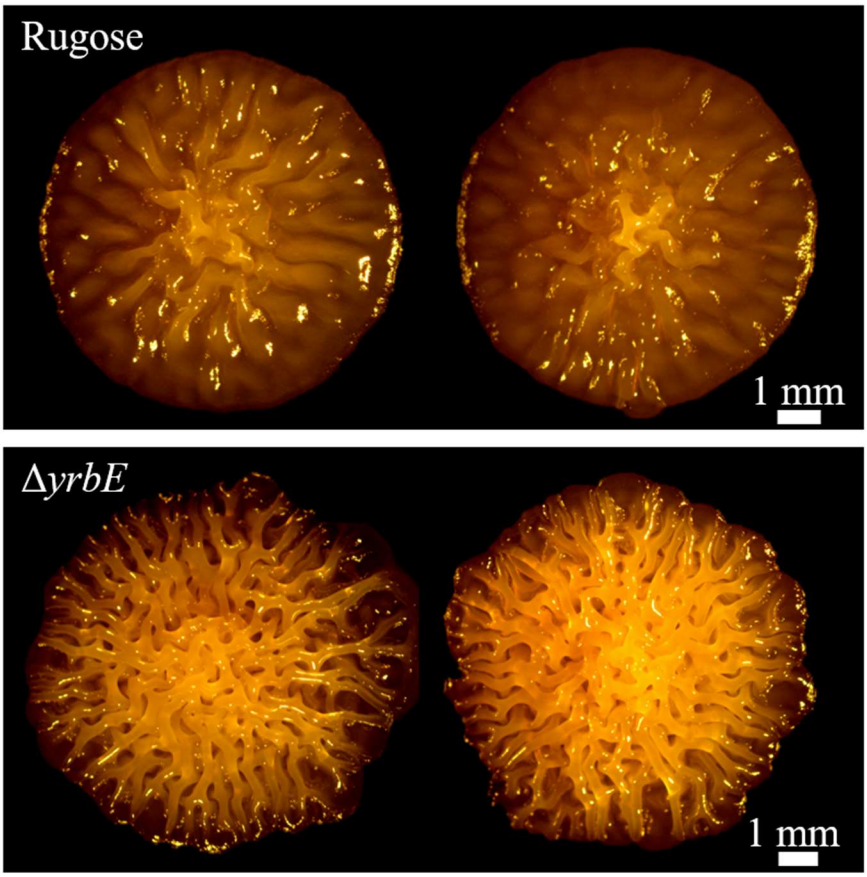
Rugose
1 mm
ΔyrbE
1 mm

Figure 3.10. Outer Membrane Vesicles Participate in *V. cholerae* Colony Biofilms. Biofilm morphologies of strains lacking the YreB permease. 100 µl of serially diluted overnight culture (final dilution of 10^{-9}) was plated on 20 ml LB agar plates. Biofilms were grown at 30°C and imaged after 120 hours. The experiment was repeated in two biological replicates. The experiment was repeated in two biological replicates, images on the right are from one trial and images on the left from the other.

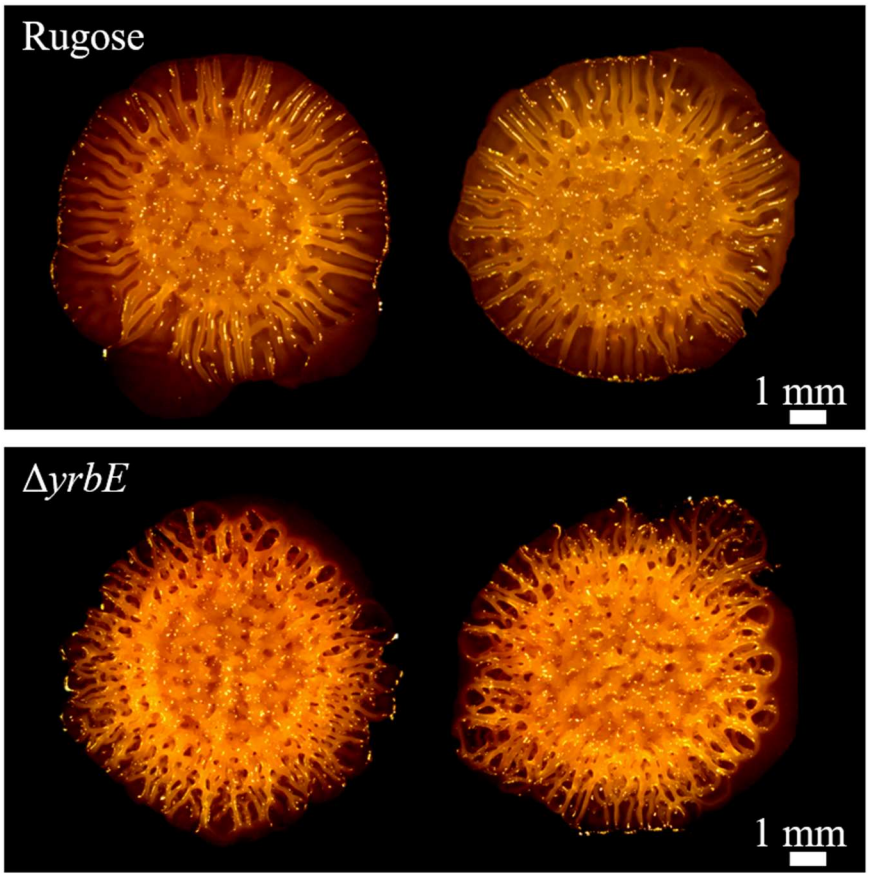
Rugose
1 mm
ΔyrbE
1 mm

Figure 3.11. Outer Membrane Vesicles Participate in *V. cholerae* Spot Biofilms Formed at Air-Solid Interface. Biofilm morphologies of strains lacking the YreB permease. 3 µl of diluted overnight culture (1:200) was plated in triplicate on 20 ml LB agar plates. Biofilms were grown at 30°C and imaged after 120 hours. The experiment was repeated in two biological replicates. The experiment was repeated in two biological replicates, images on the right are from one trial and images on the left from the other.

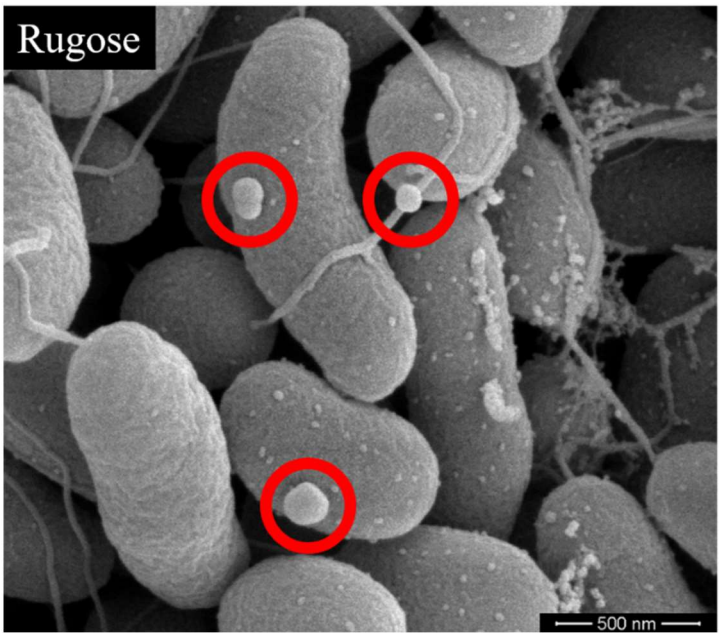
Rugose
500 nm

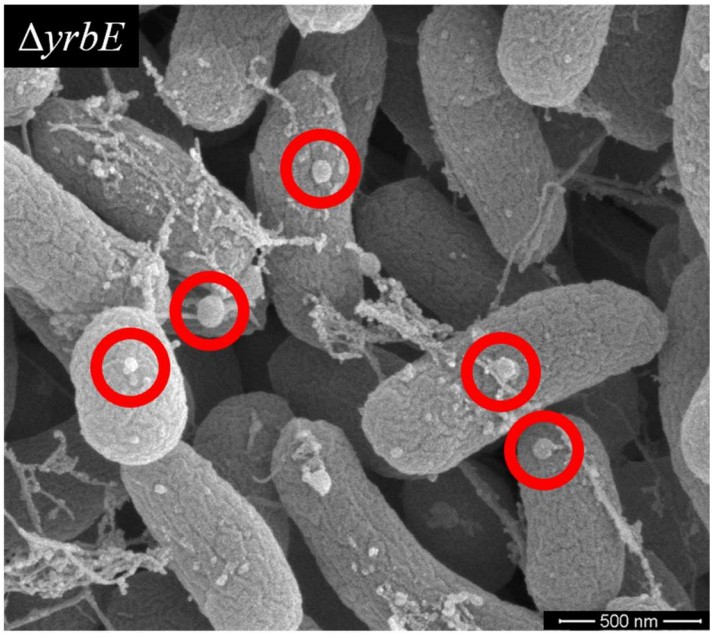
ΔyrbE
500 nm

Figure 3.12. Increased Abundance of Outer Membrane Vesicles, via Genetic Modification, in *V. cholerae* Biofilms Observed by Scanning Electron Microscopy. 100 µl of *V. cholerae* overnight culture was plated on 20 ml LB agar plates, overlaid with a single layer of sterile dialysis tubing. Biofilms were grown at 30°C and samples were prepared after 24 hours. Sterile glass coverslips were pressed into the biofilm. Retrieved samples were fixed with 2.5% glutaraldehyde and serially dehydrated with increasing concentrations of ethanol. The experiment was repeated in two biological replicates.

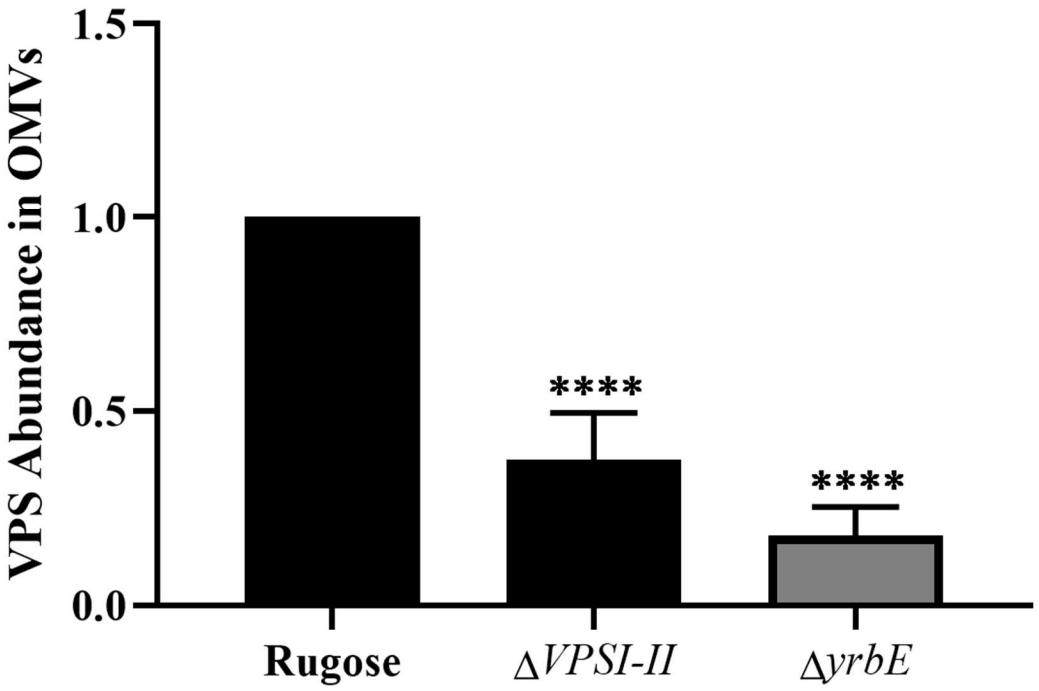
VPS Abundance in OMVs
1.5
1.0
0.5
0.0
****
****
Rugose
ΔVPSI-II
ΔyrbE

Figure 3.13. Abundance of *Vibrio* polysaccharide in Outer Membrane Vesicles Isolated from Biofilms Lacking YrbE. OMVs were isolated as previously discussed. Abundance of VPS in purified samples was determined using immunostaining and subsequently quantified using ImageJ software. The experiment was repeated in two biological replicates and two technical replicates. Presented values are the mean of these four trials.

Analysis of the Impact of Polymyxin B on *V. cholerae* Growth

It has been previously established that exposure to sub-lethal concentrations (one quarter of the minimum inhibitory concentration) of Polymyxin B (PmB) can alter the *V. cholerae* OMV proteome, increasing the association of Bap1 to OmpT[54]. In order to confirm that this concentration is also sub-lethal for our rugose variant strains, I grew both the *V. cholerae* parent and Δ*yrbE* strains in the presence of 12.5 μg/ml. Enumeration of CFUs, over numerous time points, suggests this concentration of Polymyxin B does not affect growth (Fig. 3.14). It should be noted, however, that Δ*yrbE* shows a decreased growth rate, when compared to the parent, independent of Polymyxin B.

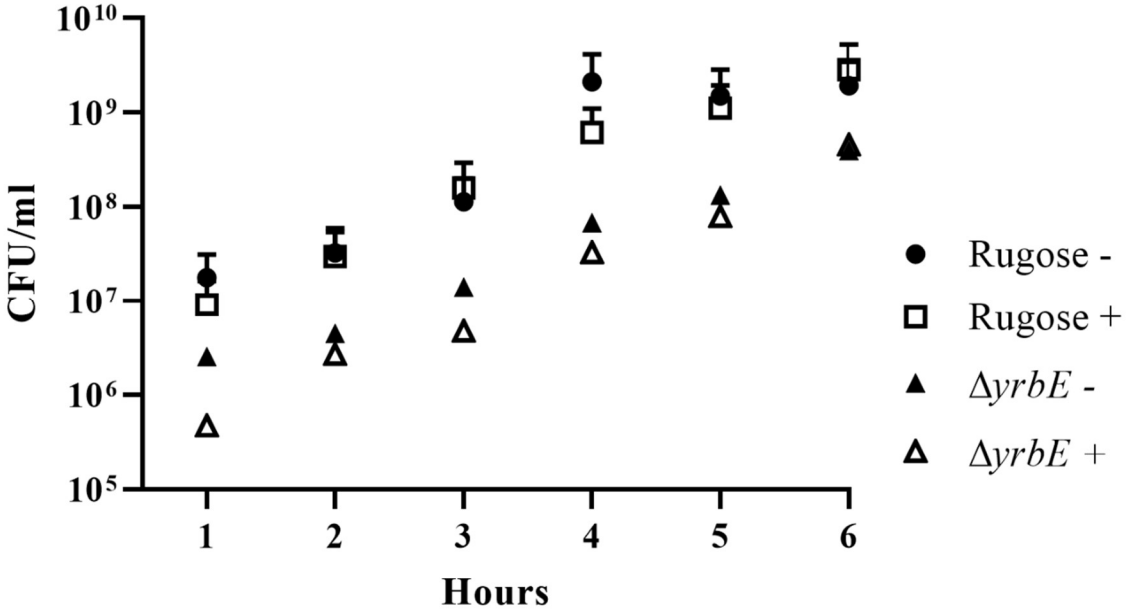
10^{10}
10^{9}
10^{8}
10^{7}
10^{6}
10^{5}
CFU/ml
1
2
3
4
5
6
Hours
Rugose -
Rugose +
Δ*yrbE* -
Δ*yrbE* +

Figure 3.14. Polymyxin B, at a Sub-Inhibitory Concentration, does not Affect *V. cholerae* Growth. Overnight grown cultures were diluted (1:200) into 50 ml fresh LB media. Polymyxin B was added to a final concentration of 12.5 μg/ml and cultures were grown at 30ºC shaking (200 rpm). 1.5 ml aliquots were taken hourly and used to measure OD_{600} and generate serial dilutions for CFU enumeration. Aliquots for serial dilutions were vortexed with glass beads for 30 seconds at 2,500xg before subsequent dilution. Each dilution was vortexed at 2,500xg for an additional 15 seconds before plating. CFU/ml was determined after 24 hours of growth at 30ºC. The experiment was repeated in two biological replicates.

Exposure to polymyxin B affects abundance of outer membrane vesicles in *V. cholerae* biofilms

Utilizing the method for OMV isolation and quantification previously described, I quantified abundance of biofilm-associated OMVs when grown in the presence of 12.5 μg/ml PmB. We do not observe variation in the abundance of OMVs in rugose treated and untreated biofilms (Fig. 3.15). Alternatively, exposure to PmB decreases abundance of biofilm-associated OMVs in the PmB-exposed Δ*yrbE* biofilm when compared to the non-exposed control (Fig. 3.15). Our data is consistent with previous work that stated that exposure of smooth *V. cholerae* to 12.5 μg/ml PmB does not alter abundance of OMVs[54]. The observation that exposure to sub-inhibitory concentrations of PmB can decrease abundance of OMV in the Δ*yrbE* mutant is novel.

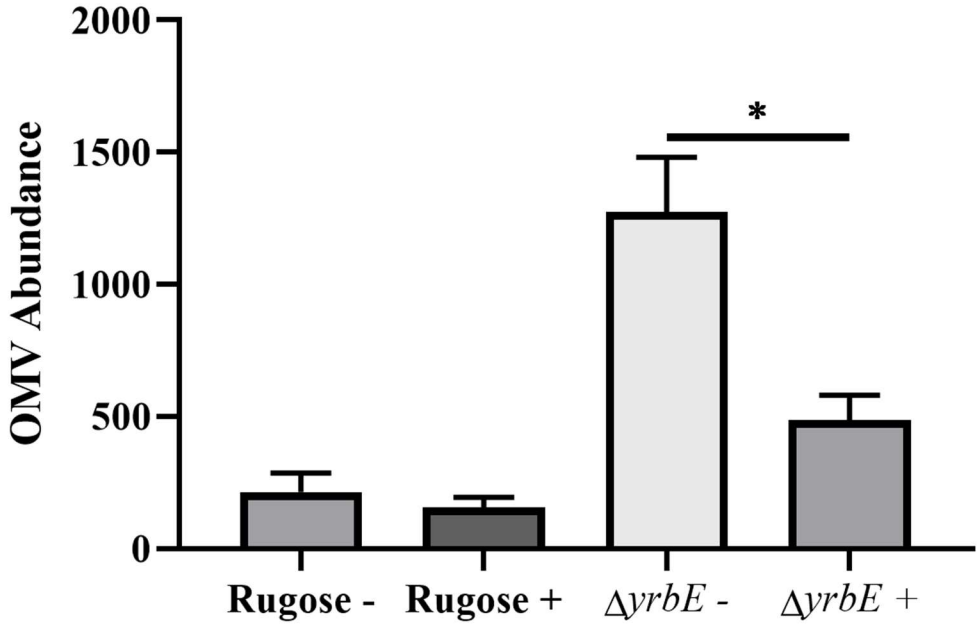
2000
1500
1000
500
0
OMV Abundance
*
Rugose -
Rugose +
ΔyrbE -
ΔyrbE +

Figure 3.15. Quantification of Outer Membrane Vesicles Isolated from *V. cholerae* Biofilms Grown in the Presence of Polymyxin B. Outer membrane vesicles were isolated as previously discussed from LB agar plates containing 12.5 μg/ml PmB. Vesicles were additionally quantified as previously discussed. Fluorescence was measured in triplicate per sample, then normalized to the rugose value. The experiment was repeated in two biological replicates.

Exposure to Polymyxin B alters *V. cholerae* biofilm morphology

Biofilms grown in the presence of 12.5 μg/ml PmB appeared more rugose, when compared to the untreated control strains (Figs. 3.16 and 3.17). Scanning electron microscopy of PmB treated and untreated *V. cholerae* biofilms showed no observable differences with respect to cell morphology or instances of cell lysis (Figs. 3.18 and 3.19).

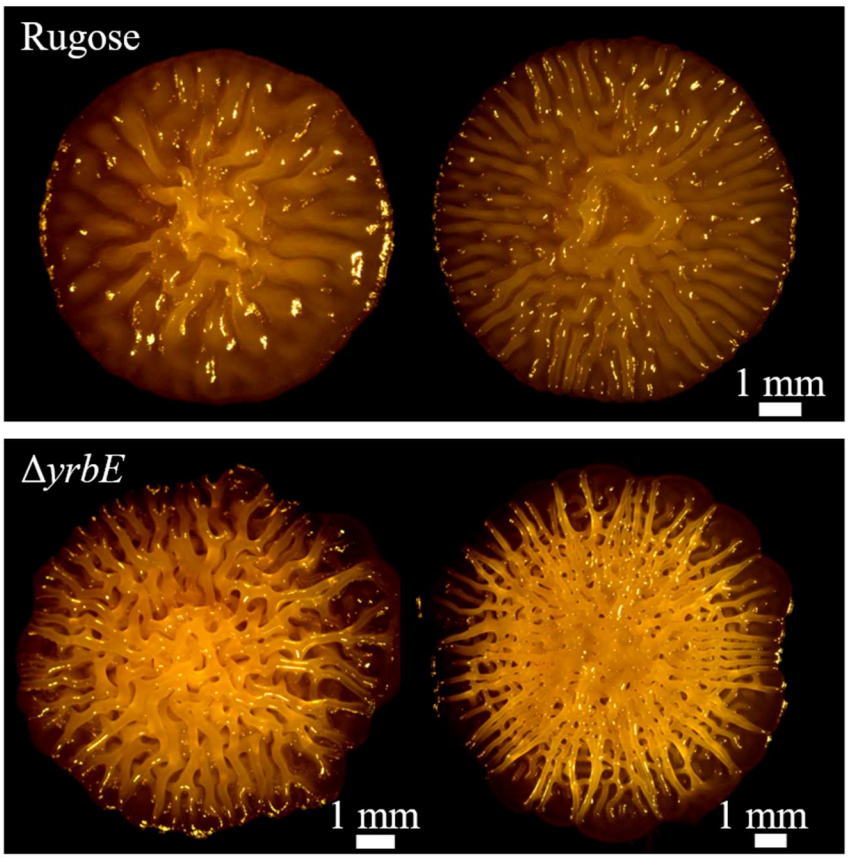
Rugose
1 mm
ΔyrbE
1 mm
1 mm

Figure 3.16. Polymyxin B, at a Sub-Inhibitory Concentration, Affects *V. cholerae* Colony Biofilms. Biofilm morphologies of parent and *yreB* strains. 100 µl of serially diluted overnight culture (final dilution of 10^{-9}) was plated on 20 ml LB agar plates, either without (left) or with (right) 12.5 µg/ml Polymyxin B. Biofilms were grown at 30°C and imaged after 120 hours. The experiment was repeated in two biological replicates.

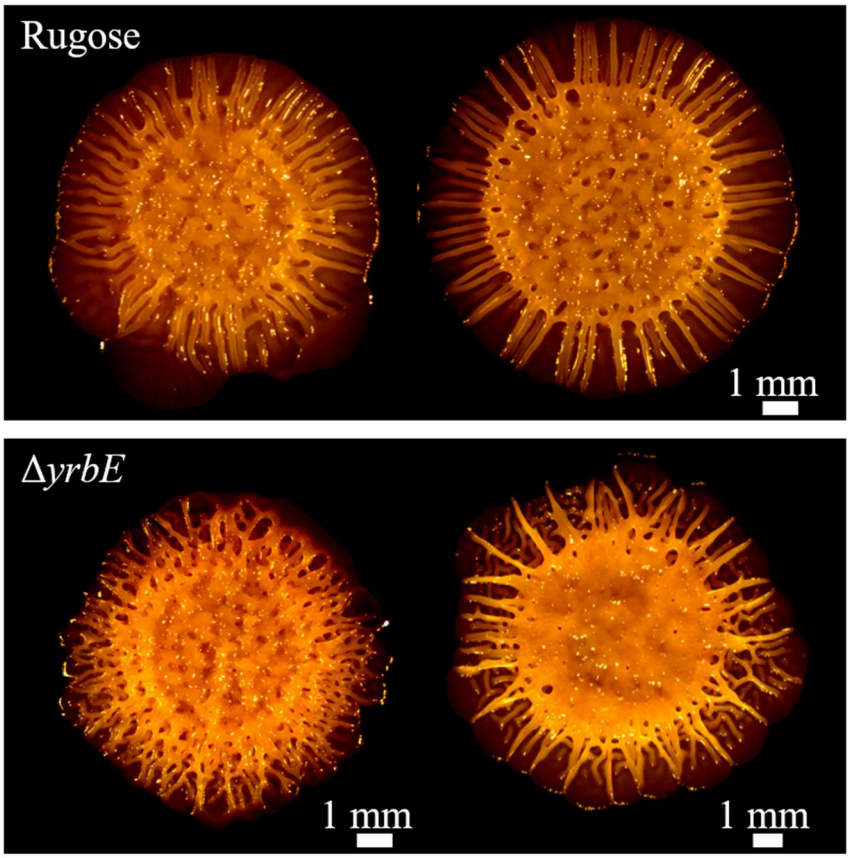
Rugose
1 mm
ΔyrbE
1 mm
1 mm

Figure 3.17. Polymyxin B, at a Sub-Inhibitory Concentration, Affects *V. cholerae* Spot Biofilms Formed at Air-Solid Interface. Biofilm morphologies of parent and *yreB* strains. 3 µl of diluted overnight culture (1:200) was plated in triplicate on 20 ml LB agar plates, either without (left) or with (right) 12.5 µg/ml. Biofilms were grown at 30°C and imaged after 120 hours. The experiment was repeated in two biological replicates.

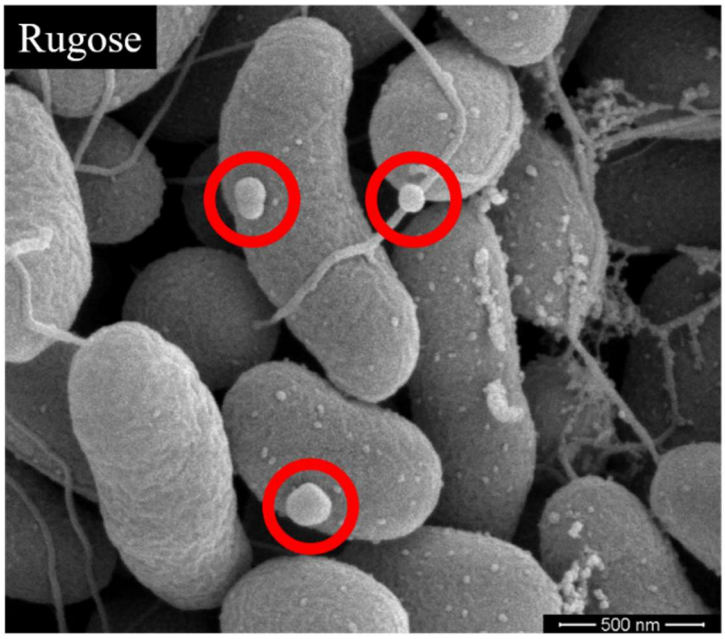
Rugose
500 nm

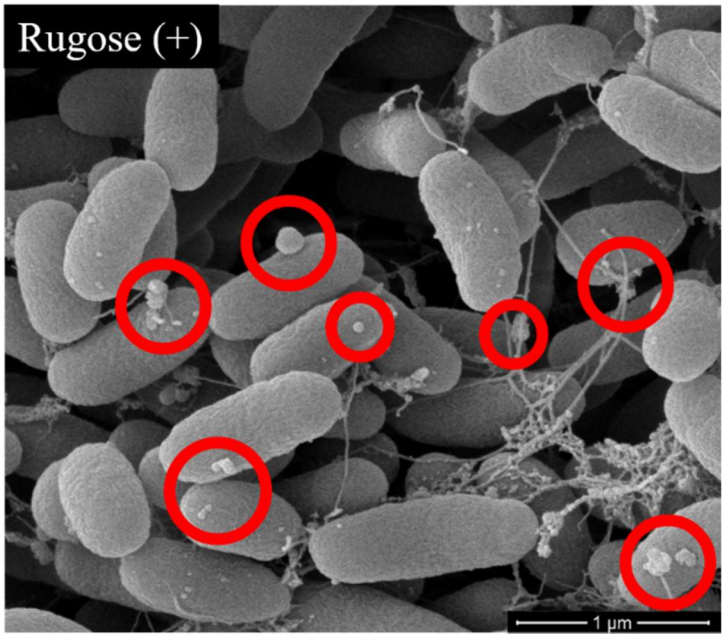
Rugose (+)
1 µm

Figure 3.18. Presence of Sub-Inhibitory Concentration of Polymyxin B Does Not Alter Cell Morphology or Lysis Events in Rugose Biofilms. 100 µl of overnight culture was plated on 20 ml LB agar plates, containing 12.5 µg/ml Polymyxin B, overlaid with a single layer of sterile dialysis tubing. Biofilms were grown at 30°C and samples were prepared after 24 hours. Sterile glass coverslips were pressed into the biofilm. Retrieved samples were fixed with 2.5% glutaraldehyde and serially dehydrated with increasing concentrations of ethanol. The experiment was repeated in two biological replicates.

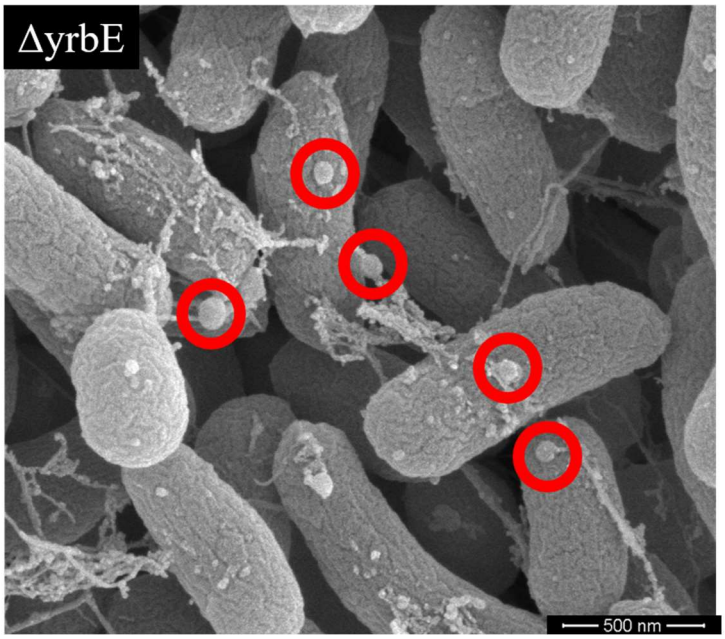
ΔyrbE
500 nm

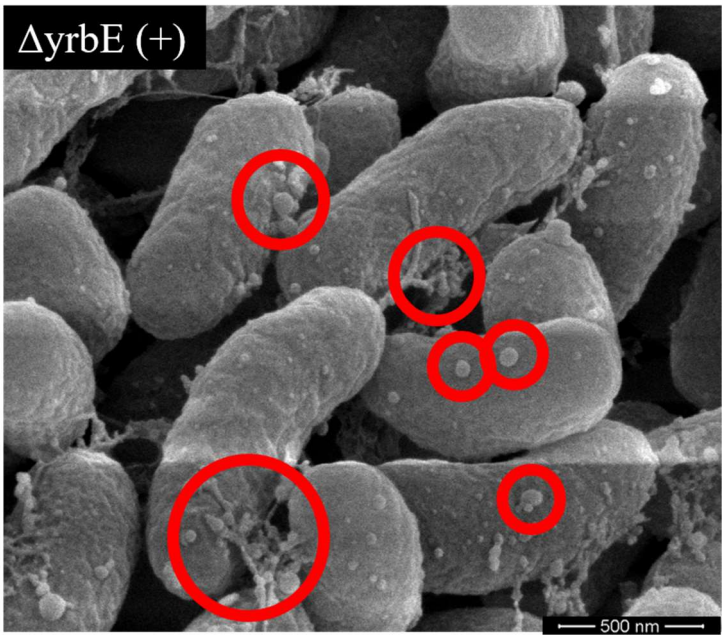
ΔyrbE (+)
500 nm

Figure 3.19. Presence of Sub-Inhibitory Concentration of Polymyxin B Does Not Alter Cell Morphology or Lysis Events in *V. cholerae* Biofilms Lacking YrbE. 100 µl of overnight culture was plated on 20 ml LB agar plates, containing 12.5 µg/ml Polymyxin B, overlaid with a single layer of sterile dialysis tubing. Biofilms were grown at 30°C and samples were prepared after 24 hours. Sterile glass coverslips were pressed into the biofilm. Retrieved samples were fixed with 2.5% glutaraldehyde and serially dehydrated with increasingly high concentrations of ethanol. The experiment was repeated in two biological replicates.

Conclusion

We have conclusively shown the existence of OMVs in *V. cholerae* biofilms. We have also shown that OMV production can be increased, resulting in the modification of biofilm morphology, through a number of means: genetic manipulation; chemical induction; or any combination thereof. This study displays that OMVs play a distinct role in the architecture of biofilms, with the increase in OMVs resulting in a hyper-rugose phenotype. Interestingly, the means of increased vesiculation, genetic or chemical modification, appear to influence the resulting, hyper-vesiculating morphology. Polymyxin B is thought to alter the charge and structure of bacterial lipopolysaccharide[157]. This modification may explain the difference in biofilm phenotype under increase OMV production via Polymyxin B compared to Δ*yreB* (Fig 3.4. and 3.5). The roles of OMVs in *V. cholerae* biofilm formation and architecture need to be further explored to understand the entirety of their contribution to the matrix as biofilm-associated OMVs have been observed to play important roles throughout biofilm-utilizing organisms. Cells from every kingdom of life, bacteria, archaea, eukaryotes, have been observed to produce extracellular vesicles, with production of vesicles being specific to each organism's biology and physiological needs[158, 159, 160]. Extracellular vesicles are also noted to be important to eukaryotic biofilms. Fungal extracellular vesicle cargo is known to contain proteins, lipids, polysaccharides, and RNA[161]. Extensive work has been done in characterizing the role of extracellular vesicles from the human pathogen, *Candida albicans* biofilms[162]. Vesicles from *C. albicans* biofilms were distinct from planktonic vesicles by size,

protein content, and abundance[163]. *C. albicans* vesicle composition has been observed to be very similar to matrix protein and polysaccharide composition, in that, there is almost a 50% overlap in matrix and vesicle proteomes[163], suggesting a role for vesicles in delivery of matrix components. Within this project, we have been able to establish matrix component delivery as an OMV function in *V. cholerae* biofilms. We have shown association of VPS and matrix proteins with OMVs. Additionally, this cargo can be of variable abundance dependent on the composition of the OMV proteome. The role of extracellular vesicles is clearly diverse but critical to biofilm formation through a number of mechanisms of participation and contribution to the matrix. We will continue to explore the role of outer membrane vesicles in biofilm formation and how the vesicle proteome contributes to the matrix as a whole.

References

1. Ali M, Lopez AL, Ae You Y, et al. The global burden of cholera. *Bull World Health Organ*. 2012;90(3):209-218. doi:10.2471/BLT.11.093427

2. Byrne JP. *Encyclopedia of Pestilence, Pandemics, and Plagues [2 Volumes]*. https://www.academia.dk/MedHist/Sygdomme/PDF/Encyclopedia_of_Pestilence_Pandemics_and_Plagues.pdf. Accessed July 7, 2019.

3. Ali M, Nelson AR, Lena Lopez A, Sack DA. Updated Global Burden of Cholera in Endemic Countries. 2015. doi:10.1371/journal.pntd.0003832

4. O'Toole G, Kaplan HB, Kolter R. Biofilm Formation as Microbial Development. *Annu Rev Microbiol*. 2000;54(1):49-79. doi:10.1146/annurev.micro.54.1.49

5. Parsek MR, Singh PK. Bacterial Biofilms: An Emerging Link to Disease Pathogenesis. *Annu Rev Microbiol*. 2003;57(1):677-701. doi:10.1146/annurev.micro.57.030502.090720

6. Donlan RM. *Biofilms: Microbial Life on Surfaces*. Vol 8.; 2002. http://www.microbelibrary.org/. Accessed July 14, 2019.

7. Vlamakis H, Chai Y, Beauregard P, Losick R, Kolter R. Sticking together: building a biofilm the Bacillus subtilis way. doi:10.1038/nrmicro2960

8. Sugimoto S, Okuda K-I, Miyakawa R, et al. Imaging of bacterial multicellular behaviour in biofilms in liquid by atmospheric scanning electron microscopy.

2016. doi:10.1038/srep25889

9. Karatan E, Watnick P. Signals, Regulatory Networks, and Materials That Build and Break Bacterial Biofilms. *Microbiol Mol Biol Rev*. 2009;73(2):310-347. doi:10.1128/MMBR.00041-08

10. Rinaudi L V., Giordano W. An integrated view of biofilm formation in rhizobia. *FEMS Microbiol Lett*. 2010;304(1):1-11. doi:10.1111/j.1574-6968.2009.01840.x

11. Faruque SM, Biswas K, Nashir Udden SM, et al. Transmissibility of cholera: In vivo-formed biofilms and their relationship to infectivity and persistence in the environment. 2006. www.pnas.orgcgidoi10.1073pnas.0601277103. Accessed July 18, 2018.

12. Gilbert P, Maira-Litran T, McBain AJ, Rickard AH, Whyte FW. The physiology and collective recalcitrance of microbial biofilm communities. *Adv Microb Physiol*. 2002;46:202-256. http://www.ncbi.nlm.nih.gov/pubmed/12073654. Accessed February 17, 2019.

13. Van Meervenne E, De Weirdt R, Van Coillie E, Devlieghere F, Herman L, Boon N. Biofilm models for the food industry: hot spots for plasmid transfer? *Pathog Dis*. 2014;70(3):332-338. doi:10.1111/2049-632X.12134

14. Remis JP, Wei D, Gorur A, et al. Bacterial social networks: Structure and composition of Myxococcus xanthus outer membrane vesicle chains. *Environ*

Microbiol. 2014;16(2):598-610. doi:10.1111/1462-2920.12187

15. Teschler JK, Zamorano-Sánchez D, Utada AS, et al. Living in the matrix: assembly and control of Vibrio cholerae biofilms. *Nat Rev Microbiol*. 2015;13(5):255-268. doi:10.1038/nrmicro3433

16. Flemming H-C, Wingender J. The biofilm matrix. *Nat Publ Gr*. 2010;8. doi:10.1038/nrmicro2415

17. Yildiz FH, Schoolnik GK. *Vibrio Cholerae O1 El Tor: Identification of a Gene Cluster Required for the Rugose Colony Type, Exopolysaccharide Production, Chlorine Resistance, and Biofilm Formation*. Vol 96.; 1999. www.pnas.org. Accessed August 29, 2018.

18. Limoli DH, Jones CJ, Wozniak DJ. *Bacterial Extracellular Polysaccharides in Biofilm Formation and Function*.; 2015. www.asmscience.org. Accessed August 18, 2018.

19. Collins RF, Beis K, Dong C, et al. *The 3D Structure of a Periplasm-Spanning Platform Required for Assembly of Group 1 Capsular Polysaccharides in Escherichia Coli*.; 2007. www.pnas.org/cgi/content/full/. Accessed August 23, 2018.

20. Cuthbertson L, Kos V, Whitfield C. ABC Transporters Involved in Export of Cell Surface Glycoconjugates. *Microbiol Mol Biol Rev*. 2010;74(3):1092-2172. doi:10.1128/MMBR.00009-10

21. Hubbard C, Mcnamara JT, Azumaya C, Patel MS, Zimmer∗ J. The Hyaluronan Synthase Catalyzes the Synthesis and Membrane Translocation of Hyaluronan. *J Mol Biol*. 2012;418:21-31. doi:10.1016/j.jmb.2012.01.053

22. Colvin KM, Gordon VD, Murakami K, Borlee BR, Wozniak DJ. The Pel Polysaccharide Can Serve a Structural and Protective Role in the Biofilm Matrix of Pseudomonas aeruginosa. *PLoS Pathog*. 2011;7(1):1001264. doi:10.1371/journal.ppat.1001264

23. Hassett MR, Parsek AK, Jeffers JG, Leid CJ, Willson ME, Shirtliff DJ. The Exopolysaccharide Alginate Protects. *J Immunol Ref*. 2005;175:7512-7518. doi:10.4049/jimmunol.175.11.7512

24. Ryu J-H, Beuchat LR. Biofilm Formation by Escherichia coli O157:H7 on Stainless Steel: Effect of Exopolysaccharide and Curli Production on Its Resistance to Chlorine. *Appl Environ Microbiol*. 2005;71(1):247-254. doi:10.1128/AEM.71.1.247-254.2005

25. Neu TR, Lawrence JR. Innovative techniques, sensors, and approaches for imaging biofilms at different scales. 2015. doi:10.1016/j.tim.2014.12.010

26. Persat A, Nadell CD, Kim MK, et al. Leading Edge The Mechanical World of Bacteria. *Cell*. 2015;161:988-997. doi:10.1016/j.cell.2015.05.005

27. Serra DO, Richter AM, Hengge R. Cellulose as an Architectural Element in Spatially Structured Escherichia coli Biofilms. 2013. doi:10.1128/JB.00946-13

28. Ryder C, Byrd M, Wozniak DJ. Role of polysaccharides in Pseudomonas aeruginosa biofilm development. 2007. doi:10.1016/j.mib.2007.09.010

29. May TB, Maharaj R, Kato J, et al. *Alginate Synthesis by Pseudomonas Aeruginosa: A Key Pathogenic Factor in Chronic Pulmonary Infections of Cystic Fibrosis Patients*. Vol 4.; 1991. https://www.ncbi.nlm.nih.gov/pmc/articles/PMC358191/pdf/cmr00043-0063.pdf. Accessed July 14, 2019.

30. Jennings LK, Storek KM, Ledvina HE, et al. Pel is a cationic exopolysaccharide that cross-links extracellular DNA in the Pseudomonas aeruginosa biofilm matrix. 2015. doi:10.1073/pnas.1503058112

31. Colvin KM, Irie Y, Tart CS, et al. The Pel and Psl polysaccharides provide Pseudomonas aeruginosa structural redundancy within the biofilm matrix. *Environ Microbiol*. 2012;14(8):1913-1928. doi:10.1111/j.1462-2920.2011.02657.x

32. Devaraj A, Justice SS, Bakaletz LO, Goodman SD. DNABII proteins play a central role in UPEC biofilm structure. *Mol Microbiol*. 2015;96(6):1119-1135. doi:10.1111/mmi.12994

33. Fong JCN, Syed KA, Klose KE, Yildiz FH. Role of Vibrio polysaccharide (vps) genes in VPS production, biofilm formation and Vibrio cholerae pathogenesis. doi:10.1099/mic.0.040196-0

34. Yildiz F, Fong J, Sadovskaya I, Grard T, Vinogradov E. Structural Characterization of the Extracellular Polysaccharide from Vibrio cholerae O1 El-Tor. *PLoS One*. 2014;9(1):86751. doi:10.1371/journal.pone.0086751

35. Lombardo M-J, Michalski J, Martinez-Wilson H, et al. *An in Vivo Expression Technology Screen for Vibrio Cholerae Genes Expressed in Human Volunteers*.; 2007. www.pnas.org/cgi/content/full/. Accessed August 29, 2018.

36. Fong JC, Rogers A, Michael AK, et al. Structural dynamics of RbmA governs plasticity of Vibrio cholerae biofilms. *Elife*. 2017;6:1-22. doi:10.7554/eLife.26163

37. Smith DR, Maestre-Reyna M, Lee G, et al. In situ proteolysis of the Vibrio cholerae matrix protein RbmA promotes biofilm recruitment. doi:10.1073/pnas.1512424112

38. Wood TK. Insights on *Escherichia coli* biofilm formation and inhibition from whole-transcriptome profiling. *Environ Microbiol*. 2009;11(1):1-15. doi:10.1111/j.1462-2920.2008.01768.x

39. Sauer FG, Mulvey MA, Schilling JD, Martinez JJ, Hultgren SJ. Bacterial pili: molecular mechanisms of pathogenesis. *Curr Opin Microbiol*. 2000;3(1):65-72. http://www.ncbi.nlm.nih.gov/pubmed/10679419. Accessed July 16, 2019.

40. Duncan MJ, Mann EL, Cohen MS, Ofek I, Sharon N, Abraham SN. The Distinct Binding Specificities Exhibited by Enterobacterial Type 1 Fimbriae

Are Determined by Their Fimbrial Shafts. *J Biol Chem*. 2005;280(45):37707-37716. doi:10.1074/jbc.M501249200

41. Beloin C, Valle J, Latour-Lambert P, et al. Global impact of mature biofilm lifestyle on Escherichia coli K-12 gene expression. *Mol Microbiol*. 2004;51(3):659-674. http://www.ncbi.nlm.nih.gov/pubmed/14731270. Accessed July 16, 2019.

42. Otto K, Hermansson M. Inactivation of ompX causes increased interactions of type 1 fimbriated Escherichia coli with abiotic surfaces. *J Bacteriol*. 2004;186(1):226-234. doi:10.1128/jb.186.1.226-234.2004

43. Ben Nasr A, Olsén A, Sjöbring U, Müller-Esterl W, Björck L. Assembly of human contact phase proteins and release of bradykinin at the surface of curli-expressing Escherichia coli. *Mol Microbiol*. 1996;20(5):927-935. http://www.ncbi.nlm.nih.gov/pubmed/8809746. Accessed July 16, 2019.

44. Sharma G, Sharma S, Sharma P, et al. Escherichia coli biofilm: development and therapeutic strategies. *J Appl Microbiol*. 2016;121(2):309-319. doi:10.1111/jam.13078

45. Cookson AL, Cooley WA, Woodward MJ. The role of type 1 and curli fimbriae of Shiga toxin-producing Escherichia coli in adherence to abiotic surfaces. *Int J Med Microbiol*. 2002;292(3-4):195-205. doi:10.1078/1438-4221-00203

46. Uhlich GA, Cooke PH, Solomon EB. Analyses of the Red-Dry-Rough Phenotype of an Escherichia coli O157:H7 Strain and Its Role in Biofilm Formation and Resistance to Antibacterial Agents. *Appl Environ Microbiol*. 2006;72(4):2564-2572. doi:10.1128/AEM.72.4.2564-2572.2006

47. Sherlock O, Vejborg RM, Klemm P. The TibA Adhesin/Invasin from Enterotoxigenic Escherichia coli Is Self Recognizing and Induces Bacterial Aggregation and Biofilm Formation. *Infect Immun*. 2005;73(4):1954-1963. doi:10.1128/IAI.73.4.1954-1963.2005

48. Tielker D, Hacker S, Loris R, et al. Pseudomonas aeruginosa lectin LecB is located in the outer membrane and is involved in biofilm formation. 2018. doi:10.1099/mic.0.27701-0

49. Martínez-Gil M, Quesada M, Ramos-González I, Soriano I, De Cristóbal RE, Espinosa-Urgel M. Interplay between extracellular matrix components of Pseudomonas putida biofilms. *Res Microbiol*. 2013;164:382-389. doi:10.1016/j.resmic.2013.03.021

50. Borlee BR, Goldman AD, Murakami K, Samudrala R, Wozniak DJ, Parsek MR. Pseudomonas aeruginosa uses a cyclic-di-GMP-regulated adhesin to reinforce the biofilm extracellular matrix. *Mol Microbiol*. 2010;75(4):827-842. doi:10.1111/j.1365-2958.2009.06991.x

51. Fong JNC, Yildiz FH. Biofilm Matrix Proteins. *Microbiol Spectr*. 2015;3(2). doi:10.1128/microbiolspec.mb-0004-2014

52. Giglio KM, Fong JC, Yildiz FH, Sondermann H. Structural Basis for Biofilm Formation via the Vibrio cholerae Matrix Protein RbmA. 2013. doi:10.1128/JB.00374-13

53. Absalon C, Ymele-Leki P, Watnick PI. The Bacterial Biofilm Matrix as a Platform for Protein Delivery. 2012. doi:10.1128/mBio.00127-12

54. Duperthuy M, Sjö strö AE, Sabharwal D, et al. Role of the Vibrio cholerae Matrix Protein Bap1 in Cross-Resistance to Antimicrobial Peptides. 2010:2010-3073. doi:10.1371/journal.ppat.1003620

55. Liu W, Chun E, Thompson AA, et al. Structural basis for allosteric regulation of GPCRS by sodium ions. *Science (80-)*. 2012;337(6091):232-236. doi:10.1126/science.1219218

56. Fong JCN, Karplus K, Schoolnik GK, Yildiz FH. Identification and Characterization of RbmA, a Novel Protein Required for the Development of Rugose Colony Morphology and Biofilm Structure in Vibrio cholerae. *J Bacteriol*. 2006;188(3):1049-1059. doi:10.1128/JB.188.3.1049-1059.2006

57. Absalon C, Van Dellen K, Watnick PI. A Communal Bacterial Adhesin Anchors Biofilm and Bystander Cells to Surfaces. Isberg RR, ed. *PLoS Pathog*. 2011;7(8):e1002210. doi:10.1371/journal.ppat.1002210

58. De ¤ S, Kaus K, Sinclair S, Case BC, Olson R. Structural basis of mammalian glycan targeting by Vibrio cholerae cytolysin and biofilm proteins. 2018.

doi:10.1371/journal.ppat.1006841

59. Heilmann C, Hussain M, Peters G, Götz F. Evidence for autolysin-mediated primary attachment of Staphylococcus epidermidis to a polystyrene surface. *Mol Microbiol*. 1997;24(5):1013-1024. doi:10.1046/j.1365-2958.1997.4101774.x

60. Ockelmann UB¨, Janke A, Kuhn R, et al. Bacterial extracellular DNAforming a de¢ned network-like structure. doi:10.1111/j.1574-6968.2006.00361.x

61. Vilain S, Pretorius JM, Theron J, Brözel VS. DNA as an Adhesin: Bacillus cereus Requires Extracellular DNA To Form Biofilms †. *Appl Environ Microbiol*. 2009;75(9):2861-2868. doi:10.1128/AEM.01317-08

62. Watanabe M, Suzuki Y, Sasaki K, Nakashimada Y, Nishio N. Flocculating property of extracellular polymeric substance derived from a marine photosynthetic bacterium, Rhodovulum sp. *J Biosci Bioeng*. 1999;87(5):625-629. doi:10.1016/S1389-1723(99)80125-X

63. Browning DF, Grainger DC, Busby SJ. Effects of nucleoid-associated proteins on bacterial chromosome structure and gene expression. 2010. doi:10.1016/j.mib.2010.09.013

64. Mulcahy H, Charron-Mazenod L, Lewenza S. Extracellular DNA Chelates Cations and Induces Antibiotic Resistance in Pseudomonas aeruginosa Biofilms. *PLoS Pathog*. 2008;4(11). doi:10.1371/journal.ppat.1000213

65. Nicas TI, Hancock REW. *Outer Membrane Protein Hi of Pseudomonas Aeruginosa: Involvement in Adaptive and Mutational Resistance to Ethylenediaminetetraacetate, Polymyxin B, and Gentamicin Downloaded From*. Vol 143.; 1980. http://jb.asm.org/. Accessed August 15, 2018.

66. Murata T, Tseng W, Guina T, Miller SI, Nikaido H. PhoPQ-Mediated Regulation Produces a More Robust Permeability Barrier in the Outer Membrane of Salmonella enterica Serovar Typhimurium Downloaded from. *J Bacteriol*. 2007;189(20):7213-7222. doi:10.1128/JB.00973-07

67. Seper A, Fengler VHI, Roier S, et al. Extracellular nucleases and extracellular DNA play important roles in Vibrio cholerae biofilm formationm mi_7867 1015..1037. 2011. doi:10.1111/j.1365-2958.2011.07867.x

68. Focareta T, Manning PA. Distinguishing between the extracellular DNases of Vibrio cholerae and development of a transformation system. *Mol Microbiol*. 1991;5(10):2547-2555. http://www.ncbi.nlm.nih.gov/pubmed/1791765. Accessed July 16, 2019.

69. Schild S, Tamayo R, Nelson EJ, Qadri F, Calderwood SB, Camilli A. Genes induced late in infection increase fitness of Vibrio cholerae after release into the environment. *Cell Host Microbe*. 2007;2(4):264-277. doi:10.1016/j.chom.2007.09.004

70. Sharpe SW, Kuehn MJ, Mason KM. Elicitation of Epithelial Cell-Derived Immune Effectors by Outer Membrane Vesicles of Nontypeable Haemophilus

influenzae. *Infect Immun*. 2011;79(11):4361-4369. doi:10.1128/IAI.05332-11

71. Kulp A, Kuehn MJ. Biological Functions and Biogenesis of Secreted Bacterial Outer Membrane Vesicles. *Annu Rev Microbiol*. 2010;64:163-184. doi:10.1146/annurev.micro.091208.073413

72. Fulsundar S, Harms K, Flaten GE, Johnsen PJ, Chopade BA, Nielsen KM. Gene Transfer Potential of Outer Membrane Vesicles of Acinetobacter baylyi and Effects of Stress on Vesiculation. 2014. doi:10.1128/AEM.04248-13

73. Malinverni JC, Silhavy TJ. An ABC transport system that maintains lipid asymmetry in the gram-negative outer membrane. *Proc Natl Acad Sci U S A*. 2009;106(19):8009-8014. doi:10.1073/pnas.0903229106

74. Roier S, Zingl FG, Cakar F, Schild S. Bacterial outer membrane vesicle biogenesis: a new mechanism and its implications. 2016;3(6). www.microbialcell.com. Accessed June 28, 2018.

75. Roier S, Zingl FG, Cakar F, et al. ARTICLE A novel mechanism for the biogenesis of outer membrane vesicles in Gram-negative bacteria. 2016. doi:10.1038/ncomms10515

76. Schwechheimer C, Kulp A, Kuehn MJ. Modulation of bacterial outer membrane vesicle production by envelope structure and content. http://www.biomedcentral.com/1471-2180/14/324. Accessed June 28, 2018.

77. Yu F, Inouye S, Inouye M. *THE JOURNAL OF BIOLOGICAL CHEMISTRY*

*Lipoprotein-28, a Cytoplasmic Membrane Lipoprotein from Escherichia Coti CLONING, DNA SEQUENCE, AND EXPRESSION OF ITS GENE**. Vol 261.; 1986. http://www.jbc.org/content/261/5/2284.full.pdf. Accessed August 12, 2018.

78. Schwechheimer C, Rodriguez DL, Kuehn MJ, Meta Kuehn CJ. NlpI-mediated modulation of outer membrane vesicle production through peptidoglycan dynamics in Escherichia coli. *Microbiologyopen*. 2015;4(3):375-389. doi:10.1002/mbo3.244

79. Cascales E, Bernadac A, Gavioli M, Lazzaroni J-C, Lloubes R. Pal Lipoprotein of Escherichia coli Plays a Major Role in Outer Membrane Integrity. *J Bacteriol*. 2002;184(3):754-759. doi:10.1128/JB.184.3.754-759.2002

80. Braun V. Covalent lipoprotein from the outer membrane of escherichia coli. *BBA - Rev Biomembr*. 1975;415(3):335-377. doi:10.1016/0304-4157(75)90013-1

81. Schwechheimer C, Kuehn MJ. Synthetic Effect between Envelope Stress and Lack of Outer Membrane Vesicle Production in Escherichia coli. 2013. doi:10.1128/JB.02192-12

82. Mashburn LM, Whiteley M. Membrane vesicles traffic signals and facilitate group activities in a prokaryote. 2005. doi:10.1038/nature03925

83. Schertzer JW, Whiteley M, Kolter R. A Bilayer-Couple Model of Bacterial

Outer Membrane Vesicle Biogenesis. 2012. doi:10.1128/mBio.00297-11

84. Florez C, Raab JE, Cooke AC, Schertzer JW. Membrane Distribution of the Pseudomonas Quinolone Signal Modulates Outer Membrane Vesicle Production in Pseudomonas aeruginosa. doi:10.1128/mBio.01034-17

85. Gaudin M, Gauliard E, Schouten S, et al. Hyperthermophilic archaea produce membrane vesicles that can transfer DNA. *Environ Microbiol Rep*. 2013;5(1):109-116. doi:10.1111/j.1758-2229.2012.00348.x

86. Rumbo C, Fernández-Moreira E, Merino M, et al. Horizontal Transfer of the OXA-24 Carbapenemase Gene via Outer Membrane Vesicles: a New Mechanism of Dissemination of Carbapenem Resistance Genes in Acinetobacter baumannii. *Antimicrob Agents Chemother*. 2011;55(7):3084-3090. doi:10.1128/AAC.00929-10

87. Kadurugamuwat JL, Beveridge TJ. *Membrane Vesicles Derived f Rom Pseudornonas Aeruginosa and Shigella Flexneri Can Be Integrated into the Surfaces of Other Gram-Negative Bacteria*. Vol 145.; 2018. www.microbiologyresearch.org. Accessed August 3, 2018.

88. Kadurugamuwa JL, Beveridge TJ. *Bacteriolytic Effect of Membrane Vesicles from Pseudomonas Aeruginosa on Other Bacteria Including Pathogens: Conceptually New Antibiotics*. Vol 178.; 1996. https://www.ncbi.nlm.nih.gov/pmc/articles/PMC178010/pdf/1782767.pdf. Accessed August 3, 2018.

89. Schaar V, Nordström T, Mörgelin M, Riesbeck K. Moraxella catarrhalis Outer Membrane Vesicles Carry-Lactamase and Promote Survival of Streptococcus pneumoniae and Haemophilus influenzae by Inactivating Amoxicillin. *Antimicrob Agents Chemother*. 2011;55(8):3845-3853. doi:10.1128/AAC.01772-10

90. Kulkarni HM, Nagaraj R, Jagannadham M V. Protective role of E. coli outer membrane vesicles against antibiotics. *Microbiol Res*. 2015;181:1-7. doi:10.1016/j.micres.2015.07.008

91. Won Kim S, Bin Park S, Pyeong Im S, et al. Outer membrane vesicles from β-lactam-resistant Escherichia coli enable the survival of β-lactam-susceptible E. coli in the presence of β-lactam antibiotics. doi:10.1038/s41598-018-23656-0

92. Premjani V, Tilley D, Gruenheid S, Le Moual H, Samis JA. Enterohemorrhagic *Escherichia coli* OmpT regulates outer membrane vesicle biogenesis. *FEMS Microbiol Lett*. 2014;355(2):185-192. doi:10.1111/1574-6968.12463

93. Yoon H, Ansong C, Adkins JN, Heffron F. Discovery of Salmonella Virulence Factors Translocated via Outer Membrane Vesicles to Murine Macrophages. *Infect Immun*. 2011;79(6):2182-2192. doi:10.1128/IAI.01277-10

94. Bomberger JM, Maceachran DP, Coutermarsh BA, Ye S, Toole O. Long-Distance Delivery of Bacterial Virulence Factors by Pseudomonas aeruginosa Outer Membrane Vesicles. *PLoS Pathog*. 2009;5(4):1000382.

doi:10.1371/journal.ppat.1000382

95. McBroom AJ, Kuehn MJ. Release of outer membrane vesicles by Gram-negative bacteria is a novel envelope stress response. *Mol Microbiol*. 2007;63(2):545-558. doi:10.1111/j.1365-2958.2006.05522.x

96. Elluri S, Enow C, Vdovikova S, et al. Outer Membrane Vesicles Mediate Transport of Biologically Active Vibrio cholerae Cytolysin (VCC) from V. cholerae Strains. Feldman MF, ed. *PLoS One*. 2014;9(9):e106731. doi:10.1371/journal.pone.0106731

97. Reyes-Robles T, Dillard RS, Cairns LS, et al. Vibrio cholerae Outer Membrane Vesicles Inhibit Bacteriophage Infection. 2018. doi:10.1128/JB.00792-17

98. Taylor RK, Millert VL, Furlong DB, Mekalanost JJ. *Use of PhoA Gene Fusions to Identify a Pilus Colonization Factor Coordinately Regulated with Cholera Toxin (Transcription Activation/Secretion/Fimbriae/Virulence/ToxR Gene)*. Vol 84.; 1987. https://www.pnas.org/content/pnas/84/9/2833.full.pdf. Accessed July 8, 2019.

99. Watnick PI, Fullner KJ, Kolter R. *A Role for the Mannose-Sensitive Hemagglutinin in Biofilm Formation by Vibrio Cholerae El Tor Downloaded From*. Vol 181.; 1999. http://jb.asm.org/. Accessed July 8, 2019.

100. Watnick PI, Lauriano CM, Klose KE, Croal L, Kolter R. *The Absence of a Flagellum Leads to Altered Colony Morphology, Biofilm Development and*

Virulence in Vibrio Cholerae O139. Vol 39.; 2001. https://onlinelibrary.wiley.com/doi/pdf/10.1046/j.1365-2958.2001.02195.x. Accessed July 8, 2019.

101. Bilecen K, Fong JCN, Cheng A, Jones CJ, Zamorano-Sánchez D, Yildiz FH. Polymyxin B Resistance and Biofilm Formation in Vibrio cholerae Are Controlled by the Response Regulator CarR. 2015. doi:10.1128/IAI.02700-14

102. Colwell RR, Huq A, Sirajul Islam M, et al. *Reduction of Cholera in Bangladeshi Villages by Simple Filtration*.; 2002. www.pnas.orgcgidoi10.1073pnas.0237386100. Accessed July 8, 2019.

103. Tamayo R, Patimalla B, Camilli A. Growth in a Biofilm Induces a Hyperinfectious Phenotype in Vibrio cholerae. *Infect Immun*. 2010;78(8):3560-3569. doi:10.1128/IAI.00048-10

104. Gupta P, Mankere B, Chekkoora Keloth S, Tuteja U, Pandey P, Chelvam KT. Increased antibiotic resistance exhibited by the biofilm of Vibrio cholerae O139. doi:10.1093/jac/dky127

105. Beyhan S, Yildiz FH. Smooth to rugose phase variation in *Vibrio cholerae* can be mediated by a single nucleotide change that targets c-di-GMP signalling pathway. *Mol Microbiol*. 2007;63(4):995-1007. doi:10.1111/j.1365-2958.2006.05568.x

106. Altindis E, Fu Y, Mekalanos JJ. Proteomic analysis of Vibrio cholerae outer

membrane vesicles. *Proc Natl Acad Sci*. 2014;111(15):E1548-E1556. doi:10.1073/pnas.1403683111

107. Absalon C, Van Dellen K, Watnick PI. A Communal Bacterial Adhesin Anchors Biofilm and Bystander Cells to Surfaces. *PLoS Pathog*. 2011;7(8):1002210. doi:10.1371/journal.ppat.1002210

108. Koebnik R, Locher KP, Van Gelder P. Structure and function of bacterial outer membrane proteins: barrels in a nutshell. *Mol Microbiol*. 2000;37(2):239-253. doi:10.1046/j.1365-2958.2000.01983.x

109. Chevalier S, Bouffartigues E, Bodilis J, et al. Structure, function and regulation of Pseudomonas aeruginosa porins. *FEMS Microbiol Rev*. 2017;41(5):698-722. doi:10.1093/femsre/fux020

110. Konovalova A, Kahne DE, Silhavy TJ. Outer Membrane Biogenesis. *Annu Rev Microbiol*. 2017;71(1):539-556. doi:10.1146/annurev-micro-090816-093754

111. Samsudin F, Ortiz-Suarez ML, Piggot TJ, Bond PJ, Khalid S. OmpA: A Flexible Clamp for Bacterial Cell Wall Attachment. *Struct Des*. 2016;24:2227-2235. doi:10.1016/j.str.2016.10.009

112. Gaddy JA, Tomaras AP, Actis LA. The Acinetobacter baumannii 19606 OmpA Protein Plays a Role in Biofilm Formation on Abiotic Surfaces and in the Interaction of This Pathogen with Eukaryotic Cells. *Infect Immun*. 2009;77(8):3150-3160. doi:10.1128/IAI.00096-09

113. Foulds J, Barrett C. *Characterization of Escherichia Coli Mutants Tolerant to Bacteriocin JF246: Two New Classes of Tolerant Mutants*.; 1973. https://www.ncbi.nlm.nih.gov/pmc/articles/PMC285459/pdf/jbacter00578-0389.pdf. Accessed August 23, 2018.

114. Prasadarao N V, Wass CA, Weiser JN, et al. *Outer Membrane Protein A of Escherichia Coli Contributes to Invasion of Brain Microvascular Endothelial Cells*. Vol 64.; 1996. http://iai.asm.org/. Accessed August 23, 2018.

115. Koebnik R. *Structural and Functional Roles of the Surface-Exposed Loops of the-Barrel Membrane Protein OmpA from Escherichia Coli Downloaded From*. Vol 181.; 1999. http://jb.asm.org/. Accessed August 23, 2018.

116. Wang Y. The Function of OmpA in Escherichia coli. 2002. doi:10.1006/bbrc.2002.6657

117. Weber BS, Kinsella RL, Harding CM, Feldman MF. The Secrets of Acinetobacter Secretion. *Trends Microbiol*. 2017;25:532-545. doi:10.1016/j.tim.2017.01.005

118. Sandkvist M, Morales V, Bagdasarian M. *A Protein Required for Secretion of Cholera Toxin through the Outer Membrane of Vibrio Cholerae (Extracellular Secretion; Secretion Genes; Recombinant DNA; Enterotoxin)*. Vol 123.; 1993.

119. Ho TD, Davis BM, Ritchie JM, Waldor MK. Type 2 Secretion Promotes Enterohemorrhagic Escherichia coli Adherence and Intestinal Colonization.

Infect Immun. 2008;76(5):1858-1865. doi:10.1128/IAI.01688-07

120. Long He X, Wang Q, Peng L, et al. Role of uropathogenic Escherichia coli outer membrane protein T in pathogenesis of urinary tract infection. *FEMS Pathog Dis*. 2015;73:6. doi:10.1093/femspd/ftv006

121. Tang X, Wang H, Liu F, Sheng X, Xing J, Zhan W. Recombinant outer membrane protein T (OmpT) of Vibrio ichthyoenteri, a potential vaccine candidate for flounder (Paralichthys olivaceus). *Microb Pathog*. 2019;126:185-192. doi:10.1016/j.micpath.2018.11.001

122. Valeru SP, Wai SN, Saeed A, Sandström G, Abd H. ToxR of Vibrio cholerae affects biofilm, rugosity and survival with Acanthamoeba castellanii. *BMC Res Notes*. 2012;5. doi:10.1186/1756-0500-5-33

123. Provenzano D, Klose KE. *Altered Expression of the ToxR-Regulated Porins OmpU and OmpT Diminishes Vibrio Cholerae Bile Resistance, Virulence Factor Expression, and Intestinal Colonization*. www.pnas.org. Accessed August 31, 2018.

124. Sperandio V, Bailey C, Girón JA, et al. Cloning and characterization of the gene encoding the OmpU outer membrane protein of Vibrio cholerae. *Infect Immun*. 1996;64(12):5406-5409. http://www.ncbi.nlm.nih.gov/pubmed/8945596. Accessed July 18, 2019.

125. Mathur J, Waldor MK. The Vibrio cholerae ToxR-Regulated Porin OmpU

Confers Resistance to Antimicrobial Peptides. *Infect Immun*. 2004;72(6):3577-3583. doi:10.1128/IAI.72.6.3577-3583.2004

126. Mathur J, Waldor MK. The Vibrio cholerae ToxR-Regulated Porin OmpU Confers Resistance to Antimicrobial Peptides. *Infect Immun*. 2004;72(6):3577-3583. doi:10.1128/IAI.72.6.3577-3583.2004

127. Chaba R, Alba BM, Guo MS, et al. Signal integration by DegS and RseB governs the σ E-mediated envelope stress response in Escherichia coli. *Proc Natl Acad Sci U S A*. 2011;108(5):2106-2111. doi:10.1073/pnas.1019277108

128. Yang JS, Kim HJ, Kang S-S, et al. TLR2, but not TLR4, plays a predominant role in the immune responses to cholera vaccines. *J Leukoc Biol*. 2015;98(4):661-669. doi:10.1189/jlb.4A1014-498R

129. Sakharwade SC, Mukhopadhaya A. Vibrio cholerae porin OmpU induces LPS tolerance by attenuating TLR-mediated signaling. *Mol Immunol*. 2015;68(2):312-324. doi:10.1016/j.molimm.2015.09.021

130. Yang JS, Jeon JH, Jang MS, et al. Vibrio cholerae OmpU induces IL-8 expression in human intestinal epithelial cells. *Mol Immunol*. 2018;93:47-54. doi:10.1016/j.molimm.2017.11.005

131. Wang S-Y, Lauritz J, Jass J, Milton DL, Milton DebraMilton D. Role for the major outer-membrane protein from Vibrio anguillarum in bile resistance and biofilm formation. doi:10.1099/mic.0.26032-0

132. Kao D-Y, Cheng Y-C, Kuo T-Y, et al. Salt-responsive outer membrane proteins of *Vibrio anguillarum* serotype O1 as revealed by comparative proteome analysis. *J Appl Microbiol*. 2009;106(6):2079-2085. doi:10.1111/j.1365-2672.2009.04178.x

133. Mathur J, Davis BM, Waldor MK. Antimicrobial peptides activate the Vibrio cholerae SigmaE regulon through an OmpU-dependent signalling pathway. *Mol Microbiol*. 2007;63(3):848-858. doi:10.1111/j.1365-2958.2006.05544.x

134. Duperthuy M, Schmitt P, Garzón E, et al. Use of OmpU porins for attachment and invasion of Crassostrea gigas immune cells by the oyster pathogen Vibrio splendidus. doi:10.1073/pnas.1015326108

135. Goo SY, Lee H-J, Kim WH, et al. Identification of OmpU of Vibrio vulnificus as a Fibronectin-Binding Protein and Its Role in Bacterial Pathogenesis. *Infect Immun*. 2006;74(10):5586-5594. doi:10.1128/IAI.00171-06

136. Stevenson G, Leavesley DI, Lagnado CA, Heuzenroeder MW, Manning PA, Manning PA. *Purification of the 25-KDa Vibrio Cholerae Major Outer-Membrane Protein and the Molecular Cloning of Its Gene: Omp V*. Vol 148.; 1985. https://febs.onlinelibrary.wiley.com/doi/pdf/10.1111/j.1432-1033.1985.tb08850.x. Accessed July 10, 2019.

137. Xu C, Ren H, Wang S, Peng X. Proteomic analysis of salt-sensitive outer membrane proteins of Vibrio parahaemolyticus. *Res Microbiol*. 2004;155(10):835-842. doi:10.1016/J.RESMIC.2004.07.001

138. Xu C, Wang S, Ren H, Lin X, Wu L, Peng X. Proteomic analysis on the expression of outer membrane proteins ofVibrio alginolyticus at different sodium concentrations. *Proteomics*. 2005;5(12):3142-3152. doi:10.1002/pmic.200401128

139. Chiu Y, Kuo T-Y, Lin C-C, Chen W-J. Proteomic analysis reveals responsive proteins of Vibrio parahaemolyticus on exposure to cationic antimicrobial peptides. *J Appl Microbiol*. 2011;110(1):80-89. doi:10.1111/j.1365-2672.2010.04856.x

140. Beketskaia MS, Bay DC, Turner RJ. Outer Membrane Protein OmpW Participates with Small Multidrug Resistance Protein Member EmrE in Quaternary Cationic Compound Efflux. 2014. doi:10.1128/JB.01483-14

141. Wu X-B, Tian L-H, Zou H-J, et al. Outer membrane protein OmpW of Escherichia coli is required for resistance to phagocytosis. 2013. doi:10.1016/j.resmic.2013.06.008

142. Givskov M, Hentzer M, Ersbøll BK, et al. Quantification of biofilm structures by the novel computer program comstat. *Microbiology*. 2000;146(10):2395-2407. doi:10.1099/00221287-146-10-2395

143. Hollenbeck EC, Fong JCN, Lim JY, Yildiz FH, Fuller GG, Cegelski L. Molecular Determinants of Mechanical Properties of V. cholerae Biofilms at the Air-Liquid Interface. *Biophysj*. 2014;107:2245-2252. doi:10.1016/j.bpj.2014.10.015

144. Yildiz H, Liu XS, Heydorn A, et al. Molecular analysis of rugosity in a Vibrio cholerae O1 El Tor phase variant. *Orig Artic Regul rugosityF*. 2004;53(2):497-515. doi:10.1111/j.1365-2958.2004.04154.x

145. Delcour AH. Outer membrane permeability and antibiotic resistance. *Biochim Biophys Acta - Proteins Proteomics*. 2009;1794(5):808-816. doi:10.1016/J.BBAPAP.2008.11.005

146. Dong H, Xiang Q, Gu Y, et al. Structural basis for outer membrane lipopolysaccharide insertion. *Nature*. 2014;511(7507):52-56. doi:10.1038/nature13464

147. Hufnagel DA, Depas WH, Chapman MR. The Biology of the Escherichia coli Extracellular Matrix. *Microbiol Spectr*. 2015;3(3). doi:10.1128/microbiolspec.MB-0014-2014

148. Chagnot C, Zorgani MA, Astruc T, Desvaux M. Proteinaceous determinants of surface colonization in bacteria: bacterial adhesion and biofilm formation from a protein secretion perspective. *Front Microbiol*. 2013;4:303. doi:10.3389/fmicb.2013.00303

149. Leo JC, Grin I, Linke D. Type V secretion: mechanism(s) of autotransport through the bacterial outer membrane. *Philos Trans R Soc B Biol Sci*. 2012;367(1592):1088-1101. doi:10.1098/rstb.2011.0208

150. Haiko J, Suomalainen M, Ojala T, Lähteenmäki K, Korhonen TK. Invited

review: Breaking barriers — attack on innate immune defences by omptin surface proteases of enterobacterial pathogens. *Innate Immun*. 2009;15(2):67-80. doi:10.1177/1753425909102559

151. Monteiro R, Ageorges V, Rojas-Lopez M, et al. A secretome view of colonisation factors in Shiga toxin-encoding *Escherichia coli* (STEC): from enterohaemorrhagic *E. coli* (EHEC) to related enteropathotypes. Clarke D, ed. *FEMS Microbiol Lett*. 2016;363(16):fnw179. doi:10.1093/femsle/fnw179

152. Schooling SR, Beveridge TJ. Membrane vesicles: An overlooked component of the matrices of biofilms. *J Bacteriol*. 2006;188(16):5945-5957. doi:10.1128/JB.00257-06

153. Dorward DW, Garon CF. *DNA Is Packaged within Membrane-Derived Vesicles of Gram-Negative but Not Gram-Positive Bacteria*. Vol 56.; 1990. https://www.ncbi.nlm.nih.gov/pmc/articles/PMC184538/pdf/aem00087-0464.pdf. Accessed August 2, 2018.

154. Yonezawa H, Osaki T, Kurata S, et al. Outer Membrane Vesicles of Helicobacter pylori TK1402 are Involved in Biofilm Formation. doi:10.1186/1471-2180-9-197

155. Bauman SJ, Kuehn MJ. Purification of outer membrane vesicles from Pseudomonas aeruginosa and their activation of an IL-8 response. *Microbes Infect*. 2006;8(9-10):2400-2408. doi:10.1016/J.MICINF.2006.05.001

156. Sonntag I, Schwarz H, Hirota Y, Henning U. Cell envelope and shape of Escherichia coli: multiple mutants missing the outer membrane lipoprotein and other major outer membrane proteins. *J Bacteriol*. 1978;136(1):280-285. http://www.ncbi.nlm.nih.gov/pubmed/361695. Accessed August 19, 2019.

157. Hankins J V, Madsen JA, Giles DK, Brodbelt JS, Trent MS. Amino acid addition to Vibrio cholerae LPS establishes a link between surface remodeling in Gram-positive and Gram-negative bacteria. doi:10.1073/pnas.1201313109

158. Brown L, Wolf JM, Prados-Rosales R, Casadevall A. Through the wall: extracellular vesicles in Gram-positive bacteria, mycobacteria and fungi. *Nat Publ Gr*. 2015;13. doi:10.1038/nrmicro3480

159. Choi DH, Kwon YM, Chiura HX, et al. Extracellular Vesicles of the Hyperthermophilic Archaeon "Thermococcus onnurineus" NA1T. *Appl Environ Microbiol*. 2015;81(14):4591-4599. doi:10.1128/AEM.00428-15

160. Juan T. Biogenesis and function of ESCRT-dependent extracellular vesicles. *Semin Cell Dev Biol*. 2018;74:66-77. doi:10.1016/J.SEMCDB.2017.08.022

161. Joffe LS, Nimrichter L, Rodrigues ML, Del Poeta M. Potential Roles of Fungal Extracellular Vesicles during Infection. 2016. doi:10.1128/mSphere.00099-16

162. Pfaller MA, Diekema DJ. Epidemiology of invasive candidiasis: a persistent public health problem. *Clin Microbiol Rev*. 2007;20(1):133-163. doi:10.1128/CMR.00029-06

163. Kristjansson L. Candida albicans biofilm–induced vesicles confer drug resistance through matrix biogenesis. *PLOS Biol*. 2018;8(2):101-108. doi:10.1371/journal.pbio.2006872